Research Report
KTC-98-1

SEISMIC ISOLATION OF A HIGHLY SKEWED, PRESTRESSED CONCRETE GIRDER BRIDGE (KYSPR 96-173)

by

Bradley Neil Robson
Formerly Research Assistant, Kentucky Transportation Center

Issam E. Harik
Professor of Civil Engineering and Head, Structures Section,
Kentucky Transportation Center

and

David L. Allen
Transportation Engineer V, Kentucky Transportation Center

Kentucky Transportation Center
College of Engineering, University of Kentucky
Lexington, Kentucky

in cooperation with

Kentucky Transportation Cabinet
Commonwealth of Kentucky

and

The Federal Highway Administration
U.S. Department of Transportation

May 1998

Commonwealth of Kentucky
Transportation Cabinet
Frankfort, Kentucky 40622

James C. Codell, III
Secretary of Transportation

Paul E. Patton
Governor

T. Kevin Flanery
Deputy Secretary

Mr. Jesse Story
Acting Division Administrator
Federal Highway Administration
330 West Broadway
Frankfort, KY 40602

September 10, 1998

Subject:
- Implementation Statement for Final Report entitled "Seismic Isolation of a Highly Skewed, Prestressed Concrete Girder Bridge."
- Study number: KYSPR 96-173
- Study title: "Seismic Rating and Evaluation of Highway Structures"

Dear Mr. Jesse Story:

The above referenced research study is divided into three major tasks:

TASK A: Experimental Dynamic Testing of the Bridge in Ballard County, Kentucky.
TASK B: Development of a Finite Element Model of the Bridge to Match Experimental Results.
TASK C: To Perform Time History Analyses with Site Specific Acceleration Records to Access the Efficacy of Seismic Isolation of the Bridge.

The main objective of this study was to quantitatively evaluate the effectiveness of seismically isolating a highly skewed, prestressed concrete, slab-on-girder bridge. The objective set forth has been achieved by conducting research in three distinct but equally important phases as mentioned in tasks A, B, and C.

The results of this study clearly show that seismic isolation is an effective means of reducing earthquake forces on bridges.

Sincerely,

David E. Smith

J. M. Yowell, P.E.
State Highway Engineer

cc: David Smith

Technical Report Documentation Page

1. Report No.	2. Government Accession No.	3. Recipient's Catalog No.
KTC-98-1	PB99-121493	

4. Title and Subtitle

SEISMIC ISOLATION OF A HIGHLY SKEWED, PRESTRESSED CONCRETE GIRDER BRIDGE (KYSPR 96-173)

5. Report Date
May 1998

6. Performing Organization Code

7. Author(s) Brad Robson, Issam Harik, and David Allen

8. Performing Organization Report No.
KTC-98-1

9. Performing Organization Name and Address

Kentucky Transportation Center
College of Engineering
University of Kentucky
Lexington, Kentucky 40506-0281

10. Work Unit No. (TRAIS)

11. Contract or Grant No.
KYSPR96-173

12. Sponsoring Agency Name and Address

Kentucky Transportation Cabinet
State Office Building
Frankfort, Kentucky 40622

13. Type of Report and Period Covered
FINAL

14. Sponsoring Agency Code

15. Supplementary Notes
Prepared in cooperation with the Kentucky Transportation Cabinet and the U.S. Department of Transportation, Federal Highway Administration

16. Abstract

A relatively new approach for designing or retrofitting highway bridges in seismic zones involves isolating the superstructure from the substructure. Through experimental and analytical investigations, this study evaluates the effectiveness of isolating one particular bridge: a highly skewed, prestressed concrete, slab-on-girder bridge. Dynamic testing of the bridge was performed using the pullback, quick-release method. A three dimensional finite element model of the bridge was created. It was refined, or calibrated, to match experimentally determined natural frequencies and mode shapes. Time-history analyzes, using site-specific acceleration records, were conducted for the seismically isolated bridge model and an identical, non-isolated bridge model.

For the bridge under consideration, seismic isolation was found to appreciably reduce forces that the bridge substructure and foundation must resist. Seismic design forces for pier columns were reduced between 43% and 86%. The results of this study clearly show that seismic isolation is an effective means of reducing earthquake forces on bridges.

17. Key Words	18. Distribution Statement
Earthquake, Seismic isolation, Base isolation, Time history, Skewed bridge, Girder bridge, Optimization, Retrofitting	Unlimited with approval of Kentucky Transportation Cabinet

19. Security Classif. (of this report)	20. Security Classif. (of this page)	21. No. of Pages	22. Price
Unclassified	Unclassified	181	

TABLE OF CONTENTS

LIST OF TABLES

LIST OF FIGURES

EXECUTIVE SUMMARY

A relatively new innovation in the design and retrofit of structures in seismic zones is base isolation. In this approach the base of the structure is connected to its supports by an isolation system. This study focuses on the quantification of the effectiveness of seismically isolating a highly skewed, prestressed concrete, slab-on-girder bridge in Ballard County, Kentucky.

To date, most research on base isolation has concentrated on laboratory testing of the isolation components themselves, or analytical investigation of real or theoretical systems. Very few full-scale bridge tests have been performed on in-service, seismically isolated bridges. Furthermore, research that combines full-scale experimental testing and analytical simulation is even more limited.

EXPERIMENTAL BRIDGE TESTING

Dynamic test results from an actual full-scale bridge is the quintessential form of model calibration for further analytical studies. Results from full-scale bridge tests are invaluable and necessary to attain a better understanding of our transportation infrastructure.

Dynamic testing of the Ballard County bridge(Fig.1,2 and 3) was performed using the pullback, quick-release method. Several new developments facilitated the quick-release testing. A simple, new quick-release mechanism was designed, constructed, and tested at the University of Kentucky. Also, for this study, a unique method of attaching the pullback cable to the bridge has been developed. This allowed the pullback force to be moved to a second pull point rapidly, without delaying the test schedule. While this attachment method is only applicable to new bridges, a modified version could easily be used on existing bridges.

Pullback, quick-release testing of the Ballard County bridge was the first of its kind ever performed. It was the first known pullback, quick-release testing of a prestressed concrete, slab-on girder bridge. Also, it was the first known pullback, quick-release test of a highly skewed bridge. The method devised to pullback, quick-release test the Ballard County bridge was found to be simple, quick, efficient, and required little site disturbance.

OPTIMIZATION OF BRIDGE MODEL

Once the experimental testing was performed and the data analyzed, the next objective of this research was to create an accurate finite element model of the bridge. Although the initial model could be developed from design plans and calculations, refinement was needed to increase correlation with measured dynamic bridge properties.

The model was refined, or calibrated, to match experimentally determined natural frequencies and mode shapes. Past researchers have refined finite element models by random manipulation or other heuristic methods. For this study, an optimization program was written to adjust specific model variables. An automated, systematic, optimization of model parameters produced an accurate analytical representation of the bridge.

SYNERGY OF EXPERIMENTAL & ANALYTICAL RESEARCH

This study synthesized both experimental and analytical research domains to better enable quantification of seismic isolation effectiveness for a particular bridge. As a result of experimental testing, an accurate, reliable finite element model was assembled. Site-specific acceleration records and time-history analyses allowed assessment of the efficacy of seismic isolation, based on an appropriate type of potential earthquakes.

This research used the best of the symbiotic relationship between experimental and analytical investigation by: (1) Creating a highly accurate finite element model based on the bridge's actual dynamic response; (2) Using site-specific acceleration histories for the Ballard County bridge site; and (3) Using nonlinear time-history analysis which incorporated the nonlinear bearing properties measured by the manufacturer. Analyses by this method produce theoretically sophisticated earthquake simulations with their foundation in experimental evidence.

RESEARCH FINDINGS AND RECOMMENDATIONS

This research has demonstrated that pullback, quick-release testing can be accomplished with a simple, inexpensive, release device. It is quick and easy to use, and produces high acceleration levels relative to the pullback force. Test results show that the method can accurately capture a bridge's dynamic signature. Similar pullback testing could be performed on existing bridges with little modification to the procedures used in this study.

Optimization has been proven to be a viable method of calibrating structural models to experimentally determined natural frequencies and mode shapes. The algorithm developed for this research can be applied to almost any application where an analytical model must be calibrated to experimental data.

From the calibration process of this research, expansion dams were found to contribute a significant amount of stiffness to the bridge's dynamic behavior. Common engineering practice is to model expansion ends of a bridge as having no longitudinal resistance. However, since expansion bearings and, more importantly, expansion dams can possess significant stiffness, it is recommended that they be included in any analytical model of a bridge.

Seismic isolation was found to appreciably reduce forces that the bridge substructure and foundation must resist. Seismic design forces for pier columns were reduced 48% to 86 % for the design earthquake. Likewise, seismic design forces for pier columns were reduced 43% to 81 % for the maximum earthquake. Thus, seismic isolation for highly skewed, prestressed concrete, slab-on-girder bridge was validated as an effective means of reducing earthquake forces on bridges.

Similar effectiveness is expected for other slab-on-girder bridge types and configurations. For this study, the importance of the expansion dam in resisting horizontal forces was obvious. For bridges without skewed substructures, the expansion dam may play little role in resisting transverse forces. It is, therefore, hypothesized that seismic isolation would be even more effective for bridges without skewed substructures.

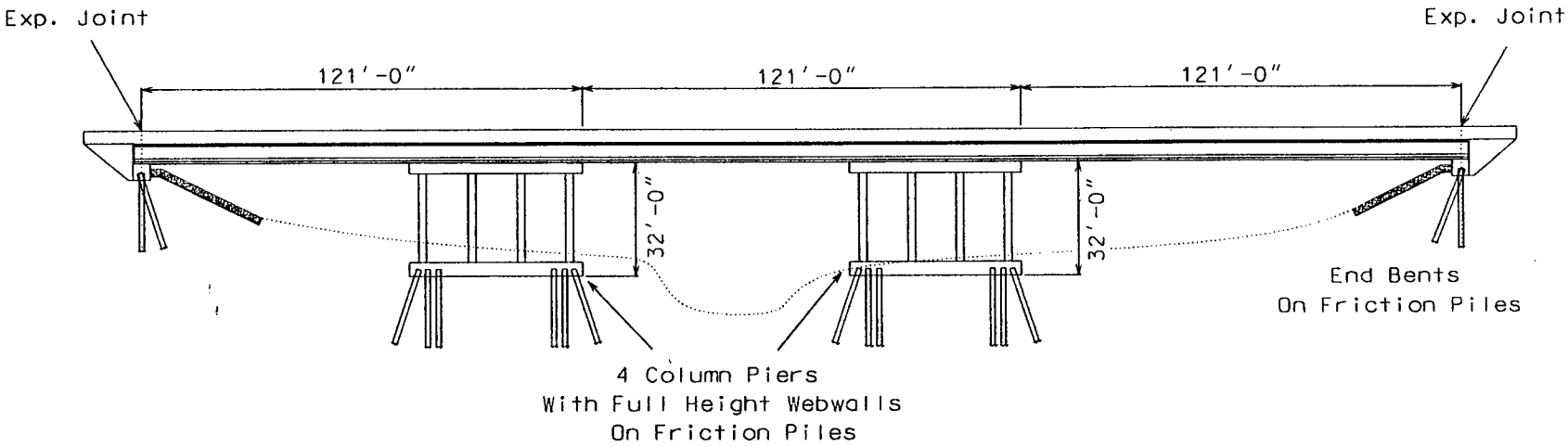

Figure 1: Elevation View of Bridge

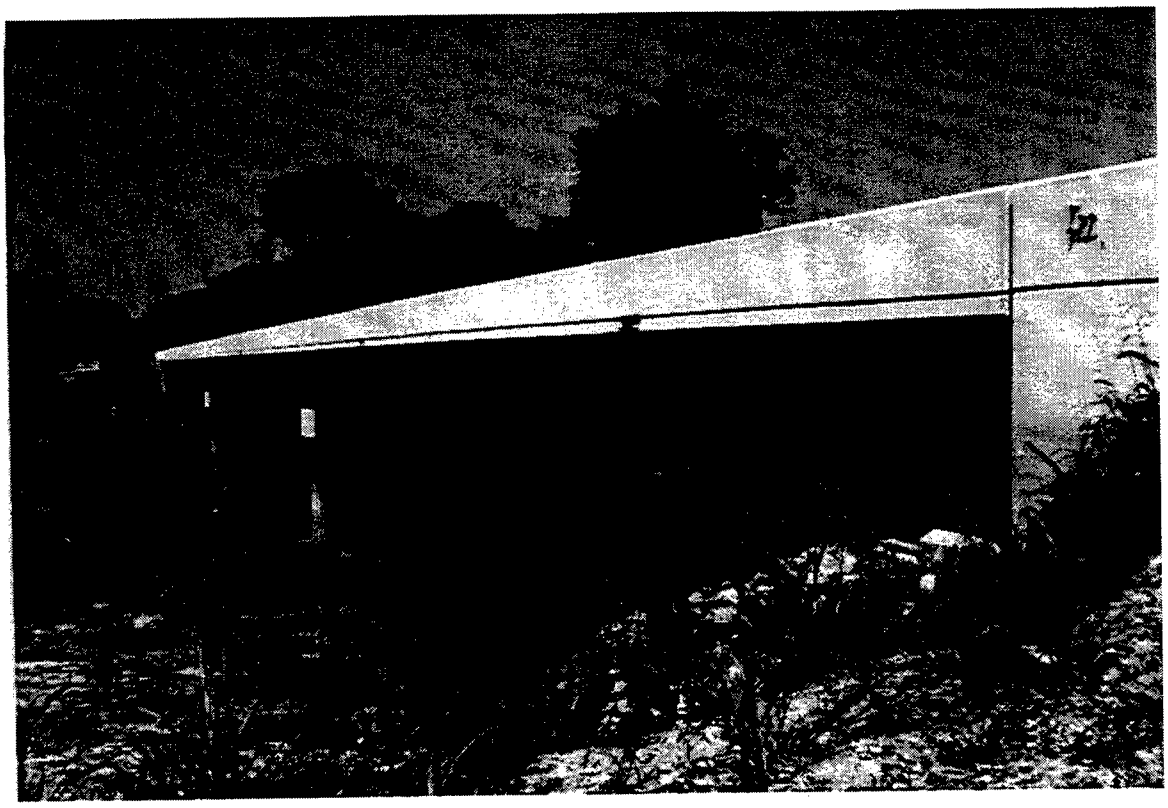

Figure 2: Elevation View Of Ballard Co. Bridge

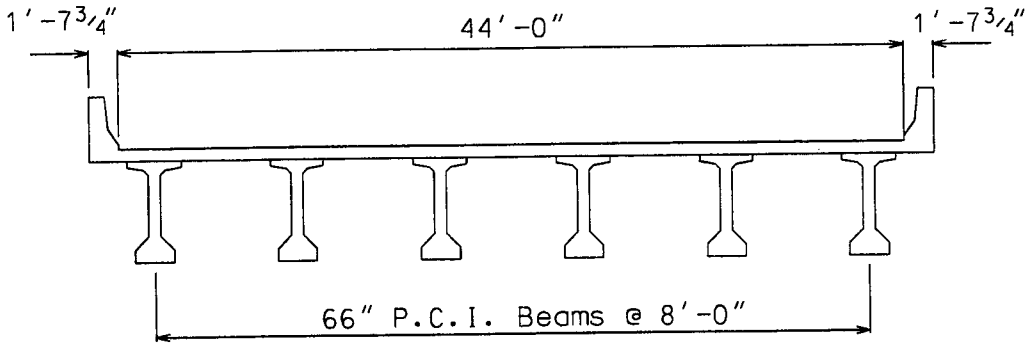

Figure 3: Typical Section

ACKNOWLEDGEMENT

The financial support for this project was provided by the Kentucky Transportation Center, the Federal Highway Administration and the National Highway Institute in the form of the Dwight David Eigenhower Transportation fellowship.

Funding, personnel, equipment, and site arrangements for the experimental portion of this work were provided by the Kentucky Transportation Cabinet and the Kentucky Transportation Center (KTC) at the University of Kentucky. The help of John Flekenstein and Clark Graves in coordinating and conducting the bridge testing is especially noteworthy. The authors would like to acknowledge the cooperation, suggestions, and advise of the members of the study advisory committee: Donald Herd(committee chairperson), Glenn Givan, Ray Greer, David Moses, Ted Noe, N.B. Shah, and David Steele.

1.0 INTRODUCTION

1.1 INTRODUCTION

Mentioning earthquakes and the United States in the same sentence usually evokes thoughts of California and its many recent quakes. Naturally, the forefront of seismic analysis and design in the United States has been pioneered in California for their type structures. Design codes such as the AASHTO (1996) code for highway bridges have gone through many iterations to reach the current provisions for seismic design. This effort has been advanced through the time-consuming process of theoretical and experimental investigation, code implementation, practical application, and post earthquake performance evaluation.

With every new earthquake, the philosophy and beliefs behind the seismic design codes are proven sufficient or found to be lacking in some respect. In order to better ensure public safety, the engineering community is constantly striving for a better understanding of the behavior of structures and the ability to protect them during earthquakes. Seismic isolation is one approach that has recently come into widespread use in the United States.

1.2 SEISMIC DESIGN PHILOSOPHIES

Engineers have long sought ways for structures to resist the damaging effects of earthquakes. Typically, peak vertical acceleration from an earthquake is smaller than the peak horizontal accelerations by a factor of approximately two thirds (Penzien 1993, Astaneh-Asl et al. 1994, AASHTO 1983). It is not surprising, then, that mainly the lateral shaking of an earthquake is responsible for damage to structures. In fact, most design codes ignore the effects of vertical acceleration on the structure.

Almost all researchers agreed with the premise of insignificant effects from intrinsic low vertical acceleration components until the October 17, 1989 Loma Prieta and the January 17, 1994 Northridge, California earthquakes proved

otherwise. During Loma Prieta, several locations recorded peak vertical acceleration greater than peak horizontal acceleration (Saadeghvaziri and Foutch 1991). The Northridge quake produced the strongest ground motions ever instrumentally recorded in an urban setting (Naeim 1995, Papageorgiou 1996). Extraordinarily high peak vertical accelerations of up to 1.67 times peak horizontal components were recorded during the Northridge earthquake at some locations (Astaneh-Asl et al. 1994). Now, the process of evaluating the significance of including vertical accelerations in structural seismic design is again underway.

A long process of trial and adjustment, along with rational analysis, has resulted in present-day design standards. Design codes are under constant scrutiny from the engineering community in order to provide the optimum in public safety without an undue economic burden from design and construction costs. While engineers are conservative in their treatment of unknown, naturally occurring forces, even the best estimates of earthquake forces can err on the unconservative side. Thus, the design of a structure must always be a tradeoff between being overly conservative and overly expensive or being rational and economically feasible but risking unanticipated large earthquake forces and structural damage.

Once the design earthquake is determined, the method utilized in the design of the structure is, many times, the choice of the engineer. Currently the three most popular methods of earthquake design are: (1) purely elastic behavior under seismic loading, (2) elastic behavior with localized plastic hinging designed into the structure, and (3) isolation of the structure from the full ground motion.

1.2.1 Elastic Design

In elastic design, the structure is merely proportioned large enough to resist all applied forces elastically. This design philosophy is iterative in nature due to the effects of mass and stiffness on the magnitude of the elastic forces. Increasing member sizes to resist seismic forces in the elastic range of the material also, usually, increases the stiffness and mass of the structure. Depending on the exact proportions of the increases, the seismic forces to be carried by the structure may then increase. This leads the designer back for another iteration of checking the capacity of the members to carry the induced seismic loads. If the members are inadequate, they are reproportioned and new seismic forces will be generated and applied to the resized structure. This process may need to be repeated several times to ensure a fully elastic design of the structure.

This design philosophy has the advantage of theoretically having no damaged structural members after the design earthquake. Additionally, the linear seismic analysis is relatively simple and many numerically well behaved analysis methods

are available. The main disadvantage to a purely elastic analysis is that the final member sizes can be significantly larger than those of other design methods. Larger members increase the initial cost of the structure and often prevent this method from being used for economic reasons.

1.2.2 Plastic Design

A second, widely used method of seismic design is to enable the structure to resist all load groups elastically except seismic loads. Members are proportioned for the non-seismic load groups and then re-analyzed for the seismic load groups. From linear elastic seismic analysis, critical locations can be pinpointed in the structure and plastic hinge zones can be designed.

In reinforced concrete members, hinging locations are designed to ensure adequate confinement, adequate ductility and proper anchorage of the reinforcing steel. In a steel structure, an engineer may purposely proportion certain members to force yielding in specific members under seismic loading (i.e. strong column-weak beam concept) in order to redistribute loads throughout the structure judiciously.

This design philosophy has the advantage of not needing multiple iterations and usually results in smaller member sizes than a purely elastic design. However, the behavior of the structure after yielding is nonlinear and hard to anticipate, especially in reinforced concrete members. Nonlinear numerical methods are available but are, in general, complex to use and require a sophisticated understanding of the analysis method and material properties to have confidence in the output.

Furthermore, this design philosophy allows substantial damage during the design earthquake which would need to be repaired afterward. Collapse of the structure, even in unanticipated large earthquakes, is theoretically prevented using detailing requirements of this method. However, the structure may be rendered useless and have to be demolished after a large event. This would be an example of protecting public safety (i.e. occupants of a building or motorists crossing a bridge), but imposing a large economic loss on the structure's owners from the resulting demolition of the structure.

1.2.3 Seismic Isolation

A relatively new innovation in the design and retrofit of structures in seismic zones is base isolation. In this approach, the base of the structure is connected to its

supports by an isolation system. Under service loads the isolation system functions in the elastic range and keeps the structure positively connected to its supports. However, during a strong earthquake, the connection becomes very flexible and dissipates energy through high damping. This flexible connection allows the structure to oscillate at a different period than the supports. In contrast, a non-isolated structure would oscillate at the same period as its supports.

Seismic isolation, or base isolation, is a relatively new technique to allow a structure to survive large seismic events with little or no damage. Seismic isolation is an alternative to the two more widely practiced design methods. In this design technique, increased structure displacements are traded for decreased substructure forces by allowing the structure to become uncoupled from the substructure or foundation during a large seismic event. This decoupling allows the structure to vibrate at a different (lower) frequency than the substructure and foundation. Shifting the structure to a longer period typically lowers its peak accelerations. Additionally, uncoupling the structure from the substructure reduces the forces that the substructure must resist.

A viable isolation system must have certain characteristic in order to provide functionality at service loads as well as the intended isolation during an earthquake. Three key components must be present in the isolation system: (1) flexibility during strong earthquake shocks with, preferably, self-centering capabilities, (2) a damping or energy dissipation mechanism during an earthquake, and (3) sufficient stiffness at service loads, such as wind loading, to not hinder everyday performance.

Advantages of seismic isolation are smaller member sizes and no damage after the design earthquake. Also, as a result of designing the substructure and/or foundation for smaller horizontal loads, substantial cost savings can sometimes be realized. Disadvantages of this design method are the complex, nonlinear analysis required to accurately predict behavior and the cost of special isolation devices required to accomplish system isolation.

1.4 HISTORY OF SEISMIC ISOLATION

Accidental seismic isolation of buildings have occurred many times throughout history. Buildings, which were not designed to resist earthquakes, were constructed above a soft clay layer which failed in shear during the earthquake shock. This inadvertent foundation or subsurface sliding effectively isolated the structure from the full effects of the earthquake.

Nearly a hundred proposals for shock absorbing or isolation systems were made prior to 1960 (Buckle and Mayes, 1990). However, none of these systems were ever implemented as far as is known. Other countries have led the way in the use of base isolation. Countries including China, France, Mexico, Japan, New Zealand, South Africa, and the former Soviet Union and Yugoslavia have all used isolation systems prior to the U.S.'s first use (Buckle and Mayes 1990, Kelly 1986). New Zealand is in the forefront of the field and had seismically isolated at least 7 structures by 1980. Mayes (1996) reported that by 1996, more than 400 seismically isolated structures have been built throughout the world. Of these, more than 75 are bridges in North America.

An isolation system was first used in the U.S. to isolate a 230 kilovolt circuit breaker for the California Department of Water Resources in 1979. In 1985 the California Department of Transportation (Caltrans) was first to use seismic isolation for a U.S. bridge as a retrofit for the Sierra Point Overcrossing. Isolation allowed existing columns to resist the design earthquake forces elastically and averted the need for column strengthening. In 1986, the U.S.'s first base isolated building was completed, the Foothill Communities Law and Justice Center in San Bernardino County, California (Buckle and Mayes, 1990).

The relatively recent acceptance and implementation of seismically isolated design is the result of three parallel developments (Buckle and Mayes, 1990). One development is reliable computer software that is able to accurately predict performance of the nonlinear bearing behavior during dynamic events. Buckle and Mayes (1990) report that correlation studies with model tests have validated the software.

Secondly, the development and construction of large, hydraulic, servo-controlled shake tables has enabled researches to reproduce recorded earthquakes in the laboratory. Such large shake tables have also led to model simulation with hypothetical earthquakes covering many possible circumstances which may not have been adequately measured during a real earthquake. Additionally, these tables allow testing of individual isolation bearings to verify their performance before they are integrated into a real structure.

The third parallel, but independent, development, according to Buckle and Mayes (1990), is the recent progress in the field of seismology. Seismologists are now able to estimate ground motion at a particular site including the effects of distance to a fault, local and global geology, and return period. Site-specific ground motions are used for time-history analysis and to generate site-specific response spectra. Dynamic response of a seismically isolated structure can then be estimated from the local seismological characteristics instead of general design ground motions.

1.5 CURRENT SEISMIC DESIGN PRACTICE FOR BRIDGES

Currently, AASHTO's Standard Specifications for Highway Bridges, Division I-A (1996) governs the seismic design of bridges throughout most of the United States. Bridge collapses from earthquakes have so far only occurred in Alaska and California. However, many of these occurred due to relatively low ground motions and seismologist have estimated that 37 of the 50 states and Puerto Rico have the potential for ground motions of a level which caused serious bridge damage in past earthquakes (Mayes et al. 1992)

The design earthquake has a peak horizontal acceleration level that has a 10% probability of being exceeded in a 50 year design life. This corresponds to an earthquake with a 475 year return period (Mayes et al. 1992). Use of the AASHTO specifications is intended: (1) to allow the structure to yield during a major earthquake, (2) to produce damage (yielding) only in areas that are accessible (visible) and repairable, and (3) to prevent collapse even during very large earthquakes (NHI 1996). Studies such as Barenberg and Foutch's (1988) have shown this design philosophy to produce safe bridges without an unacceptable initial cost.

A relatively new approach for designing or retrofitting bridges in seismic zones involves isolating the superstructure from the substructure. Base isolation can produce more economical bridges compared to standard seismic design procedures in AASHTO's Standard Specifications for Highway Bridges, Division I-A (Buckle et al. 1988, Mayes et al. 1992, O'Connor and Mayes 1992). Estimates are that new bridge costs can be lowered by up to 10% due to cost reductions for the columns and foundations of an isolated bridge (Mayes et al. 1992). Additionally, isolation designs result in bridges which do not require extensive, if any, repairs after a design earthquake. For these reasons, the overall lifetime bridge cost could be substantially less for an isolated bridge.

In bridge construction, the isolation system is located at the interface between the superstructure and the substructure. Here, the bearing system is used to isolate (dynamically) the superstructure from the ground motion that is normally transmitted from the substructure. Isolation increases the period of the superstructure and reduces the forces that the substructure must resist.

"One of the major impediments to the implementation of seismic isolation has been the lack of code requirements." (Mayes, et al. 1992) Now, AASHTO's Guide Specifications for Seismic Isolation Design (1991) imposes requirements for the analysis and performance of bridges designed with isolation systems. The analysis methods include the Single Mode Spectral Method, Multimode Spectral Method, and Time-History Method; both linear and nonlinear.

"In current engineering design practice, the determination of the maximum inelastic response of base-isolated bridges subjected to AASHTO design earthquakes or recorded ground motions is primarily based on the elastic analysis of an equivalent elastic system." (Hwang and Sheng 1993). A few shortcomings of this linearized analysis method are pointed out by Hwang and Sheng (1993) and an improved, iterative method is proposed by Hwang (1996) and Hwang et al. (1996).

AASHTO requires a linear time-history analysis be performed when the isolation system is not self-centering. Further, AASHTO requires a three-dimensional nonlinear time-history analysis be performed when the effective damping of the isolation system exceeds 30 percent. In that case, the hysteresis curves of the isolation system should be utilized in the nonlinear analysis.

Today, many isolation systems are available from many different manufacturers. Systems may encompass a range of components such as bearings, sliding plates, shock absorbers, friction pendulums, etc. Isolation systems can be roughly categorized as either: (1) elastomeric systems, (2) slide and roller systems, (3) spherical slider systems, (4) hydraulic dampers, or (5) friction dampers. Caltrans is currently conducting a systematic evaluation process to quantify and prequalify isolation systems for use on its highway bridges. The program is an Applied Research and Technology (ART) program under a federal grant of the Intermodal Surface Transportation Efficiency Act of 1991 (ISTEA). This program utilizes the Highway Innovative Technology Evaluation Center (HITEC) which is a nonprofit organization established under an agreement between the Federal Highway Administration (FHWA) and the Civil Engineering Research Foundation (CERF), a subsidiary of the American Society of Civil Engineers (ASCE). Fourteen manufacturers are participating in the study that will use full-scale dynamic tests to characterize the fundamental properties and performance characteristics of the devices. (Sultan and Sheng 1995)

Seismic isolation systems provide additional safety even in the unlikely event of the maximum credible earthquake occurring. In contrast, using the inelastic design method of plastic hinging, the structure does not have nearly the excess capacity to resist stronger earthquakes.

Because of the less rapid attenuation of ground motions with distance in the Eastern U.S. (Nuttli 1973, Johnston 1982), seismic isolation may have even more benefits for structures in the Eastern U.S. than the Western U.S. The Eastern U.S.'s ratio of ground motions between the 2500-year (maximum credible earthquake) and 500-year (design earthquake) recurrence events can measure up to twice the ratio for the Western U.S. (Khinda, Avison, and Deitch 1993). Researchers have found that, in the Eastern U.S., even if a structure is designed for the "design earthquake", the performance of the structure may be catastrophic in the event of the maximum credible earthquake (Hosahalli, Chuntavan, and Aktan

1993). An identical building in the west with an identical "design earthquake" would have a far greater chance of surviving the maximum credible earthquake.

1.6 FULL-SCALE DYNAMIC BRIDGE TESTING

Full-scale experimental testing is essential to the evaluation and predictive aspects of the design code improvement process. Without field testing, theoretical assumptions could not be validated and analytical modeling requirements could not be accurately determined. Dynamic tests on full-scale structures can be performed in a number of ways. Hudson (1977) describes the main types of full-scale dynamic testing as: (1) free vibration tests, including (a) initial displacement as in the pullback, quick-release test, and (b) initial velocity from impacts; (2) forced vibration tests, including (a) steady-state resonance testing, (b) variable frequency excitation including sweep, rundown, random and pulse sequences, and (c) transient excitations including earthquakes, wind, traffic, and explosions. Shelley (1995b) provides a very informative discussion of the advantages and disadvantages of the various test methods used on highway bridges.

Most full-scale bridge testing has been done on California-type bridges. These bridges are typified by a concrete superstructure attached monolithically to the substructure. However, the majority of bridges in many eastern states are slab-on-girder (SOG) bridges. Questions have arisen as to the applicability of the current design codes, which were calibrated to California-type bridges, for SOG bridges (Chen et al. 1993).

1.6.1 Free Vibration Testing

The simplest and most frequently used experimental method is probably the measurement of the decay of free vibrations (Clough and Penzien 1975). When a structure is in motion and there are no applied forces acting on it, the motion is known as free vibration motion. Structures can be set into free vibration by many commonly occurring actions such as wind, moving people or equipment, or passage of a vehicle over a bridge. Rarer conditions, such as earthquakes, can also induce free vibrations. During the time the event is happening, forced vibrations are occurring, but the motion after the event has ceased is free vibration. Experimentalists commonly produce free vibrations by force impulses or releasing an initial force or displacement.

1.6.1.1 Pullback, Quick-Release Testing

The idea of quick-release (sometimes called pullback or snapback) testing is to load a structure to a predetermined force or displacement and then, suddenly, release the load, thereby setting the structure into free vibration motion. For seismic bridge investigations, researchers are usually interested in transverse vibrations (i.e. perpendicular to the bridge length) because transverse earthquake forces cause most damage to bridges. Therefore, quick-release testing of bridges usually requires that forces be applied transversely to a bridge.

Quick-release testing for highway bridges was developed at the University of Nevada-Reno (Douglas 1976). So far, it has been used to test only a few SOG bridges (Chen et. al, 1993) and had never been used to test a prestressed concrete girder bridge until this project. Also, testing of a highly skewed bridge by this method had never been done. Thus, the testing performed as a part of this research yields insights into the behavior of a common bridge type found throughout the United States.

Usually, quick-release test forces are produced by either bulldozers or hydraulic jacks (Chen et al. 1993, 1994a, 1994b, 1995, Douglas 1976, Douglas and Reid 1982, Douglas et al. 1990, Mander et al. 1993, 1996, Ventura et al. 1996, Wendichansky et al. 1995). Previous release devices include mechanical release mechanisms, solenoid activated devices, explosive bolts, and fuse bars. Forces exerted on bridges in past pullback tests have ranged from 5 kips (22.2 kN) to over 150 kips (667 kN).

Douglas (1976) reported achieving peak transverse deck accelerations of between 0.5 % and 1% of gravity using pullback forces of 5 kips (22.2 kN) and 12 kips (53.4 kN). From a different quick-release test setup, Douglas et al. (1990) produced peak transverse deck-level accelerations of about 20% of gravity from the sudden release of 141 kips (627 kN). Chen et al. (1993) were able to achieve peak transverse accelerations of 6.5% gravity at bridge deck level by pulling the supporting pier with an equivalent horizontal load of 82 kips (365 kN). That pull also produced pier cap accelerations of approximately 25% gravity. On a different bridge, Chen et al. (1994) measured peak transverse accelerations at deck level of approximately 14% gravity from quick-releasing a 150 kip (667 kN) pull.

One goal achieved in the current research was the development of a simple release mechanism that produced high accelerations from a relatively small lateral force. Before this study, pullback, quick-release testing had never been performed on a prestressed concrete slab-on-girder bridge.

1.6.1.2 Drop Testing

Another method employed to dynamically test bridges is to measure free vibrations resulting from an impact (Agardh 1994, Aktan et al. 1992, 1994a, 1994b, Green and Cebon 1994, Green et al. 1995, Hogue et al. 1991, Raghavendrachar and Aktan 1992, Rotter et al. 1994, Shelley et al. 1995a, Toksoy and Aktan 1994). This commonly involves dropping a weight on the bridge deck or using a hammer to strike the bridge deck. It can also be conducted using a step function on a hydraulically controlled actuator/mass system that is positioned on the bridge. This method can be quick, inexpensive and can be performed without bridge closure in many cases. However, drop (or impact) testing excites mainly vertical modes. As such, this method primarily has applications other than determining the transverse characteristics of a bridge.

1.6.2 Forced-Vibration Testing

Other methods of dynamically field testing bridges are through the measurement of a bridge's forced vibration response. The vibrations can either be random in nature (traffic, wind, explosions, impacts, etc.) or from a controllable source that produces known vibrations. Two common forced-vibration bridge testing techniques are ambient traffic vibration testing and resonant vibration testing.

1.6.2.1 Controlled Vibration Testing

A common method using known forcing functions is through resonance testing. Typically a sinusoidal force is imparted to the structure and the steady-state response is measured. The force is usually the result of an eccentrically rotating mass positioned on the bridge. This method has been used by many researchers (Farrar et al. 1995, Maragakis et al. 1996, Shelley et al. 1995a, Stubbs et al. 1995) with excellent results. The major drawbacks to resonance testing is the expense of the mass shaker and the additional data acquisition equipment required to monitor the applied force or acceleration.

Another controllable forced vibration test method involves subjecting the bridge to random vibrations or white noise. These vibrations are usually produced by a servo-hydraulic vibration generator or seismic mass shaker (Aktan et al. 1992, 1994a, 1994b, Deger et al. 1994, Krishnan et al. 1996, Salawu and Williams 1995,

Seible et al. 1991, Williams and Salawu 1994). As with resonance testing, the major drawbacks to controlled, random vibration testing is the expense of the mass shaker and the additional data acquisition equipment required to monitor the applied force or acceleration.

1.6.2.2 Ambient Vibration Testing

Another method used to dynamically test bridges is through measurement of the bridges response to random forcing functions. These random or ambient vibrations are usually the result of normal traffic or wind. Thus, this method requires no equipment to produce the vibrations, only equipment to record the vibrations. This technique has been used successfully by a number of researchers (Alampalli and Fu 1994, Buckland et al. 1979, Doll 1994, Farrar et al. 1995, Harik et al. 1993, Paultre et al. 1995, Saiidi et al. 1994, Shahawy 1995, Ventura et al. 1994,1996, Wendichansky et al. 1995). Harik et. al. (1993) used this method with success to identify the fundamental mode shapes and frequencies of the Brent-Spence Bridge crossing the Ohio River in Cincinnati, Ohio.

Ambient vibrations from traffic usually excite vertical modes much more than horizontal modes. Transverse accelerations, for example, tend to be several orders of magnitude less than that produced from a quick-release test (Douglas and Reid 1982). Therefore, this method is also limited in its applicability in determining a bridge's transverse dynamic characteristics.

1.7 RESEARCH OBJECTIVES

The principal objective of this research was to quantitatively evaluate the effectiveness of seismically isolating a highly skewed, prestressed concrete, slab-on-girder bridge. To achieve the principal objective, research was conducted in three distinct, but equally important phases. Within each of the three phases, research objectives were formulated and accomplished.

Phase one was the experimental testing and analysis phase. Phase one's main goal was to develop a method based on pullback, quick-release testing to determine the bridge's dynamic characteristics. A quick-release pullback test on a prestressed concrete, I-girder bridge had never been performed before this research. Also, the bridge under investigation is highly skewed, which is another first for being tested by this method. Skewed bridges are thought to behave poorly during some earthquakes (Astaneh-Asl et al. 1994).

For phase one, a simple, economical, and highly effective quick-release mechanism was developed for use with low pullback forces. Using accelerometers, the bridge's natural, free vibrations were measured. From the data, mode shapes, natural frequencies and structural damping ratios were calculated. These quantities provide a unique "signature" of the bridge's dynamic behavior.

In phase two, a finite element model of the bridge was created from design information. The model was then refined, or calibrated, to better correlate with the experimentally determined natural frequencies. Parameters most affecting the vibration modes and frequencies were systematically adjusted within specified ranges by an optimization algorithm. This kind of automated model refinement is a significant research tool and more expedient than a heuristic approach.

Once the model was calibrated to the experimental results, nonlinear time-history analyses were conducted in the third research phase. Site-specific acceleration histories of artificial New Madrid earthquakes were the basis of the time-history analyses. Nonlinear bearing and expansion dam response was accounted for in the time-history analyses. Comparison to results of an identical, non-isolated bridge model quantified the effectiveness of the isolation system.

1.8 CHAPTER OUTLINE

Chapters are arranged in the sequence that the actual research was conducted. Chapter I provides a literature survey describing the past research that is relevant to this study. Chapter II is a description of the bridge that was experimentally tested by the pullback, quick-release method. Unique conditions encountered in the design of the bridge are discussed and the seismic design is reviewed. Chapter III details the pullback, quick-release test method, instrumentation, and data acquisition equipment used in the field. Method of attachment to the bridge, the quick release mechanism, and pull locations are shown.

In Chapter IV, data reduction of the experimental records are presented. Typical measurements are shown along with pertinent considerations in the analysis of the data. Mode shapes, frequencies, and damping ratios determined from testing are tabulated. Chapter V is a detailed look at the finite element model of the structure that was used in the time-history analyses. Assumptions used in the model are explained and possible areas of inconsistency are explored. The method of calibrating the model to experimental results through optimization is explained. Optimization variables are listed and the objective function is explained. Analytical mode shapes and frequencies are presented for the optimized bridge

model.

Chapter VI details the earthquake simulations for the seismically isolated bridge and an identical bridge without seismic isolation. Generation of site-specific time-history acceleration records is reviewed and the analysis method is examined. Results for the design earthquake and the maximum earthquake are presented. Design implications for this level of analysis are discussed. Chapter VII states conclusions from this research and recommendations for future research efforts to complement the current research.

2.0 SEISMICALLY ISOLATED TEST BRIDGE

2.1 INTRODUCTION

The bridge chosen to be field tested is a slab-on-girder (SOG) bridge with I-girders made of prestressed concrete. This bridge type is the most common bridge type constructed in Kentucky today and has been for many years. Additionally, this bridge type is common throughout much of the United States, especially in the Eastern United States. Therefore, the results of full-scale testing of this bridge type is applicable to a great number of bridges in existence today and to be constructed tomorrow.

2.2 BRIDGE LOCATION'S SEISMICITY

The test bridge is located in Ballard County, Kentucky, approximately one mile from the confluence of the Mississippi and Ohio Rivers. This positions the bridge in the New Madrid Seismic Zone, site of three of the largest earthquakes known to have occurred in North America (Johnston 1982, 1985, Johnston and Nava 1985, Street et al. 1996). The zone is named for the town of New Madrid, Missouri, epicenter of the third of the great earthquakes. Each of the massive earthquakes is estimated to have had a Richter magnitude above 8.0 and each of the main shocks was followed by a protracted series of strong aftershocks. The main shocks were felt throughout all of the Central United States, most of the Eastern United States, as well as parts of Canada and dramatically altered the region's landscape.

December 16, 1811 saw the first of the great earthquakes; the second of the huge quakes followed on January 23, 1812. Inhabitants reported the earth to be rolling in waves a few feet in height during the main shocks. On February 7, 1812 the third and strongest of the main shocks occurred. Denoted the "hard shock", this temblor created waterfalls on the Mississippi and caused it to flow backward, locally, for several hours. Several islands in the Mississippi disappeared altogether.

Present-day Reelfoot Lake, in Kentucky and Tennessee, was created during the February hard shock. It is estimated to have had a Richter magnitude of up to 8.8 (Johnston 1985b).

More recently, more than 2000 earthquakes had been instrumentally detected in the New Madrid Seismic Zone during the first 9 years of deployment of seismographs which began in 1974 (Johnston 1985). Although 97% of these are too small to be felt, roughly a Richter magnitude of 2.5, an earthquake occurs in the region, on average, every 48 hours (Johnston 1982). This activity makes the New Madrid Seismic Zone the most hazardous zone east of the Rocky Mountains (Johnston 1985).

2.3 BRIDGE DESCRIPTION

The test bridge carries U.S. 51 over Minor Slough and consists of three, 121 foot (36.9 m) long spans in a straight section of roadway (Figures 1 and 2). Roadway width is 44 feet (13.4 m) consisting of two 12 foot (3.66 m) wide traffic lanes and 10 foot (3.05 m) shoulders on each side. New Jersey type concrete barriers are at the edges of the shoulders. The bridge deck is 8 inches (0.203 m) thick (minimum), cast-in-place concrete and is made composite with the prestressed girders by stirrups extending into the deck. Cast-in-place concrete diaphragms are located at the third points of all spans and at the supports. There are six, 66 inch (1.68 m) deep prestressed concrete I-beams spaced 8 feet (2.44 m) center-to-center (Figure 3). Negative moment slab reinforcement and pier diaphragms make the bridge continuous for live load.

The substructure is skewed 45 degrees and consists of friction pile end bents and piers on friction piles. The bridge is symmetric except for the skewed substructure which makes the bridge antisymmetric about a transverse line through the center of the middle span. The superstructure is attached to the substructure by seismic isolation bearings.

Soil borings taken at the site prior to bridge design indicated that bedrock is more than 80 feet (24.4 m) below ground. Near-surface soil is mainly clayey silts to a depth of about 12 feet (3.66 m) with cohesion of 2500 psf (120 kPa; from unconfined compression test). The second layer is characterized as a silty sand with an internal friction angle of 34 degrees. This layer is approximately 30 feet (9.15 m) in thickness. Below that, is another layer characterized as silty sand with a friction angle of 36 degrees. The second silty sand layer had Standard Penetration Test (SPT) blow counts of 38 and above.

Bearings at the piers are 6.375 inch (0.162 m) tall shimmed rubber only (Figure 4), while each end bent bearing contains a 4.5 inch (0.114 m) diameter lead

core inside the shimmed rubber pad (Figure 5). During a strong earthquake, the lead is designed to yield and dissipate energy while resistance over the piers is only due to the much more flexible rubber bearing pads. Yielding of the lead cores, and the flexibility of the rubber itself, allow the superstructure to vibrate at a lower frequency than the substructure during a strong earthquake. This uncoupling of the structural system significantly lowers the forces that the substructure must resist. As a result, the short, stiff piers are less susceptible to damage during an earthquake.

Each of the bridge's multi-column piers have four, 3 foot (0.915 m) diameter circular reinforced concrete columns. Piers have full-height webwalls between the columns and 5 foot (1.52 m) wide by 3 foot (0.915 m) high reinforced concrete caps (Figure 6). Pier footings are 4 foot (1.22 m) thick reinforced concrete spread footing/pile caps. Each footing is 12 foot (3.66 m) wide by 67 feet 4 inches (20.5 m) long and encases 51, 16 inch (0.407 m) square, prestressed concrete piles.

Piling is arranged in three parallel rows of 17 piles each. Every other perimeter pile on the long sides are battered away from the pier at a 3 in 12 slope (14 degrees from vertical), as are all three piles on each short end. Piling was designed to be driven approximately 32 feet (9.76 m) below bottom of footing.

Reinforced concrete pile end bents with backwalls were used at both ends of the bridge. Thermal expansion of the superstructure is accommodated at the end bents with a 2 ½ inch (0.0635 m) expansion joint at each bridge end (Figure 7). Each end bent is supported by 17, 16-inch (0.406 m) square, prestressed concrete piles driven vertically. Pile lengths were designed to reach a minimum of 20 feet (6.10 m) below bottom of end bent cap.

2.4 BRIDGE DESIGN CONSIDERATIONS

The bridge was designed in accordance with the American Association of State Highway and Transportation Officials (AASHTO) *Standard Specifications for Highway Bridges*, 14th edition, 1989, with interim specifications through 1991, AASHTO's *Standard Specifications for Seismic Design of Highway Bridges* (1983, interim 1991), and the Kentucky Transportation Cabinet's Guidance Manual for Bridges (1992). Additionally, AASHTO's *Guide Specifications for Seismic Isolation Design* was used in the seismic design and analysis of the bridge after a base isolated design was adopted. Design was performed by the Kentucky Transportation Cabinet's Division of Bridges.

The bridge site presented a number of potential conditions that had to be

considered in the bridge design. Earthquake, scour, and liquefaction potential were all considered in the project. Surrounding the bridge are flood plains of the Mississippi and Ohio Rivers. These lowland areas have the potential to be inundated many times throughout the year making the likelihood of scour around the piers great. Analyses conducted by the Kentucky Transportation Cabinet's Drainage Division and the Federal Highway Administration's Regional Office calculated potential scour 22 feet (6.71 m) below grade at pier locations.

Accordingly, piers were designed assuming all soil was scoured away to a depth of 12 feet (3.66 m) below the bottom of pier footings (pier footings are 10 feet (3.05 m) below grade). In accordance with AASHTO, load combinations that include earthquakes assumed only one half of the scour potential had occurred. Therefore, anticipated scour directly affected the size, spacing, and number of piling required at each pier. The large number of piling required resulted in a very stiff foundation for the piers.

Another component contributing to the stiffness of the piers was the webwalls between the pier columns. To satisfy the Kentucky Transportation Cabinet's requirement to extend webwalls to the anticipated high water level, webwalls were installed the full height of the piers. These 15 inch (0.381 m) thick, solid concrete walls stiffen the piers in their strong axes immensely and, to a much lesser degree, also in their weak axes. In combination, the stiff foundation and extremely stiff piers attract a substantial portion of the transverse and longitudinal earthquake loads without isolation.

From the geotechnical information, the subsurface below the bottom of pier footing elevation consisted of silty sands. Such soils could possibly liquefy if saturated and subjected to sufficiently high earthquake accelerations. Pier piling extended through the first silty sand layer into a denser silty sand layer.

Since the roadway could not be relocated out of the area, mitigation measures such as removal of soil susceptible to liquefaction, densification of the susceptible soil, grouting or chemical stabilization, relief wells to increase horizontal drainage, and increasing the effective overburden were all contemplated. However, any effective mitigation measures were deemed to be cost prohibitive for this structure.

From preliminary seismic analysis using the single-mode response spectrum analysis, resisting forces and moments at piers were abnormally large. Preliminary column size for the non-isolated structure was 4 ½ foot (1.37 m) diameter. Also, the non-isolated bridge required larger footings and more piling to resist the imposed forces. The isolated structure required only 3 foot (0.915 m) diameter columns and resulted in an elastic design and a cost savings for the overall bridge, even including the cost of the seismic isolation bearings.

In August, 1992, the Kentucky Transportation Cabinet let the contract for the construction of the test bridge. The bridge was completed and opened to traffic in late 1994. Pullback, quick-release testing was conducted on August 9, 1995.

2.5 SEISMIC ISOLATION BEARINGS

The bearings used to seismically isolated the bridge are of the lead-rubber type. They consist of steel shimmed, rubber bearing pads with a cylindrical portion removed from the center of the bearing and filled with a lead plug. This type of bearing has been in use since 1978 for buildings and bridges in New Zealand (Buckle and Mayes 1990).

Use of the plastic deformation of lead as a hysteretic damper began as lead extrusion devices used on two New Zealand bridges in 1974 (Robinson and Greenbank 1976). Refinements in the technology lead to the lead-rubber bearings in common use today. Researchers have been able to produce a low cost, low maintenance, high performance mechanical energy dissipator in the lead-rubber bearing (Robinson 1982).

Lead is ideally suited for this application because it has a well defined yield stress, crystallizes at ambient temperature, is malleable, has favorable creep and/or stress relaxation properties, and has no significant fatigue characteristics. Lead's mechanical properties are such that a reasonable size lead core can be used in a bearing to elastically resist service loads such as wind, braking, and low seismic loads. For slowly applied thermal movement of a bridge, lead has approximately 25% of the resistance it has during short-term loading (DIS 1993). Thus, lead cores can effectively resist service loads without unreasonable size bearings.

During a design earthquake, lead cores of isolation bearings can undergo many cycles of plastic deformation and re-crystallization to its original properties. This return to original properties, coupled with its lack of fatigue behavior, make lead the ideal material to resist cyclical earthquake forces through hysteretic behavior.

The bearings were designed by Dynamic Isolation Systems (DIS), Inc., Berkeley, California, in conjunction with the Kentucky Transportation Cabinet. Bearings were manufactured by Furon Structural Bearings Division, Athens, Texas, where they were tested for compression stiffness and combined compression and shear. Each isolator was subjected to a minimum of five complete cycles of shear deformation of plus or minus the design displacement. Force-displacement curves were recorded for all bearings and isolator performance properties for

effective stiffness at the design displacement (K_{eff}) and yielded stiffness (K_r) were verified to be within tolerance. Also, the energy dissipated per cycle (EDC) was calculated to arrive at effective damping ratios. (DIS 1994) Figure 8 is a typical force-deflection curve for the isolation bearings at the piers and Figure 9 is a typical force-deflection curve for the lead cored bearings at the end bents.

3.0 EXPERIMENTAL SETUP

3.1 INTRODUCTION

Based on past research efforts, one goal of this full-scale bridge investigation was to identify all excited transverse modes below 20 Hz from the pullback, quick-release testing. Previous researchers have been able to identify up to four (Ventura et al. 1996), five (Douglas 1976), or six (Douglas and Reid 1982) transverse modes from quick-release bridge testing. Douglas and Reid (1982) however, were only able to determine mode shapes for four of the six identified transverse frequencies. Maximum transverse frequencies identified from previous pullback testing were 14.7 Hz (Ventura et al. 1996), 10.86 Hz (Douglas 1976), and 14.2 Hz (Douglas and Reid 1982).

Aktan et al. (1992) note that " ... extremely stringent standards are required to accurately measure 20 mass-normalized modal vectors". Out of the 21 modes (maximum frequency = 23.6 Hz) that Aktan et al. identified by vertical impact and horizontal forced-vibration tests, three were transverse modes with an identified frequency of 19.53 Hz for the third mode. Therefore, for this study, the goal was to identify all transverse modes below 20 Hz using pullback testing and complementary ambient traffic vibration testing.

3.2 A PRIORI ANALYSIS

To identify the best location for pullback points, a linear elastic eigenvalue analysis was performed. This superstructure only model consisted of beam elements connected to shell elements for the deck. The bearings were modeled as pin supports with linear translational springs in the two horizontal directions corresponding to the elastic stiffnesses that were estimated in the bearing design (DIS 1994).

It was assumed that natural frequencies below 20 Hz could be identified by snap-back testing. From the a priori analysis, five transverse modes were found to exist below 20 Hz. Pull points were located to excite as many of the first five transverse modes as possible. From plots of the transverse modes, the first transverse mode appeared as a half-sine shape and had maximum amplitude at the center of the center span. Mode two appeared to be a rigid body rotation of the

superstructure about the center of bridge and had maximum amplitude near the two ends of the bridge. Mode three showed the ends of the bridge oscillating out of phase with the center of the bridge. Mode four was a full sine wave and mode five was one and a half sine waves.

It was, therefore, decided to locate a pullback point near the center of the bridge to induce excitation of transverse modes 1,3 and 5. An additional pullback point was located at the center of one of the end spans of the bridge to try to excite modes 2 and 4.

3.3 EQUIPMENT DESCRIPTION AND CAPABILITIES

Vibrations were measured with 24 Columbia Research Laboratories, Inc. force balance accelerometers. The model SA-107B accelerometers had a ±2 G range with a system voltage of ±15 volts DC. The output from force balance accelerometers does not depend on the displacement of some internal element being a linear function of acceleration such as with LVDT, potentiometric, variable reluctance and similar type accelerometers (Columbia 1992). No additional signal conditioning was required for the accelerometers.

Sets of three accelerometers were mounted to 4 x 4 x 5 inch (10.2 x 10.2 x 12.7 cm) solid aluminum blocks. Accelerometers were mounted in order to measure in three orthogonal directions. To ensure the blocks were placed level, adjustable feet and a carpenters level was attached to each block. Accelerometers were connected to the data acquisition system by shielded cables.

The data acquisition system used during testing consisted of a DAS-1800HC hardware card installed in a 486 PC. The card, by Keithley Metrabyte, provides up to 64 channels of data acquisition. Additionally, the data acquisition system had 24 channels of simultaneous sample and hold capability for dynamic testing. Simultaneous sample and hold capability allows for sampling of all channels at the same instant, instead of sequential sampling. For dynamic testing with a high sampling rate even the small wait time that the electrical hardware has between sampling each channel sequentially may be important.

VIEWDAC Software by Keithley Metrabyte was used to set program variables, such as calibration factors, sampling rate, sampling time, etc. that affected testing. VIEWDAC also allowed viewing of data immediately after a test. This provided a quick and easy way to examine all channels to ensure data were being measured and recorded properly. Figure 10 shows the data acquisition equipment in the test trailer during the pullback, quick-release testing.

A SENSOTEC load cell capable of measuring ± 20,000 pounds (88.96 kN) was connected in-line between the bridge and the steel pullback cable. Using VIEWDAC, the load cell output was monitored and used to trigger recording of the other instrumentation channels during pullback testing. To measure displacements across an isolation bearing at a pier, an LVDT with a range of ±1 inch (2.54 cm) was used.

The pullback force was supplied by a D7 bulldozer and normal traffic provided the vibrations during ambient vibration testing. Two-way radios were used to coordinate the activities of the bulldozer operator when the data acquisition system was reset and ready for a pullback test. The two-way radios also allowed personnel on the bridge to identify approaching large trucks and signal the accelerometer recordings as the trucks crossed the bridge during the ambient vibration testing.

3.4 QUICK-RELEASE MECHANISM

During construction of the bridge, high strength DYWIDAG bars were cast in the bridge deck and allowed to protrude six inches (0.152 m) from the barrier face (Figure 11). The bars were located at the pullback points determined from the a priori analysis. On test day, a high strength steel cable connected the pullback points on the bridge to a bulldozer 100 feet (30.5 m) from the bridge. An in-line load cell was connected to the embedded Dywidag bar with a load plate and coupler (Figure 12). The load cell was used to monitor cable force and trigger accelerometer recording just prior to the quick-release.

An in-line quick-release mechanism attached the steel cable to the bulldozer. The quick-release mechanism was a simple, direct-shear device containing a pin in double shear (Figures 13 and 14). By design, at approximately 10,000 pounds (44.5 kN) of pull force, the hardened steel pin sheared, causing an almost instantaneous release of the force on the bridge. An instantaneous release produces the greatest transverse acceleration levels for a particular pull force.

Chen et al. (1994a, 1995) report that using quick unloading of a hydraulic jack to release the pullback force caused low response level due to the damping of the loading jack while evacuation of the hydraulic fluid after release. They further report that using an in-line "fuse bar", provided the nearly instantaneous release and higher transverse accelerations.

The direct-shear mechanism developed during this research is a variation of the fuse bar concept; that is, using the failure of an in-line metallic component as the release mechanism. The fuse bars, as reported by Chen et al. (1993, 1994a, 1995), were machined to a specified diameter in order to break at a predetermined load. The system developed in this study has the advantage of using commonly available, standard size, hardened steel pins to provide a brittle type shear failure. Thus, the cost of machining special fuse bars was avoided.

Figure 15 shows a typical load cell record for one pullback test. Figure 16 is an enlargement of Figure 15 and shows more clearly how rapid a complete load release was achieved with the quick-release mechanism devised for this testing.

Data acquisition software allowed the load cell to be used as a triggering mechanism to start recording of the accelerometers. The bulldozer slowly tensioned the cable until 8 kips (35.6 kN) of force was measured, then accelerometer recording began. This pre-release trigger ensured that the complete record of pre-release loading, release into free vibration, and vibration decay were recorded. Load cell, accelerometers and an LVDT were sampled at 1000 Hz for 30 seconds to assure a complete, high resolution acceleration record.

3.5 TEST METHOD

The bridge under investigation is antisymmetric about the center of the middle span (i.e. symmetric except for skewed substructure). Due to this antisymmetry, only half of the bridge had to be instrumented to obtain accurate mode shapes of the entire bridge. Accelerations at enough positions within each span were measured to ensure that the complete shape of each mode was captured. Figure 17 is a plan view of the bridge with the accelerometer locations shown.

A spacing of 20 feet (6.10 m), along each side of the bridge, provides 10 data points within a span which allowed for an accurate assessment of the mode shapes. Sets of three accelerometers were mounted to aluminum blocks in orthogonal directions. A block was positioned at each location shown in Figure 17 with the accelerometers oriented in the vertical, transverse and longitudinal directions.

Since 21 positions on the bridge deck and 4 positions on the substructure were chosen, 75 individual accelerometers would have been required if only a single pullback test was to be done. Instead, testing was conducted using a series of 4 pullbacks while moving all accelerometer blocks between pulls except a base station. Base-station testing enabled fewer accelerometers to be used to gather measurements at multiple locations. Acceleration records were then scaled to the base station magnitude to account for any variance between pulls.

Four pullback, quick-release snaps were conducted at each of the two Dywidag bar location: one at the midspan of the first span and the other at the midspan of the center span. Base stations were chosen above the pull points where the highest transverse accelerations were expected. This provided the most accurate scaling in order synthesize the multiple tests into a clear picture of the bridge's response due to the two pull locations. Figure 18 shows a technician placing an accelerometer block in position for one of the pullback tests.

To prevent any shifting of the accelerometers during testing, 25-pound bags of lead shot were laid on top of the accelerometer blocks once in position. Figure 19 shows a block in position on the end bent cap with the lead weight on top. Figure 20 shows four accelerometer blocks on the bridge deck prior to testing.

All pullback, quick-release testing was accomplished in a single day. Merely inserting a new shear pin in the quick-release mechanism allowed for expeditious testing. As can be seen in Figure 20, the shoulders were coned-off and local Kentucky Transportation Cabinet personnel provided traffic control. The bridge was only closed during the minute or so that each test required. Between tests, traffic was allowed to cross the bridge at reduced speeds. During ambient vibration tests, traffic was allowed to cross at normal highway speed.

A bulldozer, which was rented for the day of testing, provided a convenient method of applying the horizontal force. Since the force was applied directly to the superstructure, the deck level transverse accelerations were maximized. The medium sized bulldozer was easily able to supply the approximate 10 kip (44.5 kN) lateral force. Figures 21 and 22 show the bulldozer during the actual pullback testing. For safety, nylon ropes were attached to the steel cable and to the bulldozer to prevent flinging of the steel cable after release.

4.0 EXPERIMENTAL DATA, ANALYSIS, & RESULTS

4.1 INTRODUCTION

As with any dynamic testing, the ultimate goal of this research was to accurately determine the structure's natural frequencies, mode shapes, and damping ratios. Sampling at 1 millisecond for 30 seconds produced 30,000 data points for each channel, for each pullback test. This resulted in over 6 million data points from the series of eight pullback tests. Additionally, ambient vibration tests of normal traffic resulted in another 6 million data points. A data analysis program was used to process the large quantity of data gathered from the field tests. This software allowed any initial offset in the data records to be subtracted out of the record before further processing.

4.2 DATA ANALYSIS

The program DADiSP (Data Analysis and Display Software) by DSP Development Corporation, Cambridge, Massachusetts, (DADiSP 1995) was used to view and analyze the large amount of data. The program has the ability to quickly access and display the large records of 30,000 data points. Also, the program has an extensive data handling and analysis library which was needed for this research. Fast Fourier transforms of the acceleration histories were possible in a few seconds. The speed of the program made analyzing and viewing such a huge amount of data manageable.

4.3 ACCELERATION LEVELS

A typical acceleration record for transverse acceleration from the quick-release test is shown in Figure 23. Although the applied load was primarily transverse, there was enough of a vertical component (Figure 24) to allow an accurate assessment of the vertical modes of vibration also. The records shown in Figures 23 and 24 are from the midspan of span 3 at bridge deck level. This was also the location of the pullback force during this particular test.

It can be seen that peak transverse accelerations of about 7.5% of gravity were measured at the base station location. Peak vertical accelerations were approximately 4% of gravity at the base station. Lower acceleration levels were recorded at other stations and on the substructure but were easily discernible. These accelerations were the result of the application of only 10 kips (44.5 kN) of pullback force. This research demonstrates the capability of assessing the dynamic characteristics of highway bridges with a relatively small lateral load. Additional acceleration histories are shown in Appendix A.

4.4 SUBSTRUCTURE ACCELERATIONS

In addition to the accelerometers on the bridge deck, an accelerometer block was located on each end of the near end bent and each side of the near pier. These accelerometers recorded very low acceleration levels at the piers compared to the accelerometers directly above on the bridge deck. This indicates low transfer to the substructure from the superstructure acceleration. During an earthquake, the reverse happens indicating effective isolation; low transfer of acceleration from the substructure to the superstructure. End bent accelerometers also recorded very low acceleration levels from the pullback testing.

4.5 BEARING DISPLACEMENT

Additionally, relative transverse displacement between the pier cap and exterior bridge girder was measured during pullback testing using an LVDT. Figure 25 shows a typical relative displacement history across a pier bearing during a snapback test.

Figure 25 is the displacement history obtained by using a moving average 200 samples (1/5 second) wide on the displacement record. Due to this averaging, the fundamental mode is dominant in the displacement graph. A logarithmic decay of the first mode, characteristic of viscous damping, is easily seen in Figure25. Initial transverse displacement between the superstructure and substructure at the pier was approximately 0.055 inches (0.140 cm).

4.6 NATURAL FREQUENCIES

Acceleration records were transformed from the time domain to the frequency domain through the use of the Fourier transform. Equations 4.1 and 4.2 are the

mathematical definitions of the Fourier transform pair. Equation 4.1 is referred to as the Fourier transform of f(t) and the equation 4.2 as the inverse Fourier transform (Press et al. 1992, Chapra and Canale 1988).

$$F(\omega) = \int_{-\infty}^{\infty} f(t)\, e^{i\omega t}\, dt \qquad (4.1)$$

$$f(t) = \frac{1}{2\pi} \int_{-\infty}^{\infty} F(\omega)\, e^{-i\omega t}\, d\omega \qquad (4.2)$$

Where: f(t) = a function of time
$F(\omega)$ = amplitude as a function of frequency
ω = circular frequency (radians per second)

Using equations 4.1 and 4.2, a time function can be derived from a frequency function or vice versa. The problem with using equations 4.1 and 4.2 lies in the fact that a continuous function is required. For discretely sampled data, such as a dynamic bridge test, a different form of the Fourier transform is needed. A form of equation 4.1, known as the Discrete Fourier Transform (DFT), is used when points of data are known at evenly spaced intervals. Equations 4.3 and 4.4 are the Discrete forms of the Fourier transform pair.

$$f_k = \frac{1}{N} \sum_{n=0}^{N-1} F_n\, e^{-2\pi i kn/N} \qquad \text{for n = 0 to N-1} \qquad 4.3)$$

$$\text{for k = 0 to N-1} \qquad (4.3)$$

Where: N = number of sampled points
f_k = set of N sampled points

The DFT as expressed in equation 4.3 is usually the most useful in civil engineering applications where frequency components are sought from discretely sampled (digitized) data. However, the direct application of equation 4.3 requires N^2 complex mathematical operations. This becomes prohibitively time-consuming even for modest length data records. Fortunately, there is a numerical operation that reduces computing time for the DFT substantially.

The method is called the fast Fourier transform (FFT) and owes its efficiency to exploitation of the periodicity and symmetry of trigonometric functions. An FFT can be computed in approximately $N\log_2 N$ operations. For a set of 1000 data points, the FFT is approximately 100 times faster than the DFT. The first FFT is attributed to Gauss in 1805 but did not become widely known until the mid 1960's

with the advent of the Cooley-Tukey algorithm. A more complete mathematical and numerical treatment of the FFT can be found in Press et al. (1992) and Chapra and Canale (1988).

Using the Fast Fourier Transform (FFT), natural frequencies in three orthogonal directions were determined. Additional processing into a Power Spectral Density (PSD) plot, which squares the FFT amplitudes and divides out the record length, was sometimes helpful in identifying natural frequencies.

Figure 26 is a typical FFT plot of the transverse acceleration record. The fundamental frequency of 2.08 Hz is apparent from this plot. Other, less pronounced peaks show participation from many transverse modes. Lower peaks are more pronounced in the FFT's of other accelerometers, depending on the position on the bridge relative to the mode shape and the location of the pullback force. Appendix B shows FFT's for several locations along the bridge.

Two pull points on the bridge were used during the testing in an attempt to excite different modes from the different initial conditions applied to the bridge. Midspan of span 1 and midspan of span 2 were chosen based on eigenvalue analyses done prior to the field tests. Snapback testing at two points provided ample data for the determination of many transverse modes. Likewise, vertical modes were identified from pullback testing as well as from ambient traffic vibrations. Longitudinal modes were not able to be identified because of the small force component in that direction from both the pullback and ambient traffic loading. Table 1 lists the identified natural frequencies and their associated mode shapes.

4.7 TRANSVERSE MODE SHAPES

Mode shapes were determined by plotting the ratios of accelerometer FFT magnitude to base station FFT magnitude at their respective locations along the bridge. Comparing the phase angle of an FFT frequency to the base-station FFT phase angle determined the sign of the magnitude to be plotted (in-phase or out-of-phase with the base station). In this way multiple snapback tests could be incorporated into one plot of the mode shape at each of the natural frequencies.

Figures 27 to 32 are plots of the first six identified transverse modes. Plots are plan views of the entire bridge with the solid markers being positions of accelerometers on the bridge deck with their associated FFT magnitude as the ordinate (data points). The horizontal gridlines are the outline of the stationary bridge. Since only half the bridge was instrumented, the other half is plotted through extrapolation in dashed lines and open markers. The two rows of accelerometers were 40 feet (12.2 m) apart, transversely, during testing.

A fundamental transverse mode of 2.08 Hz was dominant in all FFT's of transverse acceleration. A mode is also easily visible in Figure 26 at a little over 18 Hz. Figure 30 shows the shape of this mode at 18.7 Hz This turned out to be the fourth transverse mode that was identified. It can be seen from Figures 27 to 32 that the modes with the highest participation, as determined by their Fourier magnitude, also yielded the smoothest plots of their mode shapes. Also, due to skew effects, many modes are coupled and produce transverse and vertical accelerations. In such cases, only the dominant direction of vibration is reported for the particular frequency.

4.8 VERTICAL & TORSIONAL MODE SHAPES

Vertical mode shapes were determined in a similar process as the transverse mode shapes. Having two rows of accelerometers over the two exterior girder lines enabled the detection of both vertical bending modes and torsional modes. Figures 33 and 34 show the first bending and torsional modes, respectively. The two plots show the displacement of the left and right sides of the bridge from a perspective view. The vertical lines every 20 feet (6.10 m) along the plotted lines indicate the magnitudes and direction of movement.

4.9 MODAL DAMPING

Moving averages were also used on acceleration records to filter out higher modes in order to quantify first mode equivalent viscous damping. Damping ratio estimates were obtained by the free-vibration decay method for both the LVDT displacement records and the acceleration records. Figure 35 is an example of the smoothing nature of using a moving average on Figure 23. While the magnitude of the record is greatly reduced, the underlying first mode shape becomes obvious.

Equivalent viscous damping ratios for the fundamental transverse mode was calculated using the log-decrement method for free-vibration decay (Chopra 1995, Clough and Penzien 1975). This method was applied to the smoothed records (moving average) of both the acceleration and the displacement histories. Table 2 shows the estimated modal damping ratio for the fundamental transverse frequency.

As seen from the table, the average of all accelerometers on the bridge deck, pier cap and the LVDT records at the pier bearings, the bridge has 4.0% equivalent viscous damping. Damping estimated from accelerometers on the end bent cap is significantly lower at 2.5%. Therefore, structural damping for the fundamental transverse mode in the linear elastic range can accurately be specified at 4.0% while the very stiff end bents appear to have lower damping.

5.0 ANALYTICAL MODELING & OPTIMIZATION

5.1 INTRODUCTION

Field testing a bridge provides an accurate and reliable description of its actual dynamic characteristics. A logical next step in bridge research is to create an analytical model which will correlate well to the measured dynamic properties. Many assumptions and modeling approximations must be made when creating a practical model of a bridge. For example, a finite element model requires input of the material properties which are inherently variable. This is one input where the analyst can only make a best estimate and later adjust to match the experimental results.

Refinement of the model can be done by two different methods. A structural analyst can adjust parameters heuristically, or randomly, and hope for improvement in the correlation. Or, in contrast, a systematic optimization scheme can be utilized in the form of a computer algorithm. The former can be a tedious, time consuming effort for the engineer. The latter requires minimal time for the analyst to create the proper upper and lower bounds for the variables being optimized and produces comparable or better results. Employing an optimization program provides an efficient method of refining a bridge model to improve its correlation with experimental results.

5.2 ANALYTICAL MODEL OF BRIDGE

The bridge was modeled and analyzed with the structural analysis program SAP90 and its newest version, SAP2000 (1995, 1996). In order to calibrate the bridge model to the measured frequencies and mode shapes, the entire bridge was modeled using a three dimensional model. It consisted of 720 frame elements, 352 shell elements, and 36 spring elements (Figure36). Total degrees of freedom for the model was 3048. The goal of the model was to capture the global dynamic response of the bridge. Many modeling approximations can cause local details to perform contrary to reality, but overall, the modeling is appropriate for the desired results.

5.2.1 Joints and Elements for Model

In the superstructure, shell elements were used to model the bridge deck and the concrete diaphragms at the piers and end bents. Girders are spaced 8 feet (2.44 m) apart so the deck was modeled with 8 foot (2.44 m) square shell elements between the girders, except at the ends of the bridge. There, due to the skew of the substructure, triangular shells were used. Frame elements were used to model the girders, barriers, and for rigid links to connect the girders to the slab, girders to supports, and as intermediate diaphragms. Figure 37 shows the modeling approach for the girders and slab.

Piers were modeled with frame elements at the center of each column and at the top of the pier cap while shell elements served as the webwalls (Figure 38). The piers were modeled as fixed at the top of the pile caps. This modeling assumption was considered appropriate for the very stiff substructure as described in sections 2.3 and 2.4. End bents were not modeled except as supports. Spring supports were used at the end bents which would incorporate the end bent stiffnesses indirectly as softer springs.

5.2.2 Other Modeling Considerations

After defining the nodes for the finite element model, element geometric properties were calculated. Although these properties are sometimes thought of as fixed quantities, engineering judgment is needed to estimate most properties. For example, although the moment of inertia of a girder is constant and well defined by itself, in the actual bridge it can vary continuously along the length of the bridge due to the presence of a composite haunch. In order to achieve the specified 8 inch (0.203 m) minimum slab thickness all along the girder, a haunch is used in bridge construction to account for the camber of prestressed concrete girders (Figure 38). Because the amount of camber varies along the length of the girder, the haunch must be at least the thickness of the midspan camber. For the Ballard County Bridge, the design haunch thickness was 2 inches (5.08 cm).

Another cause of increased moment of inertia of the girders is due to the slab thickening to account for the cross slope of the roadway. A cross slope of ¼ inch per foot was used on the Ballard County Bridge which creates a ¾ inch variation in slab thickness between the two sides of the 36 inch (0.914 m) wide top flange of the girders. See Figure38 for a view of this modeling consideration. Therefore, for this study, moments of inertia of the girders and slab thickness were derived from an average of the geometries. For example, the specified minimum 8 inch (0.203 m) thick slab was modeled as 8 ½ inches (0.216 m) thick. Likewise, the moments of inertia for the girders were calculated assuming a 1 inch (2.54 cm) haunch

throughout the length of the bridge. These "averaged" properties produced excellent results for the intent of the model.

Support conditions were also adjusted to yield the desired optimum model. Initially, the bridge was modeled with only spring supports for the bearing at the end bents (Figure 39). However, in the optimization process, it was noted that the translational stiffness of the end bent bearings always converged to its upper bound. These upper bounds were much higher than the measured stiffness of the bearings as reported by the manufacturer (DIS 1994).

This led to a refined model that includes translational springs for the expansion dams. Some of the joint stiffness can be explained by the stiffness of the neoprene joint seal itself. Installation specifications for expansion dams require that they be installed in "a highly compressed state" (Kentucky Transportation Cabinet 1988). Also, as Figure 7 shows, the in-situ expansion dam had a lot of gravel and debris in it which can significantly stiffen the joint in compression. Figure 39 shows the location of the expansion dam springs in the model.

One inconsistency between the model and the actual bridge is due to using one dimensional frame elements and two dimensional shell elements to model a three dimensional structure. Figure 40 shows an example of the problem with condensing dimensions of the actual structure. The node to node dimension that defines the slab span in the model is 8 feet (2.44 m). In reality, the 3-foot (0.914 m) top flange of the girders (and haunch) stiffen the slab across its width. The true unstiffened slab span for the Ballard County Bridge was only 5 feet (1.52 m) as shown in Figure 40 instead of the modeled 8 foot (2.44 m) span.

However, as mentioned earlier, the goal was to capture the overall dynamic behavior of the bridge. While the aforementioned modeling discrepancy may cause local behavior problems, their impact on the overall bridge were compensated for by adjustments of member geometric or material properties.

5.3 EIGENVALUE ANALYSIS OF BRIDGE

An eigenvalue analysis was performed with the structural analysis program SAP90 and its newest version, SAP2000 (1995, 1996), to identify the mode shapes and frequencies that corresponded to the experimentally determined ones. An eigenvalue analysis is used to determine the undamped, free vibrations of the structure. The eigensolution results in the "natural" mode shapes and frequencies of the structure. The generalized eigenvalue problem involves the solution of:

$$[\mathbf{K} - \Omega^2\mathbf{M}]\ \Phi = \mathbf{0} \qquad (5.1)$$

Where:
K = stiffness matrix
M = mass matrix
Ω^2 = the diagonal matrix of eigenvalues
Φ = matrix of corresponding eigenvectors

The eigenvalue of a mode (ω^2) is the square of the circular frequency of that mode (ω) and relates to the cyclical frequency (f) by the equation:

$$f = \frac{\omega}{2\pi} \qquad (5.2)$$

and relates to the period of vibration (T) by the equation:

$$T = \frac{2\pi}{\omega} \qquad (5.3)$$

SAP90 uses an "accelerated subspace iteration" algorithm to solve the eigenvalue problem (SAP2000 1996). The subspace iteration method was developed by Bathe in 1971 and a detailed discussion of the method and its fundamentals can be found in Bathe (1982). Various techniques have been used to "accelerate" the basic subspace iteration method and the particular algorithm used in the SAP90/SAP2000 programs can be found in Wilson and Tetsuji (1983).

5.4 CALIBRATION METHOD

Using results from the eigenvalue analysis, the bridge model was calibrated to experimentally determined mode shapes and frequencies. A perfectly calibrated model would match all experimentally determined mode shapes and frequencies exactly. To hope for such a perfect calibration is not realistic. Therefore, only the most structurally significant modes and frequencies were used in the model calibration process. Namely, the first two transverse and first two vertical modes from field testing were selected as calibration targets.

A model of the bridge was optimized (calibrated) using a simple, yet dependable constrained minimization computer program adapted for this research. The program automatically adjusted chosen structural parameters and reanalyzed the bridge using the structural analysis program SAP90 (1995) as a subprogram. Parameters were restricted by user-defined upper and lower bounds (constraints). Minimization of the error between experimental natural frequencies and analytical ones produced an optimum model for this research. Utilizing an optimization

algorithm, in combination with a structural analysis program, to match experimental frequencies provided an efficient, systematic method to obtain an optimum bridge model.

5.4.1 Optimization Algorithm

The optimization algorithm is a direct search method for single-objective, constrained minimization. This algorithm was developed by Frangopol and Klisinski (1989) at the University of Colorado at Boulder. One version of the optimization program was used by Robson with success in optimizing bridge models to match experimentally measured strains from load tests (Robson 1990, Robson, Frangopol, and Goble 1991, 1992, Robson et al. 1992, 1993). An excerpted version of the theory of the program is listed in Appendix C.

The theory that is central to this algorithm was first presented by Rosenbrock (1960). The concept of the Rosenbrock method is to allow the set of orthogonal search directions to rotate as to align one direction with the previously determined minimum direction. This method of rotating coordinates is more effective than the pattern search method which keeps the original set of orthonormal directions throughout the search process (Jacoby et al. 1972). Frangopol and Klisinski developed an extension of Rosenbrock's method for unconstrained minimization which now accommodates constraints on the variables. The resulting algorithm can, therefore, be used for constrained minimization problems such as optimizing bridge models.

The user can also decide the number of orthogonal directions to search in before updating the set of directions. Although **n** (number of optimization variables) number of orthogonal directions could be searched in before calculating a new set of **n** orthogonal directions, in practice, two directions are usually efficient for obtaining the quickest convergence.

The optimization program is terminated when a user-defined stopping criteria is met or the maximum number of iterations is reached. Because the maximum iteration number is mainly for limiting computing time for lengthy objective function evaluation, this criteria was not used in the optimization of the bridge model in this investigation.

When the program terminates, the set of optimized parameters produce a local minimum of the objective function. This is almost assuredly not the global minimum of the objective function when many parameters are optimized. To increase the chance of finding the global minimum, several sets of parameter values are used as starting points in the optimization scheme.

5.4.2 Objective Function

The optimization algorithm tries to minimize an objective function which can be defined by the analyst. For this study, the objective function was defined as the summation of the absolute differences between the experimental frequencies and the analytical frequencies for the first two transverse modes and the first two vertical modes (1 bending, 1 torsional).

In equation form the objective function used in this study is:

$$\sum_{i=1}^{4} \text{absolute}\,(f^*_i - f_i) \qquad (5.4)$$

Where: f^* = analytical frequencies

f = experimental frequencies

Using a direct search method for optimization has the advantage of not requiring derivatives of the objective function. Although the above objective function can be defined by a mathematical formula, defining a continuous, **n** variable function for this sort of objective function is impossible. Consequently, optimization methods which require gradients of the objective function are not applicable to this kind of optimization.

The choice of this objective function weights frequency differences of the four modes the same. A 1 Hz difference for mode 1 is as important as a 1 Hz difference for the second transverse mode which was the 14th analytical mode. Absolute summing inherently weights higher frequencies more heavily based on their percentage of error. For this reason, the parameters usually converge to values that yield the best model for both high and low frequencies.

5.4.3 Optimization Parameters

The model to which the optimization program converges depends on several factors. Among the more influential factors is the choice of input parameters to optimize. These choices are contingent upon what the analyst defines as important. Almost certainly, two engineers would choose different aspects which they consider significant. And just as likely, these two engineers would create two different optimized models based on their choice of objective function, and parameters to

optimize. For this study, a global optimum model was the goal: one which would match the experimental data equally well for both vertical and transverse modes

Properties to which the model is not sensitive were not included in the optimization. As was elucidated in Robson (1990), properties such as torsion constant (J) of the beam elements, Poisson's ratio (<) of the plate elements and the diaphragm properties do not significantly affect the models. Since reasonable ranges of these parameters produced negligible changes in the natural frequencies of the bridge, they were excluded from the optimization and had fixed values throughout the calibration process.

Parameters which were optimized were: modulus of elasticity (E) of the beam and shell elements, the expansion dam translational stiffness, and spring stiffnesses for the isolation bearings at the piers and end bents. Model parameters that were optimized with their initial estimates and final, optimized values are shown in Table 3. Initial parameter estimates were made based on design information. Initial estimates do not account for: (1) construction tolerances or errors that can make as-built dimensions different from design dimensions, or (2) actual strengths of materials such as the actual compressive strength of concrete, which affects its modulus of elasticity.

Translational stiffness for the bearings were estimated from the force-displacement curves from the manufacturer's tests. Rotational stiffnesses of the bearings were estimated based on the measured vertical stiffnesses of the bearings. Springs modeled individual bearings at the end bents but, represented two bearings at the piers. Initial rotational stiffnesses were estimated assuming a rigid-body rotation of the girders about the centerline of the bearing, or bearing group. Initial modulus of elasticity (E) estimates were based on design concrete strengths and the common equation for normal weight concrete relating E to concrete strength, shown in Table 3.

Expansion dam stiffness was initially assumed to be negligible and not included in the model. However, in early optimization runs, the translational stiffnesses of the bearing elements always converged to their upper bounds. Since the translational stiffness had been measured, something else was producing the stiffness that was fictitiously being included in the bearings. Expansion dams were then included in the model and found to contribute significant stiffness to the model.

As described in section 5.2, modeling inconsistencies occur whenever an analytical model of a real structure uses elements of a condensed number of dimensions. A three dimensional bridge modeled as an assemblage of one dimensional frame elements and two dimensional shell elements can not possibly account for all the nuances of a real bridge. Rather, the predominant structural behaviors are captured in a model of condensed dimensions. It is because of this

condensation of dimensions, and unmeasured actual geometries and properties, that the model is refined. In model refinement, stiffness from unmodeled components, components modeled with reduced-dimension elements, or as-built properties and dimensions different than those used in design, can be synthetically added to other components. Through optimization, unmodeled stiffness can be appropriately distributed to produce a model that behaves in a structurally accurate manner.

The bridge model was optimized for each set of spring supports separately (1 set for pier bearings, 1 set for end bent bearings). Tests showed better convergence when each support set was optimized separately instead of optimizing for all supports at once. This method is only one of a number of ways to arrive at the final model and is not professed to be the best. Figure 41 presents the strategy in flow chart form.

5.4.4 Convergence Time

The major factor that determines the time it takes to converge to an overall optimum model is the speed of the structural analysis program. The time required for the optimization algorithm is negligible compared to the time of the eigenvalue analysis. All analyses described in this report were performed on a personal computers. The computers were either 80486 or pentium based with both DOS and Windows operating systems. The optimization program was compiled with a 32 bit compiler (Microsoft FORTRAN PowerStation 1993) to take full advantage of the 32 bit microprocessors.

The number of iterations until convergence varied depending on how close property set estimates were to a local optimum. In general, the models converged to a local optimum in 15 to 20 iterations.

5.5 ANALYTICAL FREQUENCIES

Experimental frequencies used to calibrate the model and their analytical counterparts are listed in Table 4. As can be seen, the optimized frequencies matched the experimental frequencies to a high degree. Table 5 lists the experimentally determined frequencies and their analytical counterparts that were not part of the calibration and optimization process. These frequencies, as can be expected, do not match as well as the optimized ones, especially the higher frequencies. As Clough and Penzien (1975) state, "... it should be kept in mind that

the mathematical idealization of any complex structural system also tends to be less reliable in predicting the higher modes of vibration." This is usually not a problem, however, since the most structurally significant lower frequency modes match well.

5.6 ANALYTICAL MODE SHAPES

Following are views of the analytical mode shapes from the SAP90 structural analysis program. The first four (Figures 42 - 45) are the mode shapes corresponding to the optimized frequencies. They correspond to the experimentally determined Figures 27, 33, 34, and 28, respectively. The next six figures (Figures 46 - 51) correspond to experimentally identified mode shapes that were not part of the optimization process.

6.0 TIME-HISTORY ANALYSES

6.1 INTRODUCTION

The principal thrust of this research project was to gauge the effectiveness of the seismic isolation system used on the Ballard County bridge. Questions of how the bridge type would perform during Eastern U.S. earthquakes were, before this research, unanswered.

Time-history analysis is the most sophisticated analysis technique available to the structural analyst. Using this level of analysis affords the engineer a complete description of the behavior of a structure at all times throughout an earthquake. Since no strong earthquake records are available for the Eastern U.S., time-history analyses for Kentucky bridges were performed using artificial earthquake records characteristic of the New Madrid and other nearby seismic zones.

6.2 SITE-SPECIFIC ACCELERATION RECORDS

There are several important differences between ground motion associated with earthquakes in the Eastern U.S. and those in the Western U.S. Because crustal rocks in the East tend to be older, more competent, and less riddled with active faults, eastern earthquakes tend to release higher rock stresses compared to their western counterparts. This causes ground motions from eastern earthquakes to contain more high-frequency energy. Also, the ground shaking is felt more intensely over a larger distance because the earth's crust in the Eastern U.S. transmits seismic waves more efficiently (Jacob 1995).

With increasing recognition of potential damage from a large New Madrid earthquake, or other less severe quake, the Kentucky Transportation Cabinet funded the research project *Evaluation and Analysis of Innovative Concepts for Bridge Seismic Retrofit.* Research was conducted by the Kentucky Transportation Center at the University of Kentucky. Fundamental to this research project was the characterization of the seismic potential affecting Kentucky from known seismic zones as well as unknown "local" events. Results from this seismological

assessment of Kentucky were published in *Source Zones, Recurrence Rates, and Time Histories for Earthquakes Affecting Kentucky* (Street et al., 1996).

Within the report, three main tasks were covered: (1) definition and evaluation of earthquakes in seismic zones that have the potential to generate damaging ground motions in Kentucky, (2) specification of the source characteristics, accounting for the spreading and attenuation of the ground motions to top-of-bedrock at sites in Kentucky, and (3) determination of seismic zoning maps for the Commonwealth based on peak-particle accelerations, response spectra, and time-histories.

Time-histories generated in the aforementioned report were used in the current research into seismic isolation. Effects of these artificial earthquakes were calculated for bedrock elevation at the county seat of each Kentucky county. These acceleration time-histories were derived through the use of random vibration analysis and take into consideration the probability of earthquakes from nearby seismic zones, the attenuation of ground motions with distance in the Central United States, and the possibility of a random event occurring outside of the generally recognized seismic zones. Soil effects were not included in the reported time-histories (Street et al., 1996).

Time-histories representing the 50-year event and the 500-year event were generated for the vertical and two orthogonal horizontal directions in the report by Street et al. (1996). The definition of the 50-year event is: the peak horizontal particle acceleration, at the top of rock, that has a 90% probability of not being exceeded in 50 years (i.e. 10% probability of exceedance). Likewise, the 500-year event has a 90% probability of not being exceeded in 500 years. A recurrence rate (return period) can be calculated for the earthquakes which would produce the 50 and 500-year events.

The 50-year event that has a 10% probability of exceedance corresponds to AASHTO's (1995, 1996) design earthquake for highway bridges. For low probability of exceedance, the recurrence rate is approximately (National Highway Institute, 1996):

$$\text{Probability of exceedance} \cong \frac{Time}{Return\ Period} \qquad (6.1)$$

Actual return period for the 50-year event is 475 years (Mayes et al. 1992, DIS 1993). Some states require even longer return periods for their design earthquake. For example, California's Department of Transportation (Caltrans) uses a 2400-year return period, which has a 10% probability of exceedance every 250 years (DIS 1993).

For the seismic zones affecting Kentucky, the 50-year and 500-year events

defined in Street et al. (1996) correspond to the AASHTO design earthquake and near the maximum credible earthquake, respectively,. For the bridge location in this study, Ballard County, Kentucky, a time-history with peak horizontal acceleration of 30% gravity represents the AASHTO design earthquake. The time-history for the "near maximum credible earthquake" (500-year event) has a peak horizontal acceleration of 60% gravity in Ballard County. These two time-histories were used as base acceleration input to the structural analysis program SAP90 and are the bases for comparison between the seismically isolated bridge, and an identical, non-isolated bridge. Appendix E contains the input acceleration histories for the 50-year event and the 500-year event.

6.3 SOIL AMPLIFICATION

As mentioned in section 6.2, site-specific soil effects are not included in the derived time-histories. It was, therefore, necessary to add a scaling factor to multiply the time-history inputs to account for amplification due to overlying soils. AASHTO (1995, 1996) defines three site coefficients based on soil profile type. They are used to scale its response spectra in order to account for possible soil amplification of rock motion. Soil profile 1 is either rock or a stable deposit of stiff sands, gravels, or clays less than 200 feet (61.0 m) deep and has a scaling factor of 1.0 (i.e. no amplification). Soil profile 2 is a stable soil deposit of stiff sands, gravels, or clays more than 200 feet (61.0 m) deep and has a scaling factor of 1.2. Soil profile 3 includes deposits of soft to medium-stiff clays and sands, characterized by 30 feet (9.14 m) or more of soft to medium-stiff clays, with or without intervening layers of sand or other cohesionless soils. Soil profile 3 has the greatest chance of amplifying earthquake motions and has a scaling factor of 1.5.

The Ballard County bridge site, as described in sections 2.3 and 2.4, was considered most like AASHTO soil profile 2. Bridge design was completed with a site coefficient of 1.2 and, therefore, the analyses conducted for this research used a scaling factor of 1.2 to account for soil amplification. Due to limited knowledge of subsurface soil properties, modeling the complete soil profile or consideration of the very complex nature of soil-structure interaction was beyond the scope of this investigation.

Site coefficients used by AASHTO, as well as many building codes, were adopted based on research published in 1976 (Martin and Dobry 1994). Recent research has suggested expanding the site coefficients to account for nonlinear effects relating to earthquake intensity, inclusion of short period response, and other factors. Newly recommended site categories were specified in terms of

average shear wave velocity in the upper 100 feet (30.5 m) of a soil profile and/or presence of soft to medium stiff clay layers more than 10 feet (3.05 m) thick. The proposed site coefficients are particularly significant in low to moderate seismic zones such as the Eastern U.S. Dramatic increases in design forces (equivalent static) from previous codes can be anticipated where effective peak acceleration coefficient (A_a) $\leq$ 0.10 gravity if the new provisions are adopted (Martin and Dobry 1994).

6.4 ANALYSIS METHODS

The bridge was modeled and analyzed with the structural analysis program SAP90 and its newest version, SAP2000 (1995, 1996). These programs use the mode-superposition method for time-history analysis of linear or nonlinear systems. The program allows for local structural nonlinearities. Defined nonlinear elements are only active during a time-history analysis. During static or linear dynamic analyses, an effective linear stiffness is used in the analysis.

Traditionally, mode-superposition analysis was performed using a structure's eigenvectors as the basis for the analysis. Research (Wilson, Yuan, and Dickens, 1982) indicates that this is not the best starting point for a mode-superposition time-history analysis. Instead, a special set of load-dependent, orthogonal Ritz vectors yields more accurate results than the same number of natural mode shapes. Ritz vector analysis significantly reduces computing time and automatically includes the proven numerical techniques of static condensation, Guyan reduction, and static correction due to higher mode truncation (SAP2000 1996).

The reason that Ritz vector analysis yields better results than an equal number of eigenvectors is because the Ritz vectors take into account the spatial distribution of dynamic loading. In fact, the spatial distribution of loading serves as a starting load vector to begin the process of finding appropriate Ritz vectors. Subsequent Ritz vectors are formed based on the preceding Ritz vector and the neglected inertial effects.

In contrast, the eigenvectors are computed from the stiffness and mass matrices only (equation 5.1) and, therefore, can not account for the spatial distribution of loading. Eigenvectors that are orthogonal to loading do not participate in the structural response even if they are at or near the forcing frequency. A more detailed presentation of the Ritz vector analysis method used can be found in Appendix F.

Types of nonlinear elements available in SAP90/SAP2000 include: viscoelastic dampers, gap or hook elements (compression only or tension only, respectively), uniaxial plasticity, biaxial-plasticity base isolator, and friction-pendulum base isolator (SAP2000 1996). For the Ballard County bridge model, biaxial-plasticity base isolators were used to model the seismic isolation bearings and gap elements (compression only) were used to model the effects of the expansion dam and backwall at the ends of the bridge.

Bearing elements exhibit coupled plasticity for the two horizontal translational (bearing shear) degrees of freedom. Input parameters used to define the hysteretic property of the bearing elements were (for each shear direction): elastic stiffness for nonlinear force-deformation relationship (initial stiffness = unloading stiffness), yield force, ratio of post yield stiffness to elastic stiffness, and effective stiffness for linear analysis. These input properties were determined from the force-deformation curves of the actual bearing tests by the manufacturer (DIS 1994). A more detailed description of the coupled plasticity model can be found in the SAP2000 Analysis Reference (1996).

As determined in the calibration of the bridge model (section 5.4), the expansion dams at the ends of the bridge were found to exhibit significant stiffness. It was presumed that the stiffness of the expansion joint would be most influential when the joint is closing. Further, it was assumed that insignificant stiffness would result from the joint opening. Therefore, a gap (compression only) element was modeled at the bridge ends, at each beam line, and given zero initial opening. This produced the effect of a linear stiffness when the superstructure displacements close the joint and zero stiffness when movement opens the joint.

Classical modal analysis is precluded from being used with nonlinear elements since the equations cannot be decoupled into independent modal equations. Despite this apparent obstacle, the mode superposition method can still be used efficiently for some systems. Systems which can be accurately modeled for dynamic response by a structure composed of linear subsystems connected through nonlinear elements are ideal for a modified version of the mode superposition method (Chopra 1995, Ibrahimbegovic and Wilson 1988). The number of significant modes (J) is much smaller than the total degrees of freedom (N) of the system. That much smaller set of coupled equations can be solved in modal coordinates instead of the much larger set of N coupled equations in nodal coordinates. A more detailed presentation of the nonlinear time-history analysis method used can be found in Appendix F.

6.5 TIME-HISTORY RESULTS

Time-history analysis produces a very large quantity of output. Presenting all of the thousands of time step results, for the thousands of nodes and elements, would be unduly burdensome to both the author and the reader. Therefore, in order to interpret results between different bridge models or different earthquakes, a few, select response characteristics must be chosen for comparison. Maximum magnitudes from the response histories are presented for each category. Results presented in the following sections capture a succinct picture of the overall response of the two bridge models (isolated and non-isolated) for two artificial earthquakes.

6.5.1 Design Earthquake

The design earthquake is the 50-year event as described in section 6.2. For the Ballard County bridge site, peak horizontal bedrock acceleration for this artificial earthquake is 30% gravity. For comparison, AASHTO's map (1996) of peak horizontal acceleration places the Ballard County bridge site in, approximately, the 25% gravity contour for the same probability event. Earthquake duration is 10.24 seconds consisting of 2049 data points at 0.005 second intervals and is plotted in Appendix E.

Tables 6 to 8 present the maximum response attributes representative of the entire bridge. Results are presented for three elevation levels in the bridge that are, generally, of most interest to the bridge engineer.

Maximum deck-level displacements are listed in Table 6 for the two horizontal directions. Since the deck behaves mostly as a rigid body across the deck width, only displacements above the exterior girders are tabulated. These displacements would typically be used to size expansion joints for seismic movement so that the backwalls of the end bents would not be impacted by the superstructure.

Also, maximum forces in the compression only springs, which model the expansion dam, are listed in Table 6. Since one spring at each beamline is used to model a continuous expansion joint, spring forces represent the total expansion dam resistance for 11.3 feet (3.45 m) of joint [8 ft. (2.44 m) beam spacing along 45 deg skew].

Table 7 shows maximum horizontal displacement across bearings and their corresponding maximum force components. Again, exterior bearings were chosen to be listed for brevity in presenting response characteristics. Accurate interpolations can be made for maximum displacements and forces of interior bearings due to the rigid body nature of the deck and the supporting substructure.

Table 8 presents peak pier forces, some of the most important information for the bridge engineer. Maximum pier column moments, shears, and dynamic axial loads at the base of the columns are listed. Seismic isolation was devised as a means of lowering these pier-level forces as well as those transferred on down to the supporting foundation. These forces control the size and number of pier columns, as well as governing the design of the supporting foundation.

Tables 9 to 11 present the maximum response attributes of a bridge model without seismic isolation bearings. Transverse and longitudinal displacements of the superstructure are fixed to the top of piers and transverse displacement at the end bents is inhibited. Otherwise, the non-isolated bridge model is identical to the isolated bridge.

Kentucky Transportation Cabinet's standard detail for a fixed pier consists of two smooth, 1 ½ inch diameter, steel dowels cast in the pier cap at each beamline with the concrete pier diaphragms cast around the dowels. End bent supports are modeled with conventional neoprene bearing pad stiffnesses longitudinally, and very stiff transverse springs simulating the shear keys. This is the configuration that the bridge would likely have been without the addition of the seismic isolation bearings.

6.5.2 Maximum Earthquake

The earthquake considered the "maximum" earthquake for this study is the 500-year event as described in section 6.2. For the Ballard County bridge site, peak horizontal acceleration for this earthquake is 60% gravity. Earthquake duration is 20.48 seconds consisting of 4097 data points at 0.005 second intervals and is plotted in Appendix E. Tables 12 to 14 present maximum response attributes representative of the entire bridge. As for the design earthquake, results are presented for three elevation levels in the bridge. Response locations are shown in Figures 52 to 54 of section 6.5.1.

Tables 15 to 17 present the maximum response attributes of a bridge model without seismic isolation bearings subjected to the maximum earthquake. The bridge model represents the configuration that the bridge would likely have been

without the application of seismic isolation.

6.6 NONLINEAR ELEMENT RESPONSE

The seismic isolation bearings used on the Ballard County bridge are the lead-rubber type as described in chapter 2. Lead cores were used only at the end bents while the pier bearings were rubber only. Figure 55 shows a typical force-displacement history for a pier bearing during the design earthquake.Figure56 shows a typical force-displacement history for an end bent bearing during the design earthquake. The area encompassed by the bearing response is a measure of its hysteretic damping. As seen in Figures 55 and 56, the hysteretic damping is much higher in the end bent bearings due to the yielding of the lead core.

Also, the directional response is evident in the two figures. This is due to the presence of the expansion dams at the ends of the bridge. Since the substructure was skewed 45 degrees, both longitudinal and transverse movements were influenced. The expansion dam had the effect of limiting movement in one direction (closing the joint) while not affecting movement in the opposite direction (opening the joint). Bearing response was, thus, much greater in the direction away from the backwall. Figure 57 is a typical displacement history for an expansion dam element and Figure 58 depicts the compression only nature of the expansion dam element. Similar bearing response to the maximum earthquake can be seen in Figures 59 and 60. Figure 59 is a typical pier bearing response in the transverse direction to the maximum earthquake. Figure 60 is a typical end bent bearing response in the transverse direction to the maximum earthquake.

Figures 59 and 60 can be compared to the force-displacement curves from tests by the manufacturer as shown in Figures 8 and 9, respectively. Figure 59 is approximately twice as stiff as the manufacture's test plot because one bearing element was used to model two bearings at the piers. Figure 60 reproduces the manufacturer's results closely for the end bent bearing.

6.7 EFFECTIVENESS OF SEISMIC ISOLATION

Time-history results from section 6.5 provide a method of quantifying the effectiveness of seismically isolating this bridge type. In essence, the reason for seismic isolation is to reduce the forces acting on the substructure and foundation. Further, the most damaging seismic effects are from transverse accelerations so a reduction in transverse forces is the principal goal of seismic isolation.

A compromise with using seismic isolation is the increase in displacements of the superstructure. Results from the time-histories conducted for this study confirm these basic tenets of seismic isolation: a reduction in substructure forces with increased superstructure displacements. Following, in Tables 18 to 20, are comparisons of the isolated bridge's response, presented in section 6.5, as percentages of the non-isolated bridge's response.

Table 18 shows that, in general, superstructure displacements are greater for the seismically isolated bridge (SIB) than for the non-isolated bridge (NIB). Of particular interest are the transverse displacements at the piers. There, the isolation effects are most pronounced because the rubber-only bearings allow the superstructure to easily become uncoupled from the substructure. Transverse pier displacements for the SIB were 209% to 311% of NIB's displacements during the design earthquake and 250% to 414% of NIB for the maximum earthquake. The percentages for transverse displacement at the end bents are not meaningful since shear keys modeled for the non-isolated bridge prevented significant transverse movement of the superstructure.

Also, with the increased displacements, expansion dam forces for the SIB are higher than for the NIB. Table 18 shows that the SIB longitudinal compression force components increased to 124% of NIB's for the design earthquake and up to 159% of NIB's forces for the maximum earthquake. Transverse maximum forces increased up to 338% of NIB for the design earthquake and up to 912% of NIB for the maximum earthquake.

Table 19 provides a means of quantifying the effectiveness of seismic isolation by the percentage of NIB's force transferred through the bearing locations to the top of piers. Transverse force transfer at the pier bearing locations was only 6% to 8% of that transferred in the NIB for the design earthquake and 5% to 6% of NIB for the maximum earthquake. Likewise, at the piers, longitudinal SIB force transfer at bearing locations was only 11% to 15% of NIB for the design earthquake and 12% to 17% for the maximum earthquake. Again, percentages for transverse displacement at the end bents are not meaningful since shear keys modeled for the NIB inhibited transverse movement of the superstructure.

As seen in Table 20, seismic isolation reduced maximum pier column moments to 38% to 68% of NIB moments for the design earthquake and 51% to 66% of NIB for the maximum earthquake. Maximum axial dynamic column loads were reduced to 12% to 18% of NIB for exterior columns and 42% to 63% of NIB for interior columns during the design earthquake. Maximum dynamic axial column loads were reduced to 15% to 21% of NIB for exterior columns and to 49% to 72% of NIB for interior columns during the maximum earthquake. Maximum column shears were reduced to 34% to 70% of NIB for the design earthquake and to 51% to

68% of NIB for the maximum earthquake.

6.8 DESIGN IMPLICATIONS

As mentioned previously, the goal of seismic isolation is to lessen the damaging effects of earthquakes on a bridge's substructure and foundation. It is likely that the use of seismic isolation and time-history analysis could reduce the number or size of some bridge components. For example, to design the pier columns, one method would be to use the force envelope of the peak values from all columns. Since the maximum forces come from different columns, at different periods in time, the envelope of peak forces is conservative for design.

Since the two piers are identical, they would have been designed for the same forces because opposite directions for the acceleration histories could easily have reversed the critical pier. Also, although the eight individual columns have their own unique peak forces, envelope forces from all eight columns would probably have been used for the design of all columns. Thus, one column design would have been sufficient for all columns. Table 21 shows the envelopes of peak pier column force components from all eight columns.

Round columns were used on the Ballard County bridge so the two orthogonal shears and moments can be combined vectorially (square root of the sum of the squares). The resultant is then used to design columns bending about a single axis. Table 22 shows the seismic design force envelopes and the percentage of force reduction from the non-isolated bridge to the isolated bridge.

From Table 22 it is seen that seismic isolation appreciably lowers seismic design forces. The significant role of the expansion dams in resisting the seismic forces may have prevented further reduction.

Common modeling of expansion ends is to assume no longitudinal stiffness from expansion bearings or expansion dams. This research indicates that expansion ends contribute a substantial stiffness to the bridge.

Also, due to the skewed substructure, transverse translation of the superstructure always closes one expansion dam while opening the other. In contrast, a non-skewed bridge would allow transverse translation of the superstructure without expansion joint closure. It is therefore postulated that seismic isolation would be even more effective for non-skewed bridges.

7.0 CONCLUSIONS & FURTHER RESEARCH

7.1 INTRODUCTION

In this study, the primary interest was quantification of the effectiveness of seismically isolating a highly skewed, prestressed concrete, slab-on-girder bridge. In order to realize this goal, the research was composed of three distinct, yet interrelated phases. Within each phase, noteworthy accomplishments were achieved in pursuit of the overall project objective. Following, sections detail those significant accomplishments, state conclusions about the research, and list research which would complement this study.

7.2 SIGNIFICANCE OF RESEARCH

Seismic isolation is a relatively new technique, having been applied to bridges in the United States only since 1985. To date, most research has concentrated on laboratory testing of the isolation components themselves, or analytical investigation of real or theoretical systems. Very few full-scale bridge tests have been performed on in-service, seismically isolated bridges. Furthermore, research which combines full-scale experimental testing and analytical simulation is even more limited.

7.2.1 Experimental Bridge Testing

Full-scale, dynamic bridge testing has been performed several times over the past few decades. Without these full-scale experimental explorations, design codes, and the resulting designs, would be based on only scaled-down lab tests and purely theoretical research. Using test results from an actual bridge is the quintessential form of model calibration for further analytical studies. Researchers involved in full-scale experimental testing of bridges will affirm that theory, sometimes, has no practical application in the field. Results from full-scale bridge tests are invaluable and necessary to attain a better understanding of our Nation's transportation infrastructure.

Dynamic testing of the Ballard County bridge was performed using the pullback, quick-release method. Several new developments facilitated the quick-release testing. A simple, new quick-release mechanism was designed, constructed, and tested at the University of Kentucky. The mechanism uses the failure of an inexpensive shear pin to release the pullback load instantaneously. Monitoring the applied pullback load allowed accelerometer recording to be triggered just before the quick-release.

Also, for this study, the method of attaching the pullback cable to the bridge was unique. A high-strength Dywidag bar was cast in the bridge deck during construction and allowed to protrude 6 inches from the side of the bridge. On test day, a load plate was coupled to the protruding bar in seconds. This allowed the pullback force to be moved to a second pull point rapidly, without delaying the test schedule. While this attachment method is only applicable to new bridges, a modified version could easily be used on existing bridges.

Pullback, quick-release testing of the Ballard County bridge was the first of its kind ever performed. It was the first known pullback, quick-release testing of a prestressed concrete, slab-on girder bridge. Also, it was the first known pullback, quick-release test of a highly-skewed bridge. The method devised to pullback, quick-release test the Ballard County bridge was found to be simple, quick, efficient, and required little site disturbance.

7.2.2 Optimization of Bridge Model

Once the experimental testing was performed and the data analyzed, the next objective of this research was to create an accurate finite element model of the bridge. Although the initial model could be developed from design plans and calculations, refinement was needed to increase correlation with measured dynamic bridge properties.

The model was refined, or calibrated, to match experimentally determined natural frequencies and mode shapes. Past researchers have refined finite element models by random manipulation or other heuristic methods. For this study, an optimization program was written to adjust specific model variables. An automated, systematic, optimization of model parameters produced an accurate analytical representation of the bridge. This is the first known application of optimization, used in this manner, to calibrate a finite element bridge model based on dynamic test data.

7.2.3 Synergy of Experimental & Analytical Research

Most research into the effectiveness of seismic isolation has been wholly experimental or entirely analytical. This study synthesized both research domains to better enable quantification of seismic isolation effectiveness for a particular bridge. As a result of experimental testing, an accurate, reliable finite element model was assembled. Site-specific acceleration records and time-history analyses allowed assessment of the efficacy of seismic isolation, based on an appropriate type of potential earthquakes.

In short, this research used the best of the symbiotic relationship between experimental and analytical investigation by: (1) Creating a highly accurate finite element model based on the bridge's actual dynamic response (2) Using site-specific acceleration histories for the Ballard County bridge site (3) Using nonlinear time-history analysis which incorporated the nonlinear bearing properties measured by the manufacturer. Analyses by this method produce theoretically sophisticated earthquake simulations with their foundation in experimental evidence.

7.3 CONCLUSIONS

This research has demonstrated that pullback, quick-release testing can be accomplished with a simple, inexpensive, release device. It is quick and easy to use and produces high acceleration levels relative to the pullback force. Test results show that the method can accurately capture a bridge's dynamic signature. Similar pullback testing could be performed on existing bridges with little modification to the procedures used in this study.

Optimization has been proven to be a viable method of calibrating structural models to experimentally determined natural frequencies and mode shapes. The algorithm developed for this research can be applied to almost any application where an analytical model must be calibrated to experimental data.

From the calibration process of this research, expansion dams were found to contribute a significant amount of stiffness to the bridge's dynamic behavior. Common engineering practice is to model expansion ends of a bridge as having no longitudinal resistance. However, since expansion bearings and, more importantly, expansion dams can possess significant stiffness, it is recommended that they be included in any analytical model of a bridge.

Seismic isolation was found to appreciably reduce forces that the bridge substructure and foundation must resist. Seismic design forces for pier columns were reduced 48 to 86 % for the design earthquake. Likewise, seismic design forces for pier columns were reduced 43 to 81 % for the maximum earthquake. Thus, seismic isolation for highly skewed, prestressed concrete, slab-on-girder bridges was validated as an effective means of reducing earthquake forces on bridges.

Similar effectiveness is expected for other slab-on-girder bridge types and configurations. For this study, the importance of the expansion dam in resisting horizontal forces was obvious. For bridges without skewed substructures, the expansion dam may play little role in resisting transverse forces. It is, therefore, hypothesized that seismic isolation would be even more effective for bridges without skewed substructures.

7.4 RECOMMENDED FURTHER RESEARCH

Research is scholarly or scientific investigation according to lexicologists, but, for the researcher, it is more. It is prospecting in the unknown, advancing insight and invention, elucidating the ambiguous, or creating the unimaginable. Mostly, research builds upon the accomplishments of past investigators so, with this in mind, the following suggestions are made which would complement the results of this research.

7.4.1 Complementary Experimental Research

Several experimental investigations could be conducted which would complement this study. Pullback, quick-release testing of non-skewed bridges would help quantify the influence of a skewed substructure on a bridge's dynamic characteristics. Further dynamic testing could also help quantify the influence of expansion dams at the ends of bridges.

Experimentally investigating soil amplification/attenuation potential for various areas throughout Kentucky would be beneficial for earthquake analysis. An assessment of well defined soil types, their distribution throughout the State, and their potential for soil amplification or attenuation of bedrock accelerations would allow engineers to accurately account for that phenomenon.

Also, an ideal supplement to this research would be to set up a seismic monitoring station at the Ballard County bridge site. Set to trigger in the event of an earthquake, the station would measure the free field ground accelerations, and the bridge's substructure and superstructure accelerations. After an earthquake, measured ground accelerations could be used in a time-history analysis. Time-history results could then be compared to the bridge's measured response.

7.4.2 Complementary Analytical Research

Supplemental analytical investigations would enhance our understanding of the behavior of seismically isolated bridges. Time-history analyses, identical to this study's, for models without skewed substructures, both isolated and non-isolated, could be used to quantify skew effects. Additionally, more time-history analyses with this study's model, using acceleration histories representative of different areas in Kentucky, could be used for comparison of seismic isolation effectiveness depending on location within the Commonwealth.

Analytical complexity could be increased by including soil-structure interaction in the time-history investigations. This would probably have to be done in conjunction with experimental research to quantify soil properties needed for the analysis. Moreover, including soil-structure interaction in the analysis does not guarantee a more accurate evaluation of a bridge's response to unknown earthquakes.

REFERENCES

AASHTO, (1996), *Standard Specifications for Highway Bridges*, 16th Edition, American Association of State Highway and Transportation Officials, Washington D.C.

AASHTO, (1995), *Standard Specifications for Highway Bridges*, 15th Edition, American Association of State Highway and Transportation Officials, Washington D.C., 1992 with interim specifications through 1995.

AASHTO, (1983), *Standard Specifications for Seismic Design of Highway Bridges*, American Association of State Highway and Transportation Officials, Washington D.C., 1983 with interim specifications through 1991.

AASHTO, (1991), *Guide Specifications for Seismic Isolation Design,* American Association of State Highway and Transportation Officials, Washington D.C., 1991.

Agardh, L., (1994), "Impact Excitation of Concrete Highway Bridges," Proceedings of the *12th International Modal Analysis Conference*, Honolulu, Hawaii, pp. 1329-1334.

Aktan, A.E., et al., (1992), "Structural Identification of a Steel Stringer Bridge," *Transportation Research Record 1393*, Transportation Research Board, Washington D.C., pp. 175-185.

Aktan, A.E., et al., (1994a), "Destructive Testing of Two 80-Year-Old truss Bridges," Paper No. 940255 Presented at the Transportation Research Board's 73rd Annual Meeting, Washington D.C., January, 1994.

Aktan, A.E., et al., (1994b), "Multireference Modal Testing for Bridge Diagnostics," Paper Presented at Structural Materials Technology, An NDT Conference, Atlantic City, New Jersey, February, 1994.

Alampalli, S., and Fu, G., (1994), "Instrumentation for Remote and Continuous Monitoring of Structural Condition," Paper No. 940261 Presented at the Transportation Research Board's 73rd Annual Meeting, Washington D.C., January, 1994.

Astaneh-Asl, A., et al., (1994), "Seismic Performance of Steel Bridges During the 1994 Northridge Earthquake," Report No. UCB/CE-Steel-94/01 to the California Department of Transportation, University of California, Berkeley, California.

Barenberg, M.E., and Foutch, D.A., (1988), "Evaluation of Seismic Design Procedures for Highway Bridges," *Journal of Structural Engineering*, Vol. 114, No. 7, pp. 1588-1605.

Bathe, K.J., (1982), *Finite Element Procedures in Engineering Analysis*, Prentice-Hall, Inc., Englewood Cliffs, New Jersey, chapter 12.

Buckland, P.G., et al., (1979), "Suspension Bridge Vibrations: Computed and Measured," *Journal of the Structural Division*, Vol. 105, No. ST5, pp. 859-874.

Buckle, I.G., and Mayes, R.L., (1990), "Seismic Isolation: History, Application, and Performance - A World View," *Earthquake Spectra*, Vol. 6, No. 2, pp. 161-201.

Buckle, I.G., Knight, R.P., and Mayes, R.L., (1988), "An Intelligent Approach to the Design of Bearing Systems for Bridge Superstructures," Presented at The International Road and Bridge Maintenance/Rehabilitation Conference and Exposition, Atlanta, Georgia.

Chapra, S.C., and Canale, R.P., (1988), *Numerical Methods for Engineers*, 2nd Edition, McGraw-Hill, Inc., New York, New York, Chapter 13.

Chen, S.S., et al., (1993), "Quick-Release Behavior of Two Eastern U.S. Highway Bridges," Proceedings of the *10th Annual International Bridge Conference*, Pittsburgh, Pennsylvania, pp. 175-182.

Chen, S.S., et al., (1994a), "Field Testing of a Seismically Isolated Bridge," Year 1 Research Summary of Task 106-F-4.3(A), April, 1994.

Chen, S.S., et al., (1994b), "In-Situ Efficacy of Aseismic Bearing Retrofits" Paper No. IBC-94-61 Presented at the *11th Annual International Bridge Conference*, Pittsburgh, Pennsylvania, June, 1994.

Chen, S.S., et al., (1995), "Field Testing of a Seismically Isolated Bridge," Year 2 Research Summary of Task 106-F-4.3.1(A), April, 1995.

Chopra, A.K., (1995), *Dynamics of Structures: Theory and Applications to Earthquake Engineering*, Prentice-Hall, Inc., Englewood Cliffs, New Jersey.

Clough, R.W., and Penzien, J., (1975), *Dynamics of Structures*, McGraw-Hill, Inc., New York, New York.

Columbia Bulletin 103, (1992), "Inertial Products Division," Columbia Research Laboratories, Inc., Woodlyn, PA.

DADiSP 4.0 User Manual, (1995), DSP Development Corporation, Cambridge, Massachusetts.

Deger, Y., Cantieni, R., and Pietrzko, S., (1994), "Modal Analysis of an Arch Bridge: Experiment, Finite Element Analysis and Link," Proceedings of *the 12th International Modal Analysis Conference*, Honolulu, Hawaii, 1994, pp. 425-432.

DIS, (1993), "AASHTO Design Procedures for Seismically Isolated Bridges," Dynamic Isolation Systems, Inc., Berkeley, California.

DIS, (1994), "Test Results for D.I.S. Seismic Isolation Bearings for US 51 over Minor Slough Ballard County, Kentucky," D.I.S. Report No. 5875-01, Dynamic Isolation Systems, Inc., Berkeley, California.

Doll, H., (1994), "Eigenfrequencies and Normal Modes of the Norderelb Bridge Near Hamburg: Numerical and Measuring Investigations," Proceedings of *the 12th International Modal Analysis Conference*, Honolulu, Hawaii, pp. 449-455.

Douglas, B.M., (1976), "Quick Release Pullback Testing and Analytical Seismic Analysis of a Six-Span Composite Girder Bridge," Engineering Report No. 44, Dept. of Civil Engineering, University of Nevada, Reno, Nevada.

Douglas, B.M., Maragakis, E.A., and Nath, B., (1990), "Static Deformations of Bridges from Quick-Release Dynamic Experiments," *Journal of Structural Engineering*, Vol. 116, No. 8, pp. 2201-2213.

Douglas, B.M., and Reid, (1982), W.H., "Dynamic Tests and System Identification of Bridges," *Journal of the Structural Division*, Proceedings of the American Society of Civil Engineers, Vol. 108, No. ST10, October, 1982, pp. 2295-2312.

Eggers, D.W., and Stubbs, N., (1994), "Structural Assessment Using Modal Analysis Techniques," Proceedings of the *12th International Modal Analysis Conference*, Honolulu, Hawaii, pp. 1595-1601.

Farrar, C., White, K., and Mayes, R., (1995), "Vibration Testing of the I-40 Bridge Before and After the Introduction of Damage," Presented at the North-American Workshop on Instrumentation and Vibration Analysis of Highway Bridges, Cincinnati, Ohio, July, 1995.

Frangopol, D.M., and Klisinski, M., (1989), "Material Behavior and Optimum

Design of Structural Systems," *Journal of Structural Engineering*, Vol. 115, No. 5, pp. 1054-10

Green, M.F., Cebon, D., and Cole, D.J., (1995), "Effects of Vehicle Suspension Design on Dynamics of Highway Bridges," *Journal of Structural Engineering*, Vol. 121, No. 2, pp. 272-282.

Green, M.F., and Cebon, D., (1994), "Dynamic Response of Highway Bridges to Heavy Vehicle Loads: Theory and Experimental Validation," *Journal of Sound and Vibration*, No. 170 (1), pp. 51-78.

Harik, I.E., et al., (1993), "Seismic Analysis of the Brent-Spence Bridge," Research Report KTC-93-15, Kentucky Transportation Center, University of Kentucky, Lexington, Kentucky, August, 1993.

Hogue, T.D., Aktan, A.E., and Hoyos, A., (1991), "Localized Identification of Constructed Facilities," *Journal of Structural Engineering*, Vol. 117, No. 1, pp. 128-148.

Hosahalli, S., Chuntavan, C., and Aktan, A.E., (1993), "Fundamental Issues in Seismic Sagety in Midwestern U.S. Due to Hazard/Vulnerability Relation," Proceedings of the Symposium on Structural Engineering in Natural Hazards Mitigation, Irvine, California, pp. 434-439.

Hudson, D.E., (1977), "Dynamic Tests of Full-Scale Structures," Journal of the Engineering Mechanics Division, Vol. 103, No. EM6, pp. 1141-1157.

Hwang, J.S., (1996), "Evaluation of Equivalent Linear Analysis Methods of Bridge Isolation," *Journal of Structural Engineering*, Vol. 122, No. 8, pp. 972-976.

Hwang, J.S., and Sheng, L.H, (1993), "Effective Stiffness and Equivalent Damping of Base-Isolated Bridges," *Journal of Structural Engineering*, Vol. 119, No. 10, pp. 3094-3101.

Hwang, J.S., et al., (1996), "A Refined Model for Base-Isolated Bridges with Bi-Linear Hysteretic Bearings," *Earthquake Spectra*, Vol. 12, No. 2, May, 1996, pp. 245-273.

Ibrahimbegovic, A., and Wilson, E.L., (1989), "Simple Numerical Algorithms for the Mode Superposition Analysis of Linear Structural Systems with Non-Proportional Damping," *Computers & Structures*, Vol. 33, No. 2, pp. 523-531.

Jacob, K., (1995), "Geotechnical and Seismological Aspects of New York Seismic

Code Provisions," *National Center for Earthquake Engineering Research Bulletin*, Vol. 9, No. 3, July, 1995.

Jacoby, S.L.S., Kowalik, J.S., and Pixxo, J.T., (1972), *Iterative Methods for Nonlinear Optimization Problems*, Prentice-Hall, Inc., Englewood Cliffs, New Jersey, pp. 73-93.

Johnston, A.C., (1982), "A Major Earthquake Zone on the Mississippi," *Scientific American*, Vol. 246, No. 4, pp. 60-68.

Johnston, A.C., (1985), "A Brief Overview of the Geology, Seismicity and Seismic Hazard of the Central Mississippi Valley Area," Presented at A Regional Seminar on Earthquake Fundamentals for the Mississippi Valley, Memphis, Tennessee, October, 1985.

Johnston, A.C., and Nava, S.J., (1985), "Recurrence Rates and Probability Estimates for the New Madrid Seismic Zone," *Journal of Geophysical Research*, Vol. 90, No. B8, pp. 6737-6753.

Kelly, J.M., (1986), "Progress and Prospects in Seismic Isolation," Proceedings of a *Seminar and Workshop on Base Isolation and Passive Energy Dissipation*, Applied Technology Council, San Francisco, California.

Kentucky Transportation Cabinet, (1988), *Standard Specifications for Road and Bridge Construction*, Commonwealth of Kentucky, Transportation Cabinet, Department of Highways, Frankfort, Kentucky.

Khinda, J.S., Avison, R.L., and Deitch, I., (1993), "Rehabilitation and Seismic Retrofit of Bridges in New York City," Proceedings of the 10th Annual *International Bridge Conference*, Pittsburgh, Pennsylvania, pp. 246-253.

Krishnan, K., Seible, F., and Pardoen, G., (1996), "Evaluation of Bridge Strengthening Measures Using Forced Vibration Tests," Proceedings of the 14th *ASCE Structures Congress*, Chicago, Illinois, pp. 845-852.

Mander, J.B., Kim, J.H., and Chen, S.S., (1993), "Some Implications Regarding Different Bearing Types on the Seismic Performance of Bridges in the Eastern United States," Proceedings of the *10th Annual International Bridge Conference*, Pittsburgh, Pennsylvania, pp. 277-284.

Mander, J., et al., (1996), "Field and Laboratory Studies on the Seismic Performance of Bridge Bearings," *National Center for Earthquake Engineering Research Bulletin*, Vol. 10, No. 3, July, 1996,

Maragakis, E., et al., (1996), "Full-Scale Resonance Tests of a Railway Bridge," Proceedings of the 14th *ASCE Structures Congress*, Chicago, Illinois, pp. 183-190.

Martin, G.R., and Dobry, R., (1994), "Earthquake Site Response and Seismic Code Provisions," *National Center for Earthquake Engineering Research Bulletin*, Vol. 8, No. 4, October, 1994.

Mayes, R.L., et al., (1992), "AASHTO Seismic Isolation Design Requirements for Highway Bridges," *Journal of Structural Engineering*, Vol. 118, No. 1, pp. 284-304.

Mayes, R.L., (1996), "Seismic Isolation of Bridges Using Elastomeric Isolation Systems," Proceedings of the 14th *ASCE Structures Congress*, Chicago, Illinois, pp. 33-40.

Microsoft FORTRAN PowerStation, (1993), User's Guide, Microsoft Corporation, Redmond, Washington.

Naeim, F., (1995), "On Seismic Design Implications of the 1994 Northridge Earthquake Records," *Earthquake Spectra*, Vol. 11, No. 1, February, 1995, pp. 91-109.

National Highway Institute (NHI) Course No. 13063, (1996), "Seismic Bridge Design Applications," Notes from Sessions 1 & 2.

Nuttli, O.W., (1973), "Seismic-wave attenuation and magnitude relations for eastern North America," *Journal of Geophysical Research* 78, pp. 876-885.

O'Connor, T.F., and Mayes, R.L., (1992), "Controlling Lateral Load Distribution in Bridges to Achieve Overall Economy," Proceedings of the 9th Annual *International Bridge Conference*, Pittsburgh, Pennsylvania.

Papageorgiou, A.S., (1996), "Synthesis of Strong Ground Motion of the Northridge Earthquake: Comparison with Observed Damage Distribution in the San Fernando Valley," *National Center for Earthquake Engineering Research Bulletin*, Vol. 10, No. 2, April, 1996.

Paultre, P., Proulx, J., and Talbot, M., (1995), "Dynamic Testing Procedures for Highway Bridges Using Traffic Loads," *Journal of Structural Engineering*, Vol. 121, No. 2, pp. 362-376.

Penzien, J., (1993), "Seismic Design Criteria for Transportation Structures," Proceedings of the Symposium on Structural Engineering in Natural Hazards

Mitigation, Irvine, California, pp. 4-36.

Press, W.H., et al., (1992), *Numerical Recipes in FORTRAN: The Art of Scientific Computing*, 2nd Edition, Cambridge University Press, New York, New York, chapter 12.

Raghavendrachar, M., and Aktan, A.E., (1992), "Flexibility by Multireference Imact Testing for Bridge Diagnostics," *Journal of Structural Engineering*, Vol. 118, No. 8, pp. 2186-2203.

Robinson, W.H., (1982), "Lead-Rubber Hysteretic Bearings Suitable for Protecting Structures During Earthquakes," *Earthquake Engineering and Structural Dynamics*, Vol. 10, pp. 593-604.

Robinson, W.H., and Greenbank, L.R., (1976), "An Extrusion Energy Absorber Suitable for the Protection of Structures During an Earthquake," *Earthquake Engineering and Structural Dynamics*, Vol. 4, pp. 251-259.

Robson, B.N., (1990), "Predicting Structural Response in Highway Bridges," Masters Thesis, University of Colorado, Boulder, Colorado.

Robson, B.N., Frangopol, D.M., and Goble, G.G., (1991), "Optimized Models for Predicting Structural Response in Highway Bridges," Proceedings of the *Tenth Conference on Electronic Computation*, Indianapolis, Indiana, April, 1991.

Robson, B.N., Frangopol, D.M., and Goble, G.G., (1992), "Improving Correlation Between Experimental Bridge Strains and Analytical Models Through Optimization," Third International Workshop on Bridge Rehabilitation, Darmstadt, Germany, June, 1992.

Robson, B.N., and Harik, I.E., (1996), "Effectiveness of Seismic Isolation in Prestressed I-Girder Bridges," Paper #IBC-96-48 *13th Annual International Bridge Conference*, Pittsburgh, Pennsylvania, June, 1996.

Robson, B.N., et al., (1992), "Realistic Modeling of Highway Bridges," 8th U.S.-Japan Bridge Engineering Workshop, Chicago, Illinois, May, 1992.

Robson, B.N., et al., (1993), "Modeling of Field-Tested Highway Bridges," Paper No. 930165 Presented at the Transportation Research Board's 72rd Annual Meeting, Washington D.C., January, 1993.

Rosenbrock, H.H., (1960), "An Automatic Method for Finding the Greatest or Least Value of a Function," *The Computer Journal*, Vol. 3, pp. 175-184.

Rotter, T., Kohoutek, R., and Marusiak, (1994), G., "Modal Analysis of Railway Bridge in Mlada Boleslav," Proceedings of the *12th International Modal Analysis Conference*, Honolulu, Hawaii, pp. 1316-1320.

Saadeghvaziri, M.A., and Foutch, D.A., (1991), "Dynamic Behaviour of R/C Highway Bridges Under the Combined Effect of Vertical and Horizontal Earthquake Motions," *Earthquake Engineering and Structural Dynamics*, Vol. 20, pp. 535-549.

Saiidi, M., Douglas, B., and Feng, S., (1994), "Prestress Force Effect on vibration Grequency of Concrete Bridges," *Journal of Structural Engineering*, Vol. 120, No. 7, pp. 2233-2241.

Salawu, O.S., and Williams, C., (1995), "Bridge Assesment Using Forced-Vibration Testing," *Journal of Structural Engineering*, Vol. 121, No. 2, pp. 161-173.

SAP2000 6.0, (1996), User Manuals, Computers & Structures, Inc., Berkeley, California.

SAP90 6.0 Beta Release, (1995), User's Manual, Computers & Structures, Inc., Berkeley, California.

Seible, F., Nigel Priestley, M.J., and Krishnan, K., (1991), "Bridge Superstructure Rehabilitation and Strengthening," *Transportation Research Record 1290*, Transportation Research Board, Washington D.C., pp. 59-67.

Shahawy, M.A., (1995), "Non Destructive Strength Evaluation of Florida Bridges," Proceedings of SPIE Nondestructive Evaluation of Aging Infrastructure Conference, Oakland, California, June, 1995.

Shelley, S.J. et al., (1995), "Active-Control and Forced-Vibration Studies on Highway Bridge," *Journal of Structural Engineering*, Vol. 121, No. 9, pp. 1306-1312.

Shelley, S.J., et al., (1995), "Dynamic Testing (Vibration Analysis) of Highway Bridges," Notes Presented at the *North-American Workshop on Instrumentation and Vibration Analysis of Highway Bridges*, Cincinnati, Ohio, July, 1995.

Street, R., et al., (1996), "Source Zones, Recurrence Rates, and Time Histories for Earthquakes Affecting Kentucky," Research Report KTC-96-4, Kentucky Transportation Center, University of Kentucky, Lexington, Kentucky, March, 1996.

Stubbs, N., Kim, J.T., and Farrar, C.R., (1995), "Field Verification of a

Nondestructive Damage Localization and Severity Estimation Algorithm," Proceedings of the *13th International Modal Analysis Conference*, Nashville, Tennessee, pp. 210-218.

Sultan, M., and Sheng, L.H., (1995), "Application of NDE Methods to Bridge Structures - A California Perspective," Presented at the North-American Workshop on Instrumentation and Vibration Analysis of Highway Bridges, Cincinnati, Ohio, July, 1995.

Toksoy, T., and Aktan, A.E., (1994), "Bridge-Condition Assessment by Modal Flexibility," *Experimental Mechanics*, September, 1994 pp. 271-278.

Ventura, C.E., Felber, A.J., and Stiemer, S.F., (1996), "Determination of the Dynamic Characteristics of the Colquitz River Bridge by Full-Scale Testing," *Canadian Journal of Civil Engineering*, No. 23, pp. 536-548.

Ventura, C.E., Felber, A.J., and Prion, G.L., (1994), "Seismic Evaluation of a Long Span Bridge by Modal Testing," Proceedings of the *12th International Modal Analysis Conference*, Honolulu, Hawaii, pp. 1309-1315.

Wendichansky, D.A., Chen, S.S., and Mander, J.B., (1995), "In-Situ Performance of Rubber Bearing Retrofits," Presented at National Seismic Conference on Bridges and Highways, San Diego, California, December, 1995.

Williams, C., and Salawu, O.S., (1994), "Modal Identification of a Full-Scale Highway Bridge," Proceedings of the *12th International Modal Analysis Conference*, Honolulu, Hawaii, pp. 724-730.

Wilson, E.L., (1993), "An Efficient Computational Method for the Base Isolation and Energy Dissipation Analysis of Structural Systems," ATC17-1, *Proceedings of the Seminar on Seismic Isolation, Passive Energy Dissipation, and Active Control*, Applied Technology Council, Redwood City, California.

Wilson, E.L., and Tetsuji, I.J., (1983), "An Eigensolution Strategy for Large Systems," *Computers and Structures*, Vol. 16, pp. 259-265.

Wilson, E.L., Yuan, M.W., and Dickens, J.M., (1982), "Dynamic Analysis by Direct Superposition of Ritz Vectors," *Earthquake Engineering and Structural Dynamics*, Vol. 10, pp. 813-821.

TABLE 1

IDENTIFIED NATURAL FREQUENCIES

Mode	Frequency (Hz)	Direction-Shape
1	2.08	Transverse - (Symmetric)
2	3.42	Vertical - Bending
3	4.21	Vertical - Torsional
4	5.99	Vertical - Torsional
5	8.20	Transverse - (Symmetric)
6	11.2	Transverse-(Anti-Symmetric)
7	13.2	Vertical - Bending
8	18.7	Transverse - (Symmetric)
9	24.7	Transverse-(Anti-Symmetric)
10	30.2	Transverse - (Symmetric)

TABLE 2

STRUCTURAL DAMPING

Percent of Critical Damping for First Transverse Mode	
LVDT Displacements @ Pier Bearings	3.9%
Accelerometers on Bridge Deck	4.0%
Accelerometers on Pier Cap	4.0%
Accelerometers on End Bent Cap	2.5%

TABLE 3

OPTIMIZATION PARAMETERS

Model Parameter	Initial Estimate	Comments	Optimized Value
Abutment Bearing Stiffness - Horizontal (x & y) Translation	40 kips/inch (70 kN/cm)	Initial estimate from bearing manufacturer's test	85 (149)
Abutment Bearing Stiffness - Strong Axis Beam Rotation	10,000 inch*kip/radian (1130 kN*m/rad)	model not sensitive to this parameter in reasonable range	6300 (711)
Abutment Bearing Stiffness - Weak Axis Beam Rotation	100,000 inch*kip/radian (11,300 kN*m/rad)	Includes some of Unmodeled diaphragm stiffness	88,600,000 (10,000,000)
Pier Bearing Stiffness - Horizontal (x & y) Translation	25 kips/inch (43.8 kN/cm)	Initial estimate from bearing manufacturer's test	35 (61.3)
Pier Bearing Stiffness - Strong Axis Beam Rotation	1,000,000 inch*kip/radian (113,000 kN*m/rad)	model not sensitive to this parameter in reasonable range	1,000,000 (113,000)
Pier Bearing Stiffness - Weak Axis Beam Rotation	100,000 inch*kip/radian (11,300 kN*m/rad)	Includes some of Unmodeled diaphragm stiffness	446,000,000 (50,400,000)
Expansion Dam Stiffness - Horizontal (x & y) Translation	0 kips/inch (0 kN/cm)	1 spring per beam line; Not modeled initially	600 (1051)
Modulus of Elasticity - Beam Concrete	4600 kips/inch^2 (31,700 MPa)	Initial estimate $E = 57\sqrt{f_c'}$ (ksi)	4548 (31,400)
Modulus of Elasticity - Slab Concrete	3600 kips/inch^2 (24,800 MPa)	Initial estimate $E = 57\sqrt{f_c'}$ (ksi)	3545 (24,400)

TABLE 4

OPTIMIZED FREQUENCIES (HZ)

Mode Shape	Initial Analytical Model	Experimental	Optimized Analytical Model
1st Transverse (Symmetric)	1.10	2.08	2.08
1st Vertical (Bending)	2.96	3.42	3.43
2nd Vertical (1st Torsional)	3.94	4.21	4.22
2nd Transverse (Symmetric)	3.94	8.20	8.22

TABLE 5

NON-OPTIMIZED FREQUENCIES (HZ)

Mode Shape	Experimental	Analytical
3rd Vertical (Torsional)	5.99	5.98
3rd Transverse (Anti-Symmetric)	11.2	10.9
4th Vertical (Bending)	13.2	11.3
4th Transverse (Symmetric)	18.7	16.5
5th Transverse (Anti-Symmetric)	24.7	21.6
6th Transverse (Symmetric)	30.2	26.2

TABLE 6

MAXIMUM DECK-LEVEL RESPONSE
FOR ISOLATED BRIDGE - DESIGN EARTHQUAKE

		Maximum Horizontal Displacement		Maximum Expansion Dam Compression Force	
Location	Node #	Longitudinal (X)	Transverse (Y)	Longitudinal (X)	Transverse (Y)
End Bent 1	106	0.472 in (1.20 cm)	0.559 in (1.42 cm)	216 kips (961 kN)	144 kips (641 kN)
End Bent 1	601	0.406 in (1.03 cm)	0.518 in (1.32 cm)	188 kips (836 kN)	52.0 kips (231 kN)
Pier 1	121	0.461 in (1.17 cm)	0.875 in (2.22 cm)	----[a]	----[a]
Pier 1	616	0.428 in (1.09 cm)	0.721 in (1.83 cm)	----[a]	----[a]
Pier 2	136	0.420 in (1.07 cm)	1.03 in (2.62 cm)	----[a]	----[a]
Pier 2	631	0.465 in (1.18 cm)	1.02 in (2.59 cm)	----[a]	----[a]
End Bent 2	151	0.384 in (0.975 cm)	1.05 in (2.67 cm)	224 kips (996 kN)	53.8 kips (239 kN)
End Bent 2	646	0.467 in (1.19 cm)	1.08 in (2.74 cm)	274 kips (1219 kN)	92.0 kips (409 kN)

[a] There are no expansion dams at Piers 1 and 2.

TABLE 7

MAXIMUM BEARING-LEVEL RESPONSE
FOR ISOLATED BRIDGE - DESIGN EARTHQUAKE

		Maximum Horizontal Bearing Displacement		Maximum Bearing Shear Force	
Location	**Element**	**Longitudinal (X)**	**Transverse (Y)**	**Longitudinal (X)**	**Transverse (Y)**
End Bent 1	6101	0.469 in (1.19 cm)	0.556 in (1.41 cm)	25.6 kips (114 kN)	23.8 kips (106 kN)
End Bent 1	6106	0.407 in (1.03 cm)	0.520 in (1.32 cm)	24.4 kips (109 kN)	22.1 kips (98.3 kN)
Pier 1	6001	0.388 in (0.986 cm)	0.816 in (2.07 cm)	12.2 kips (54.3 kN)	18.4 kips (81.8 kN)
Pier 1	6006	0.431 in (1.10 cm)	0.667 in (1.69 cm)	11.7 kips (52.0 kN)	15.3 kips (68.1 kN)
Pier 2	7001	0.392 in (0.996 cm)	1.00 in (2.54 cm)	12.4 kips (55.2 kN)	21.3 kips (94.7 kN)
Pier 2	7006	0.415 in (1.05 cm)	0.948 in (2.41 cm)	12.6 kips (56.0 kN)	20.2 kips (89.9 kN)
End Bent 2	7101	0.395 in (1.00 cm)	1.05 in (2.67 cm)	24.3 kips (108 kN)	31.3 kips (139 kN)
End Bent 2	7106	0.479 in (1.22 cm)	1.08 in (2.74 cm)	24.2 kips (108 kN)	32.5 kips (145 kN)

TABLE 8

MAXIMUM PIER-LEVEL RESPONSE
FOR ISOLATED BRIDGE - DESIGN EARTHQUAKE

		Maximum Dynamic Axial Load		Maximum Shear Force		Maximum Bending Moments	
Location	Element	Comp.	Tension	V_x	V_y	M_{xx}	M_{yy}
Pier 1	4015	45.4 k (202 kN)	56.7 k (252 kN)	17.3 k (77.0 kN)	17.3 k (77.0 kN)	3060 in-k (346 kN-m)	3110 in-k (351 kN-m)
Pier 1	4016	26.9 k (120 kN)	34.2 k (152 kN)	20.6 k (91.6 kN)	22.3 k (99.2 kN)	3487 in-k (394 kN-m)	3387 in-k (383kN-m)
Pier 1	4017	25.6 k (114 kN)	42.5 k (189 kN)	20.7 k (92.1 kN)	21.1 k (93.9 kN)	3334 in-k (377 kN-m)	3331 in-k (376 kN-m)
Pier 1	4018	53.1 k (236 kN)	70.0 k (311 kN)	21.6 k (96.1 kN)	21.0 k (93.4 kN)	3304 in-k (373 kN-m)	3332 in-k (376 kN-m)
Pier 2	5015	51.7 k (230 kN)	46.5 k (207 kN)	22.9 k (102 kN)	23.1 k (103 kN)	3843 in-k (434 kN-m)	3788 in-k (428 kN-m)
Pier 2	5016	25.7 k (114 kN)	31.2 k (139 kN)	26.2 k (117 kN)	26.2 k (117 kN)	4226 in-k (kN-m)	4151 in-k (469 kN-m)
Pier 2	5017	24.9 k (111 kN)	34.1 k (152 kN)	24.1 k (107 kN)	24.5 k (109 kN)	3850 in-k (435 kN-m)	3854 in-k (435 kN-m)
Pier 2	5018	48.4 k (215 kN)	62.2 k (277 kN)	21.9 k (97.4 kN)	21.3 k (94.7 kN)	3579 in-k (404 kN-m)	3643 in-k (412 kN-m)

TABLE 9

MAXIMUM DECK-LEVEL RESPONSE FOR NON-ISOLATED BRIDGE - DESIGN EARTHQUAKE

		Maximum Horizontal Displacement		Maximum Expansion Dam Compression Force	
Location	**Node #**	**Longitudinal (X)**	**Transverse (Y)**	**Longitudinal (X)**	**Transverse (Y)**
End Bent 1	106	0.459 in (1.17 cm)	0.082 in (0.208 cm)	214 k (952 kN)	43.5 k (194 kN)
End Bent 1	601	0.347 in (0.881 cm)	0.036 in (0.091 cm)	153 k (681 kN)	15.4 k (68.5 kN)
Pier 1	121	0.430 in (1.09cm)	0.418 in (1.06 cm)	----[a]	----[a]
Pier 1	616	0.366 in (0.930 cm)	0.347 in (0.881 cm)	----[a]	----[a]
Pier 2	136	0.345 in (0.876 cm)	0.331 in (0.841 cm)	----[a]	----[a]
Pier 2	631	0.418 in (1.06 cm)	0.402 in (1.02 cm)	----[a]	----[a]
End Bent 2	151	0.309 in (0.785 cm)	0.037 in (0.094 cm)	180 k (801 kN)	15.9 k (70.7 kN)
End Bent 2	646	0.417 in (1.06 cm)	0.093 in (0.236 cm)	244 k (1085 kN)	37.6 k (167 kN)

[a] There are no expansion dams at Piers 1 and 2.

TABLE 10

MAXIMUM BEARING-LEVEL RESPONSE FOR NON-ISOLATED BRIDGE - DESIGN EARTHQUAKE

		Maximum Horizontal Bearing Displacement		Maximum Bearing Shear Force	
Location	Element	Longitudinal (X)	Transverse (Y)	Longitudinal (X)	Transverse (Y)
End Bent 1	6101	0.481 in (1.22 cm)	0.080 in (0.203 cm)	28.8 k (128 kN)	240 k (1068 kN)
End Bent 1	6106	0.347 in (0.881 cm)	0.035 in (0.089 cm)	20.8 k (92.5 kN)	105 k (467 kN)
Pier 1	6001	0	0	205 k (911 kN)	170 k (756 kN)
Pier 1	6006	0	0	165 k (734 kN)	140 k (623 kN)
Pier 2	7001	0	0	145 k (645 kN)	142 k (632 kN)
Pier 2	7006	0	0	209 k (930 kN)	171 k (761 kN)
End Bent 2	7101	0.324 in (0.823 cm)	0.036 in (0.091 cm)	19.4 k (86.3 kN)	107 k (476 kN)
End Bent 2	7106	0.454 in (1.15 cm)	0.089 in (0.226 cm)	27.2 k (121 kN)	268 k (1192 kN)

TABLE 11

MAXIMUM PIER-LEVEL RESPONSE
FOR NON-ISOLATED BRIDGE - DESIGN EARTHQUAKE

		Maximum Dynamic Axial Load		Maximum Shear Force		Maximum Bending Moments	
Location	Element	Comp.	Tension	V_x	V_y	M_{xx}	M_{yy}
Pier 1	4015	380 k (1690 kN)	355 k (1579 kN)	50.9 k (226 kN)	44.9 k (200 kN)	7637 in-k (863 kN-m)	8270 in-k (934 kN-m)
Pier 1	4016	63.7 k (283 kN)	55.3 k (246 kN)	53.9 k (240 kN)	48.9 k (218 kN)	7809 in-k (882 kN-m)	8401 in-k (949 kN-m)
Pier 1	4017	48.8 k (217 kN)	68.2 k (303 kN)	50.2 k (223 kN)	45.7 k (203 kN)	7312 in-k (826 kN-m)	7822 in-k (884 kN-m)
Pier 1	4018	347 k (1544 kN)	382 k (1699 kN)	42.2 k (188 kN)	37.0 k (165 kN)	6321 in-k (714 kN-m)	6859 in-k (775 kN-m)
Pier 2	5015	386 k (1717 kN)	347 k (1544 kN)	37.6 k (167 kN)	33.1 k (147 kN)	5630 in-k (636 kN-m)	6181 in-k (698 kN-m)
Pier 2	5016	51.2 k (228 kN)	49.8 k (222 kN)	43.8 k (195 kN)	38.9 k (173 kN)	6304 in-k (712 kN-m)	6807 in-k (769 kN-m)
Pier 2	5017	50.2 k (223 kN)	80.9 k (360 kN)	46.3 k (206 kN)	43.3 k (193 kN)	6935 in-k (784 kN-m)	7341 in-k (829 kN-m)
Pier 2	5018	337 k (1499 kN)	401 k (1784 kN)	45.4 k (202 kN)	42.1 k (187 kN)	7043 in-k (796 kN-m)	7646 in-k (864 kN-m)

TABLE 12

MAXIMUM DECK-LEVEL RESPONSE
FOR ISOLATED BRIDGE - MAXIMUM EARTHQUAKE

		Maximum Horizontal Displacement		Maximum Expansion Dam Compression Force	
Location	**Node #**	**Longitudinal (X)**	**Transverse (Y)**	**Longitudinal (X)**	**Transverse (Y)**
End Bent 1	106	0.725 in (1.84 cm)	3.51 in (8.92 cm)	429 k (1908 kN)	451 k (2006 kN)
End Bent 1	601	0.805 in (2.05 cm)	3.48 in (8.84 cm)	392 k (1744 kN)	290 k (1290 kN)
Pier 1	121	0.725 in (1.84 cm)	3.05 in (7.75 cm)	----[a]	----[a]
Pier 1	616	0.824 in (2.09 cm)	3.16 in (8.03 cm)	----[a]	----[a]
Pier 2	136	0.772 in (1.96 cm)	2.54 in (6.45 cm)	----[a]	----[a]
Pier 2	631	0.755 in (1.92 cm)	2.46 in (6.25 cm)	----[a]	----[a]
End Bent 2	151	0.822 in (2.09 cm)	3.06 in (7.77 cm)	487 k (2166 kN)	178 k (792 kN)
End Bent 2	646	0.690 in (1.75 cm)	3.08 in (7.82 cm)	408 k (1815 kN)	412 k (1833 kN)

[a] There are no expansion dams at Piers 1 and 2.

TABLE 13

MAXIMUM BEARING-LEVEL RESPONSE
FOR ISOLATED BRIDGE - MAXIMUM EARTHQUAKE

		Maximum Horizontal Bearing Displacement		Maximum Bearing Shear Force	
Location	**Element**	**Longitudinal (X)**	**Transverse (Y)**	**Longitudinal (X)**	**Transverse (Y)**
End Bent 1	6101	0.725 in (1.84 cm)	3.49 in (8.87 cm)	27.9 k (124 kN)	57.3 k (255 kN)
End Bent 1	6106	0.819 in (2.08 cm)	3.49 in (8.87 cm)	28.0 k (125 kN)	56.2 k (250 kN)
Pier 1	6001	0.693 in (1.76 cm)	2.79 in (7.09 cm)	16.3 k (72.5 kN)	44.9 k (198 kN)
Pier 1	6006	0.825 in (2.10 cm)	2.91 in (7.39 cm)	18.6 k (82.7 kN)	46.2 k (205 kN)
Pier 2	7001	0.828 in (2.10 cm)	2.26 in (5.74 cm)	16.9 k (75.2 kN)	37.6 k (167 kN)
Pier 2	7006	0.823 in (20.9 cm)	2.31 in (5.87 cm)	19.0 k (84.5 kN)	37.1 k (165 kN)
End Bent 2	7101	0.834 in (2.12 cm)	3.07 in (7.80 cm)	30.0 k (133 kN)	53.0 k (236 kN)
End Bent 2	7106	0.707 in (1.80 cm)	3.06 in (7.77 cm)	28.3 k (126 kN)	53.1 k (236 kN)

TABLE 14

MAXIMUM PIER-LEVEL RESPONSE
FOR ISOLATED BRIDGE - MAXIMUM EARTHQUAKE

		Maximum Dynamic Axial Load		Maximum Shear Force		Maximum Bending Moments	
Location	**Element**	**Comp.**	**Tension**	**V_x**	**V_y**	**M_{xx}**	**M_{yy}**
Pier 1	4015	123 k (547 kN)	125 k (556 kN)	47.9 k (213 kN)	45.7 k (203 kN)	7761 in-k (877 kN-m)	7777 in-k (879 kN-m)
Pier 1	4016	71.2 k (317 kN)	75.8 k (337 kN)	59.7 k (266 kN)	61.6 k (274 kN)	9154 in-k (1034 kN-m)	9023 in-k (1019 kN-m)
Pier 1	4017	65.6 k (292 kN)	80.0 k (356 kN)	61.4 k (273 kN)	62.7 k (279 kN)	9220 in-k (1042 kN-m)	9099 in-k (1028 kN-m)
Pier 1	4018	116 k (516 kN)	105 k (467 kN)	46.3 k (206 kN)	46.2 k (206 kN)	7404 in-k (837 kN-m)	7323 in-k (827 kN-m)
Pier 2	5015	146 k (649 kN)	123 k (547 kN)	42.1 k (187 kN)	39.5 k (176 kN)	6908 in-k (781 kN-m)	6963 in-k (787 kN-m)
Pier 2	5016	67.2 k (299 kN)	80.4 k (358 kN)	55.9 k (249 kN)	57.4 k (255 kN)	8855 in-k (1000 kN-m)	8774 in-k (991 kN-m)
Pier 2	5017	65.4 k (291 kN)	78.8 k (351 kN)	58.3 k (259 kN)	59.0 k (262 kN)	9349 in-k (1056 kN-m)	9290 in-k (1050 kN-m)
Pier 2	5018	120 k (534 kN)	145 k (645 kN)	51.2 k (228 kN)	51.0 k (227 kN)	8570 in-k (968 kN-m)	8538 in-k (965 kN-m)

TABLE 15

MAXIMUM DECK-LEVEL RESPONSE FOR NON-ISOLATED BRIDGE - MAXIMUM EARTHQUAKE

		Maximum Horizontal Displacement		Maximum Expansion Dam Comp. Force	
Location	**Node #**	**Longitudinal (X)**	**Transverse (Y)**	**Longitudinal (X)**	**Transverse (Y)**
End Bent 1	106	0.862 in (2.19 cm)	0.194 in (0.493 cm)	511 k (2273 kN)	111 k (494 kN)
End Bent 1	601	0.598 in (1.52 cm)	0.069 in (0.175 cm)	353 k (1570 kN)	31.8 k (141 kN)
Pier 1	121	0.858 in (2.18 cm)	0.945 in (2.40 cm)	----[a]	----[a]
Pier 1	616	0.680 in (1.73 cm)	0.763 in (1.94 cm)	----[a]	----[a]
Pier 2	136	0.717 in (1.82 cm)	0.814 in (2.07 cm)	----[a]	----[a]
Pier 2	631	0.872 in (2.22 cm)	0.985 in (2.50 cm)	----[a]	----[a]
End Bent 2	151	0.660 in (1.68 cm)	0.074 in (0.188 cm)	307 k (1366 kN)	38.4 k (171 kN)
End Bent 2	646	0.929 in (2.36 cm)	0.197 in (0.500 cm)	423 k (1882 kN)	85.2 k (379 kN)

[a] There are no expansion dams at Piers 1 and 2.

TABLE 16

MAXIMUM BEARING-LEVEL RESPONSE FOR NON-ISOLATED BRIDGE - MAXIMUM EARTHQUAKE

		Maximum Horizontal Bearing Displacement		Maximum Bearing Shear Force	
Location	**Element**	**Longitudinal (X)**	**Transverse (Y)**	**Longitudinal (X)**	**Transverse (Y)**
End Bent 1	6101	0.874 in (2.22 cm)	0.188 in (0.478 cm)	52.5 k (234 kN)	565 k (2513 kN)
End Bent 1	6106	0.613 in (1.56 cm)	0.066 in (0.168 cm)	36.8 k (164 kN)	199 k (885 kN)
Pier 1	6001	0	0	352 k (1566 kN)	292 k (1299 kN)
Pier 1	6006	0	0	337 k (1499 kN)	275 k (1223 kN)
Pier 2	7001	0	0	281 k (1250 kN)	244 k (1085 kN)
Pier 2	7006	0	0	411 k (1828 kN)	315 k (1401 kN)
End Bent 2	7101	0.689 in (1.75 cm)	0.072 in (0.183 cm)	41.3 k (184 kN)	216 k (961 kN)
End Bent 2	7106	0.947 in (2.41 cm)	0.191 in (0.485 cm)	56.8 k (253 kN)	574 k (2553 kN)

TABLE 17

MAXIMUM PIER-LEVEL RESPONSE FOR NON-ISOLATED BRIDGE - MAXIMUM EARTHQUAKE

		Maximum Dynamic Axial Load		Maximum Shear Force		Maximum Bending Moments	
Loc.	**Elmt**	**Comp.**	**Tension**	**V_x**	**V_y**	**M_{xx}**	**M_{yy}**
Pier 1	4015	698 k (3105 kN)	662 k (2945 kN)	85.0 k (378 kN)	84.9 k (378 kN)	14129 in-k (1596 kN-m)	14267 in-k (1612 kN-m)
Pier 1	4016	136 k (605 kN)	129 k (574 kN)	94.9 k (422 kN)	95.7 k (426 kN)	14684 in-k (1659 kN-m)	14553 in-k (1644 kN-m)
Pier 1	4017	133 k (592 kN)	111 k (494 kN)	91.0 k (405 kN)	94.2 k (419 kN)	14232 in-k (1608 kN-m)	13894 in-k (1570 kN-m)
Pier 1	4018	633 k (2816 kN)	682 k (3034 kN)	70.2 k (312 kN)	74.1 k (330 kN)	12064 in-k (1363 kN-m)	11429 in-k (1291 kN-m)
Pier 2	5015	713 k (3171 kN)	633 k (2816 kN)	80.9 k (360 kN)	76.7 k (341 kN)	13409 in-k (1515 kN-m)	13111 in-k (1481 kN-m)
Pier 2	5016	130 k (578 kN)	137 k (609 kN)	88.2 k (392 kN)	94.3 k (419 kN)	15310 in-k (1730 kN-m)	14400 in-k (1627 kN-m)
Pier 2	5017	131 k (583 kN)	128 k (569 kN)	95.0 k (423 kN)	102 k (454 kN)	16417 in-k (1855 kN-m)	15406 in-k (1741 kN-m)
Pier 2	5018	579 k (2575 kN)	764 k (3398 kN)	97.1 k (432 kN)	99.7 k (444 kN)	16795 in-k (1898 kN-m)	15935 in-k (1800 kN-m)

TABLE 18

ISOLATED BRIDGE DECK-LEVEL RESPONSE
AS A PERCENTAGE OF NON-ISOLATED BRIDGE RESPONSE

Earthquake	Location	Node	% of Maximum Horizontal Displacement		% of Maximum Expansion Dam Force	
			Longitudinal (X)	Transverse (Y)	Longitudinal (X)	Transverse (Y)
Design	EB 1	106	103	682	101	331
	EB 1	601	117	1455	123	338
	Pier 1	121	107	209	----[a]	----[a]
	Pier 1	616	117	208	----[a]	----[a]
	Pier 2	136	122	311	----[a]	----[a]
	Pier 2	631	111	254	----[a]	----[a]
	EB 2	151	124	2876	124	338
	EB 2	646	112	1165	112	245
Maximum	EB 1	106	84	1800	84	406
	EB 1	601	135	5073	111	912
	Pier 1	121	84	323	----[a]	----[a]
	Pier 1	616	121	414	----[a]	----[a]
	Pier 2	136	108	312	----[a]	----[a]
	Pier 2	631	87	250	----[a]	----[a]
	EB 2	151	125	4141	159	464
	EB 2	646	74	1564	97	484

[a] There are no expansion dams at Piers 1 and 2.

TABLE 19

ISOLATED BRIDGE BEARING-LEVEL RESPONSE
AS A PERCENTAGE OF NON-ISOLATED BRIDGE RESPONSE

Earthquake	Location	Element	% of Maximum Horizontal Bearing Displacement		% of Maximum Bearing Force	
			Longitudinal (X)	Transverse (Y)	Longitudinal (X)	Transverse (Y)
Design	EB 1	6101	98	694	89	10
	EB 1	6106	117	1490	117	21
	Pier 1	6001	----[a]	----[a]	6	11
	Pier 1	6006	----[a]	----[a]	7	11
	Pier 2	7001	----[a]	----[a]	8	15
	Pier 2	7006	----[a]	----[a]	6	12
	EB 2	7101	122	2941	125	29
	EB 2	7106	106	1211	89	12
Maximum	EB 1	6101	83	1856	53	10
	EB 1	6106	134	5272	76	28
	Pier 1	6001	----[a]	----[a]	5	15
	Pier 1	6006	----[a]	----[a]	6	17
	Pier 2	7001	----[a]	----[a]	6	15
	Pier 2	7006	----[a]	----[a]	5	12
	EB 2	7101	121	4270	73	25
	EB 2	7106	75	1600	50	9

[a] Translation is fixed at pier bearing locations for non-isolated bridge.

TABLE 20

ISOLATED BRIDGE PIER-LEVEL RESPONSE AS A PERCENTAGE OF NON-ISOLATED BRIDGE RESPONSE

Earthquake	Loc.	Element	% Maximum Dynamic Axial Load		%Maximum Shear Force		% Maximum Bending Moments	
			Comp	Tension	Vx	Vy	Mxx	Myy
Design	Pier 1	4015	12	16	34	39	40	38
	Pier 1	4016	42	62	38	46	45	40
	Pier 1	4017	52	62	41	46	46	43
	Pier 1	4018	15	18	51	57	52	49
	Pier 2	5015	13	13	61	70	68	61
	Pier 2	5016	50	63	60	67	67	61
	Pier 2	5017	50	42	52	57	55	52
	Pier 2	5018	14	16	48	51	51	48
Maximum	Pier 1	4015	18	19	56	54	55	55
	Pier 1	4016	52	59	63	64	62	62
	Pier 1	4017	49	72	68	67	65	66
	Pier 1	4018	18	15	66	62	61	64
	Pier 2	5015	21	19	52	52	52	53
	Pier 2	5016	52	59	63	61	58	61
	Pier 2	5017	50	62	61	58	57	60
	Pier 2	5018	21	19	53	51	51	54

TABLE 21

ENVELOPE OF PIER COLUMN PEAK FORCES

Earthquake	Force Component	Seismically Isolated Bridge	Non-Isolated Bridge
Design	Dynamic Axial Compression	53.1 k (236 kN)	386 k (1717 kN)
	Dynamic Axial Tension	70.0 k (311 kN)	401 k (1784 kN)
	Shear V_x	26.2 k (117 kN)	53.9 k (240 kN)
	Shear V_y	26.2 k (117 kN)	48.9 k (218 kN)
	Moment M_{xx}	4226 in-k (478 kN-m)	7809 in-k (882 kN-m)
	Moment M_{yy}	4151 in-k (469 kN-m)	8401 in-k (949 kN-m)
Maximum	Dynamic Axial Compression	146 k (649 kN)	713 k (3171 kN)
	Dynamic Axial Tension	145 k (645 kN)	764 k (3398 kN)
	Shear V_x	61.4 k (273 kN)	97.1 k (432 kN)
	Shear V_y	62.7 k (279 kN)	99.7 k (444 kN)
	Moment M_{xx}	9349 in-k (1056 kN-m)	16795 in-k (1898 kN-m)
	Moment M_{yy}	9290 in-k (1050 kN-m)	15935 in-k (1800 kN-m)

TABLE 22

SEISMIC DESIGN FORCE ENVELOPES

Earthquake	Force Component	Seismically Isolated Bridge	Non-Isolated Bridge	Force Reduction
Design	Dynamic Axial Compression	53.1 k (236 kN)	386 k (1717 kN)	86.2 %
	Dynamic Axial Tension	70.0 k (311 kN)	401 k (1784 kN)	82.5 %
	Design Shear	37.0 k (165 kN)	72.8 k (324 kN)	49.2 %
	Design Moment	5924 in-k (669 kN-m)	11470 in-k (1296 kN-m)	48.4 %
Maximum	Dynamic Axial Compression	146 k (649 kN)	713 k (3171 kN)	79.5 %
	Dynamic Axial Tension	145 k (645 kN)	764 k (3398 kN)	81.0 %
	Design Shear	87.8 k (391 kN)	139 k (618 kN)	36.8 %
	Design Moment	13180 in-k (1489 kN-m)	23152 in-k (2616 kN-m)	43.1 %

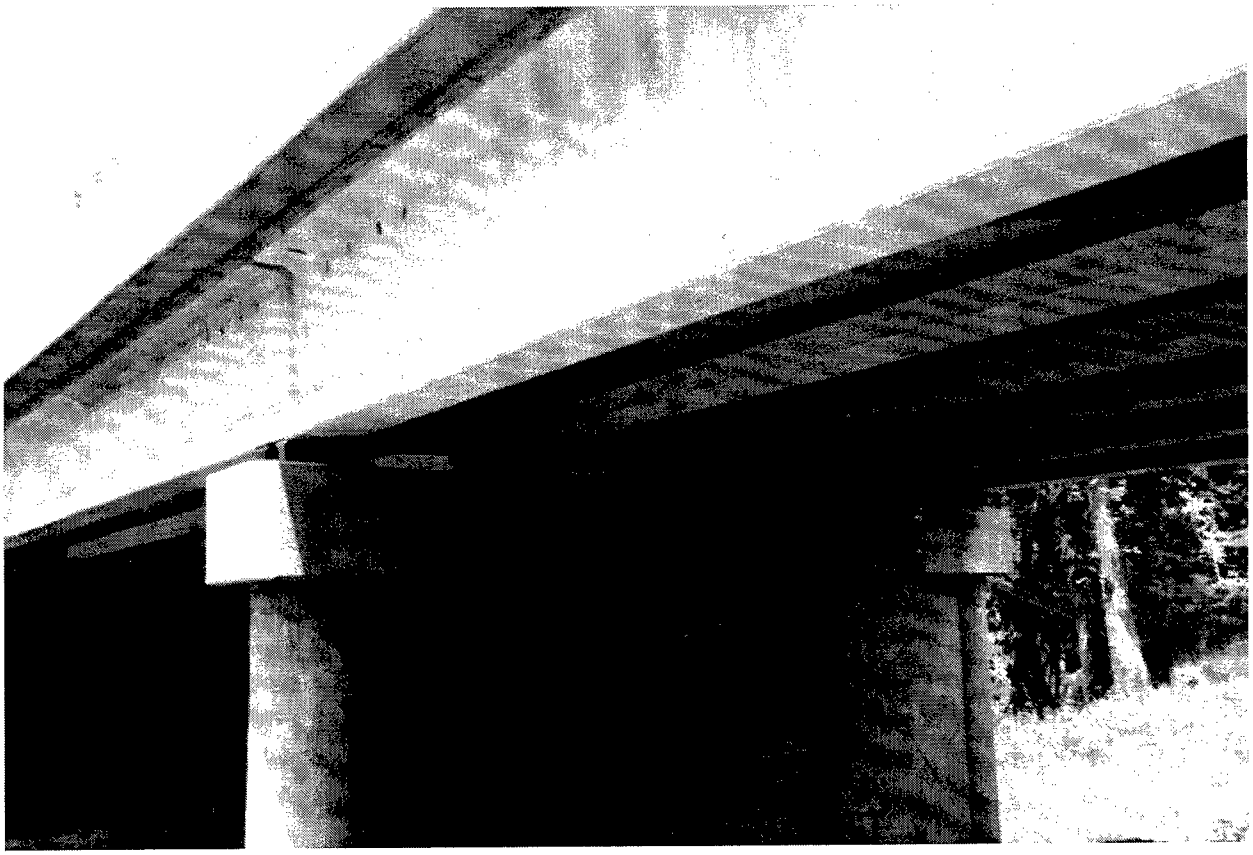

Figure 4: Isolation Bearings at Piers

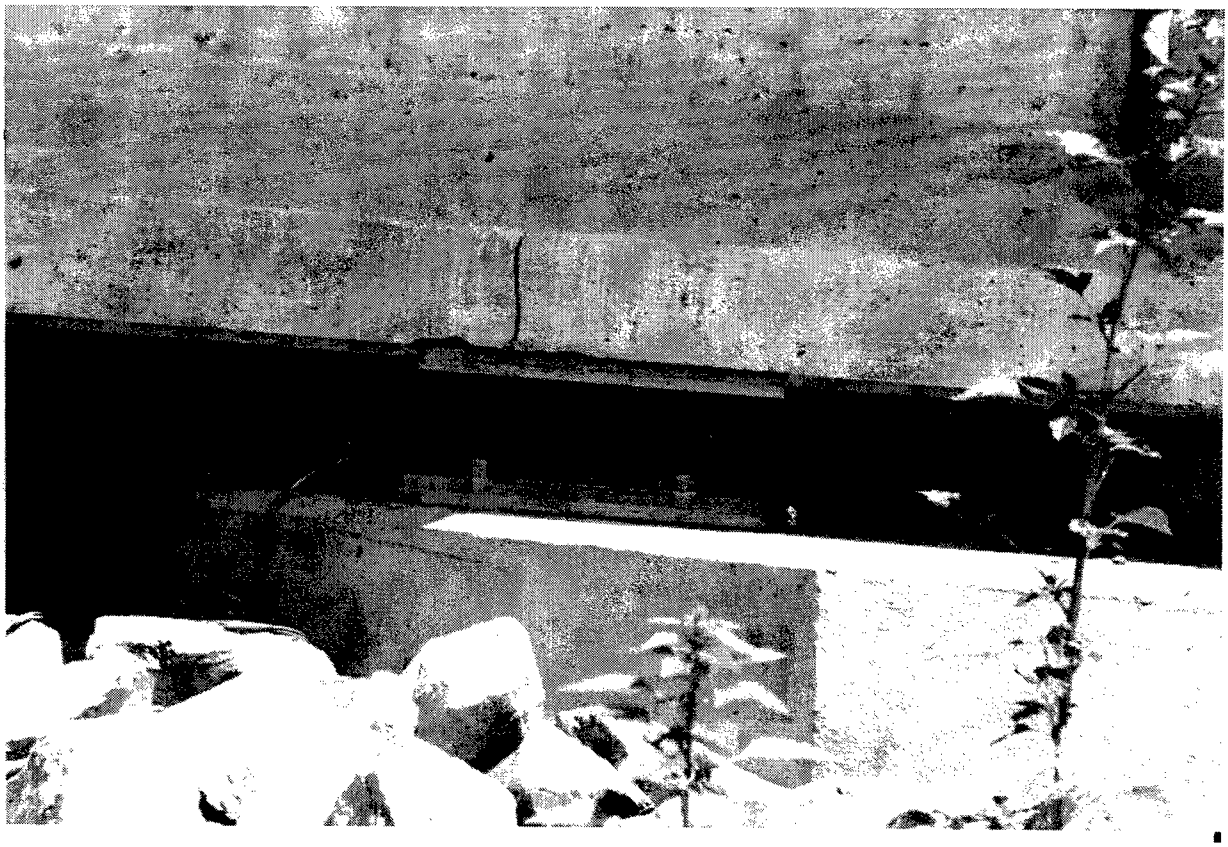

Figure 5: Isolation Bearings at End Bent

Figure 6: Four Column Piers with Webwalls During Bridge Construction

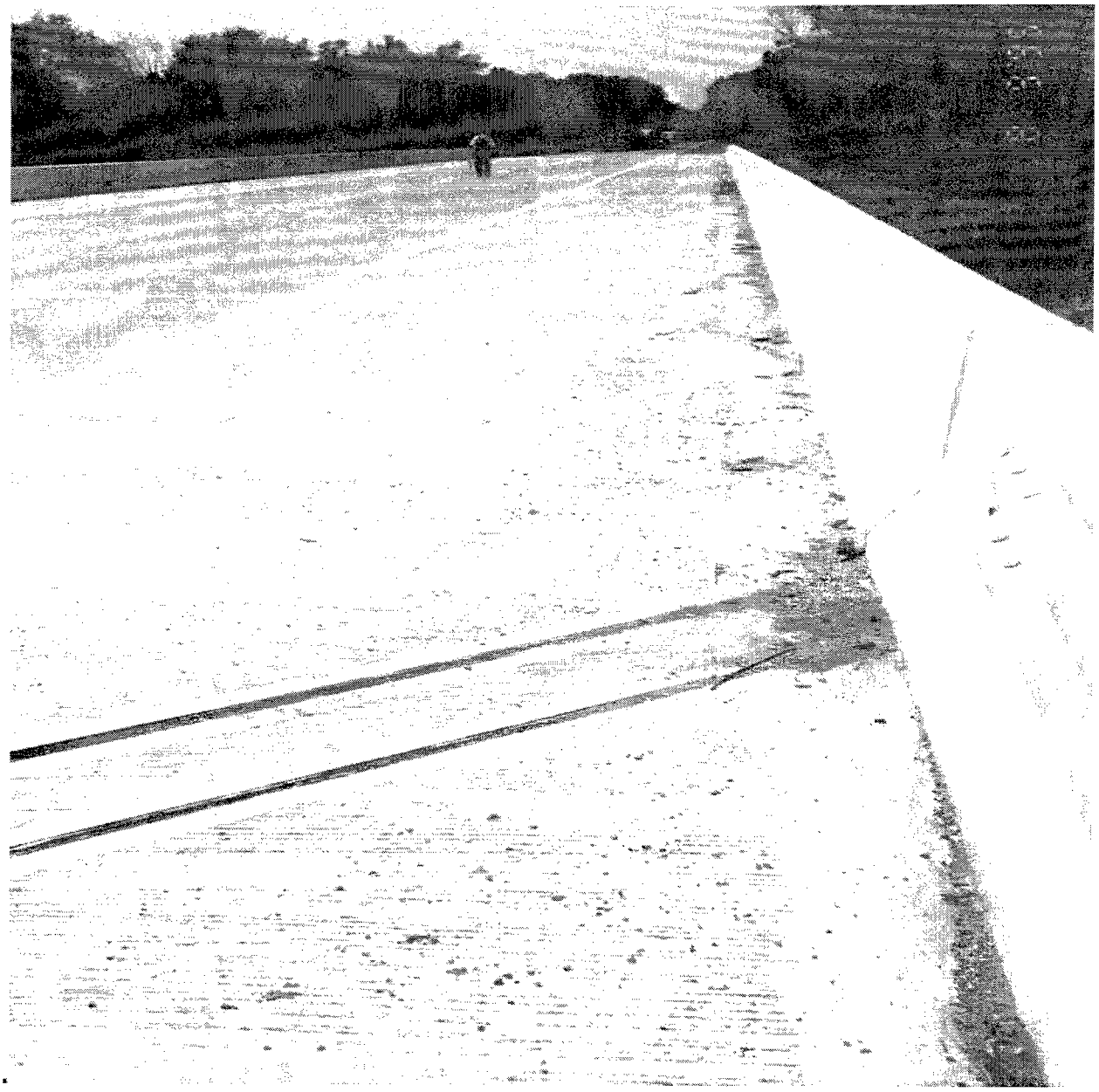

Figure 7: Expansion Joint at End of Bridge

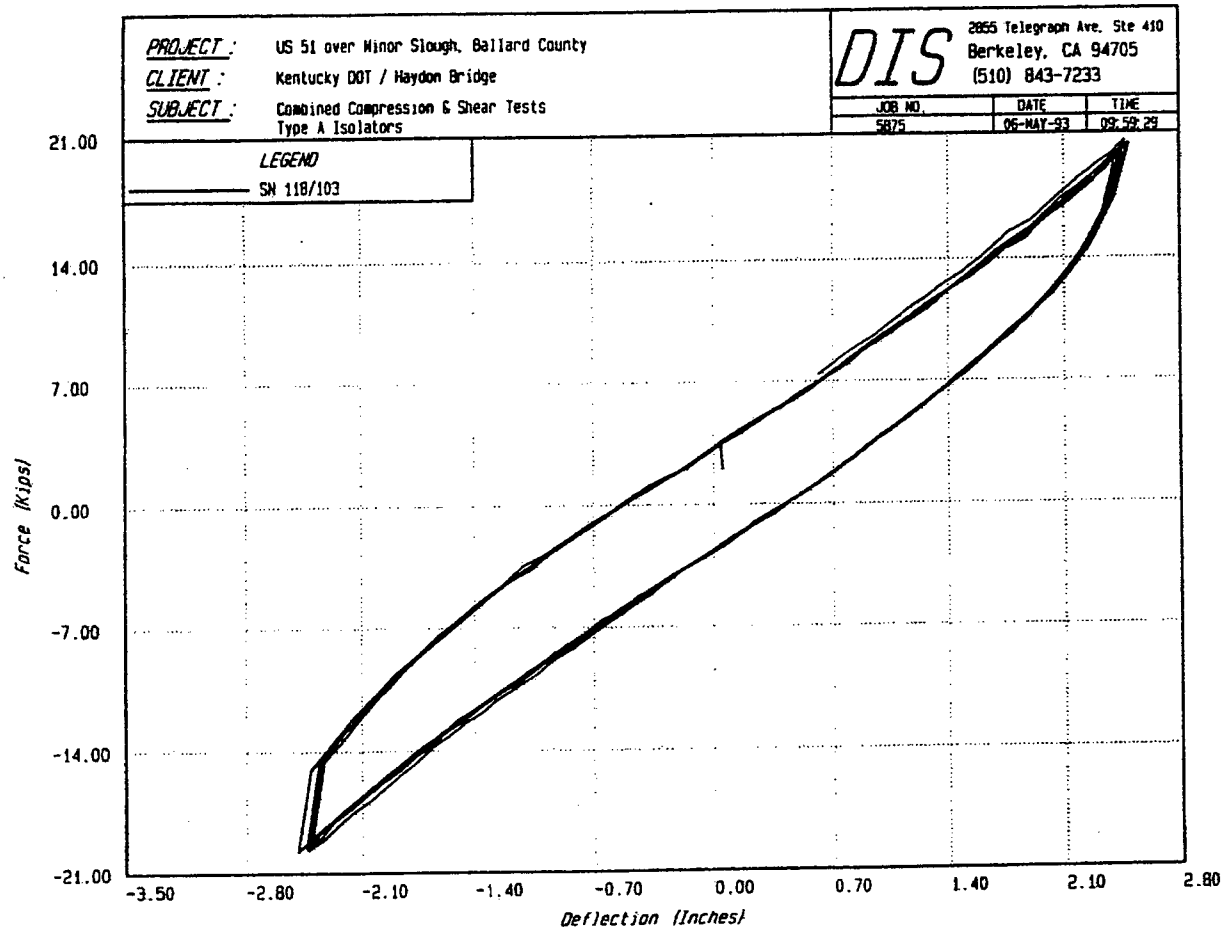

Figure 8: Typical Force-Deflection Curve of Pier Isolation Bearing

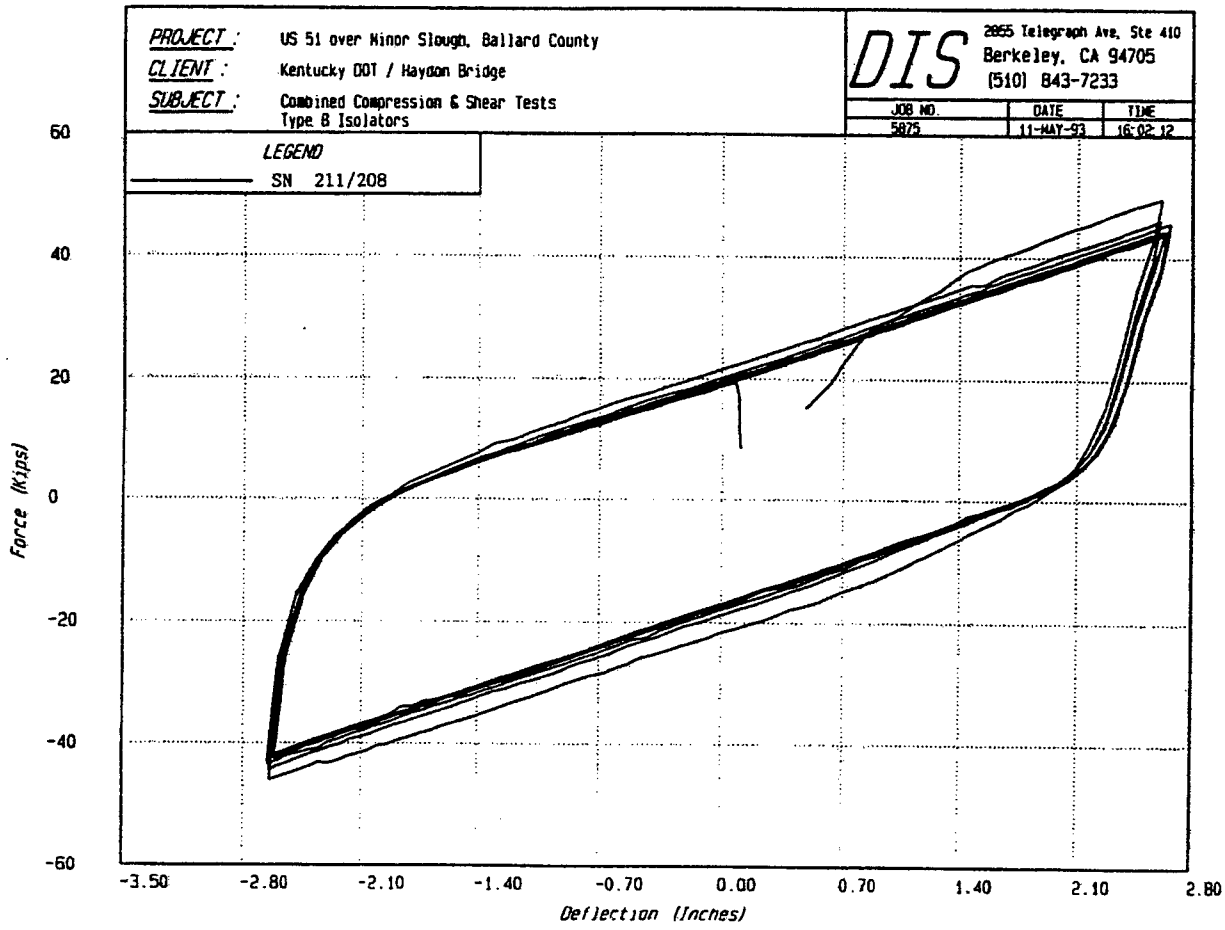

Figure 9: Typical Force-Deflection Curve of End Bent Isolation Bearing

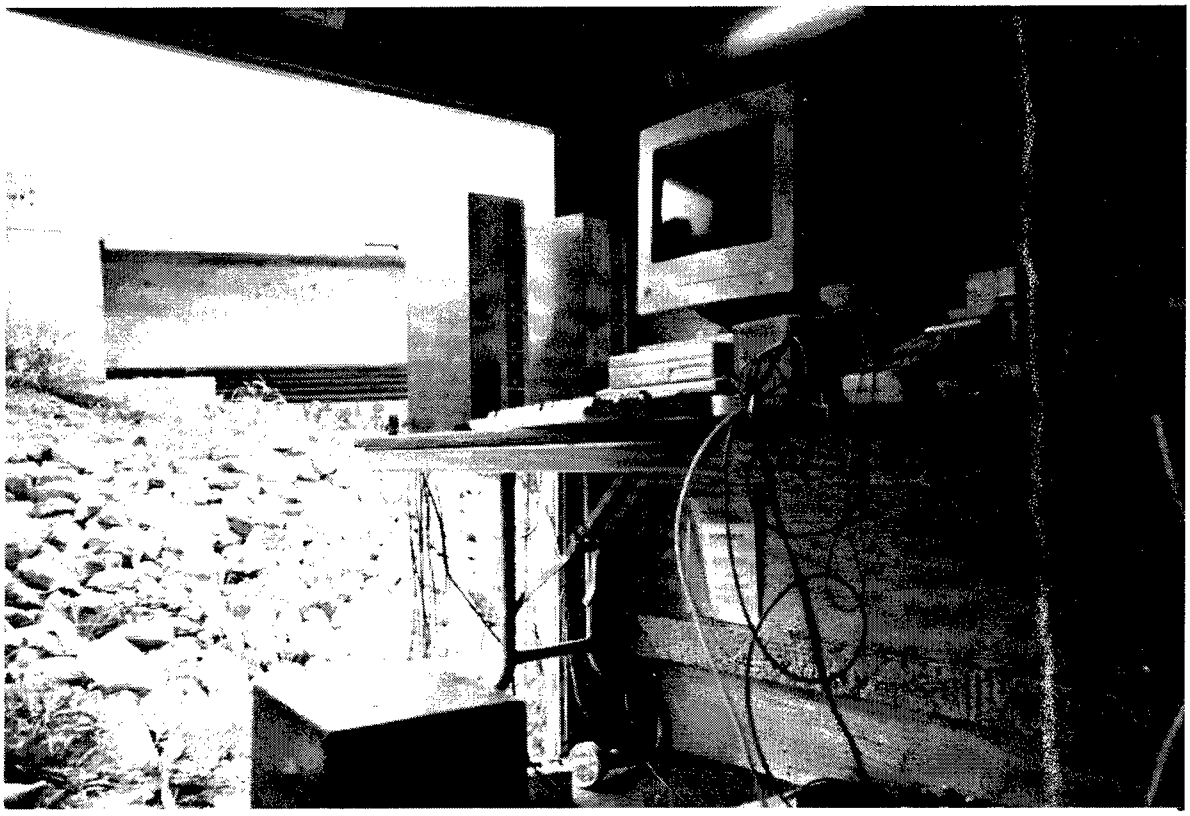

Figure 10: Data Acquisition Equipment at Bridge Site

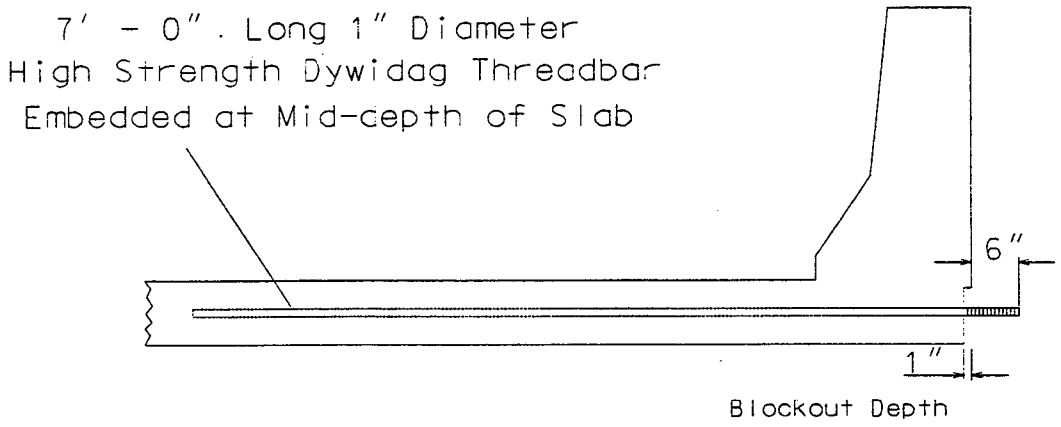

Figure 11: Embedded Dywidag Bar Used for Pullback

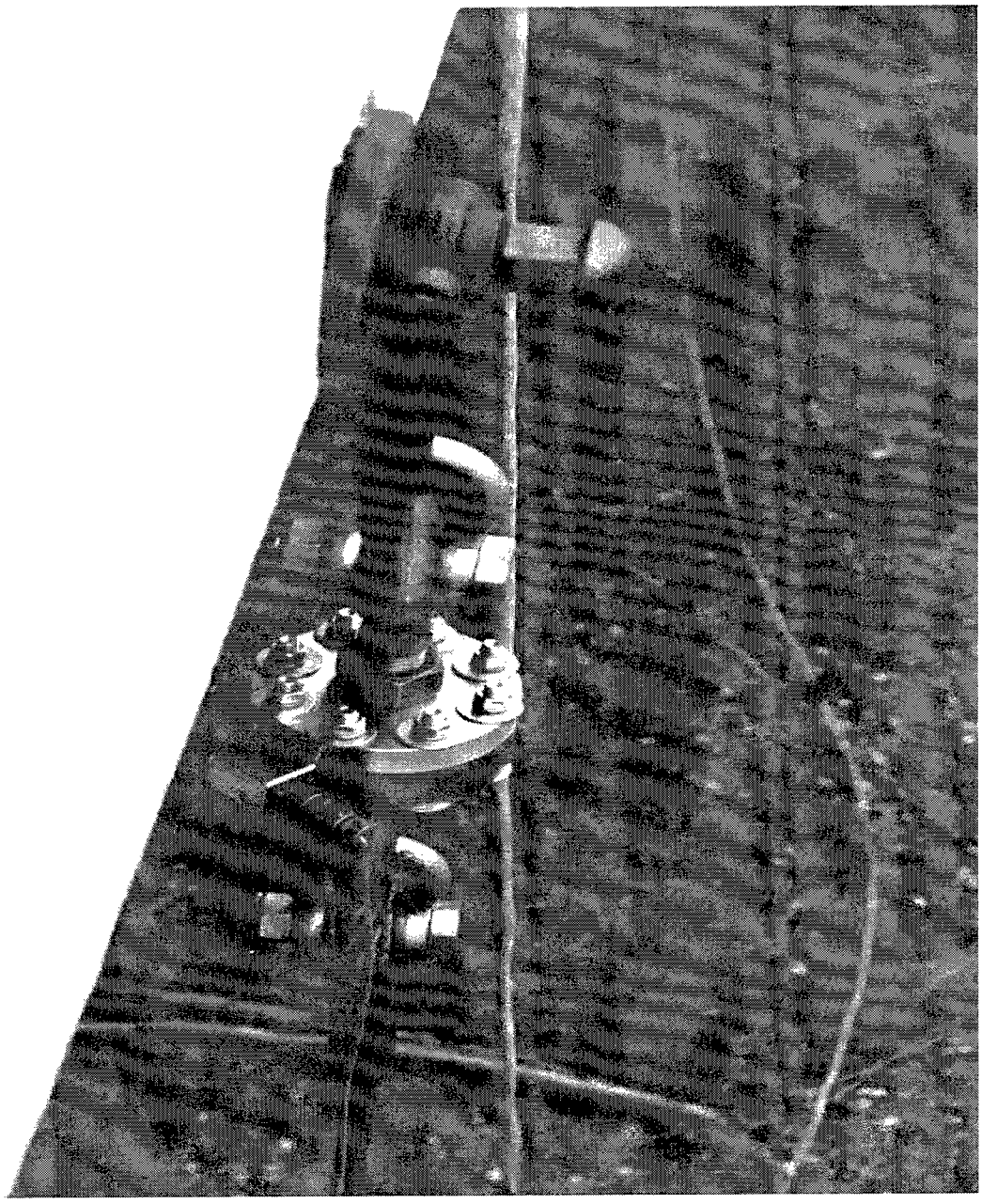

Figure 12: Connection to Embedded Dywidag Bar & Load Cell

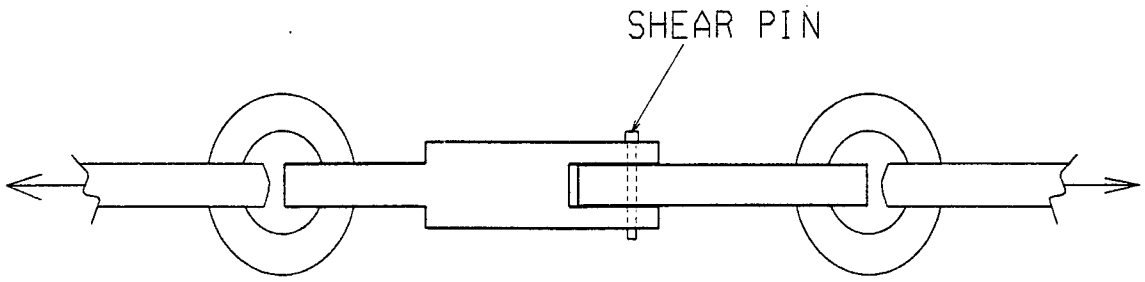

Figure 13: Quick-Release Mechanism

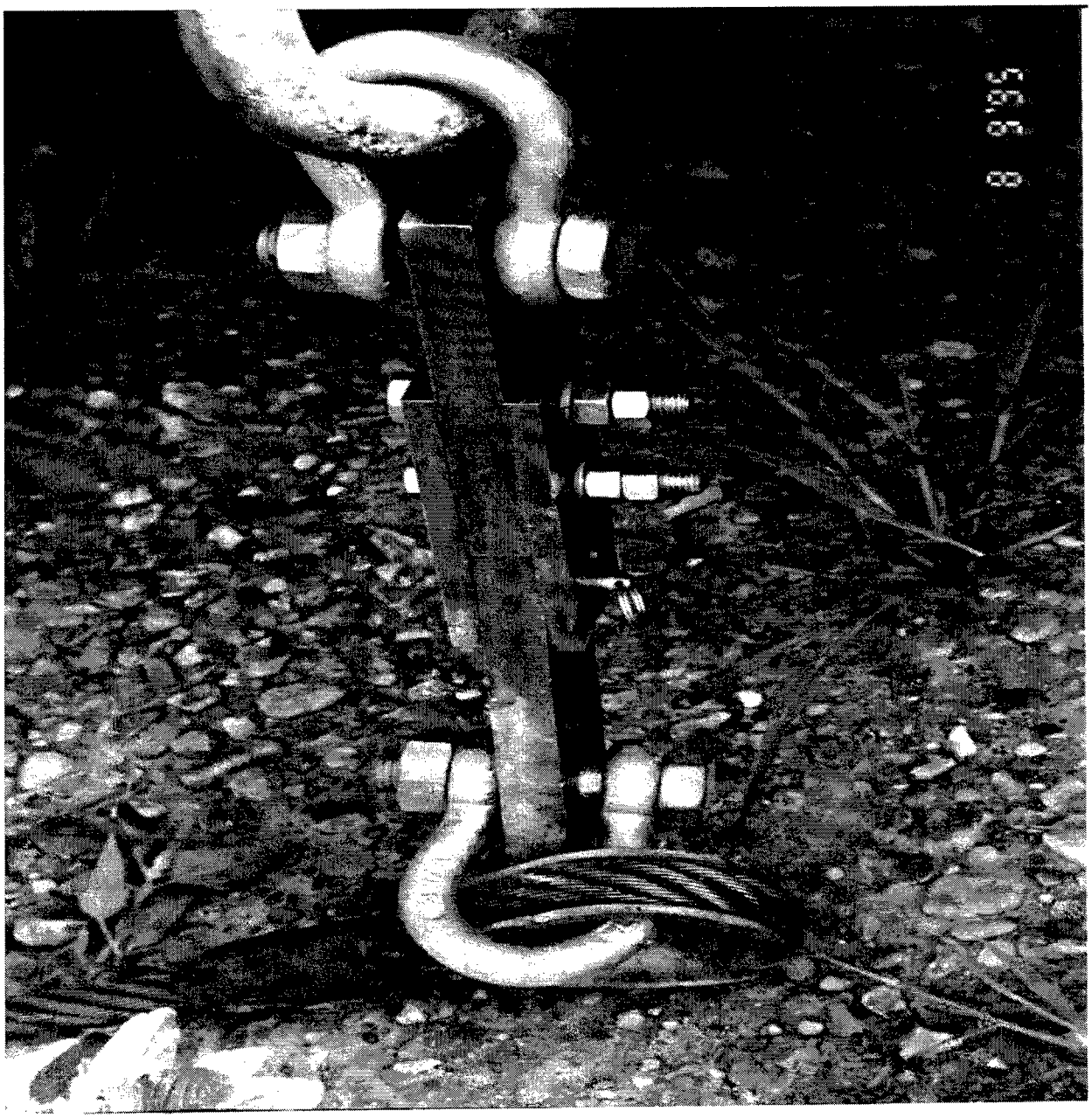

Figure 14: Quick-Release Mechanism

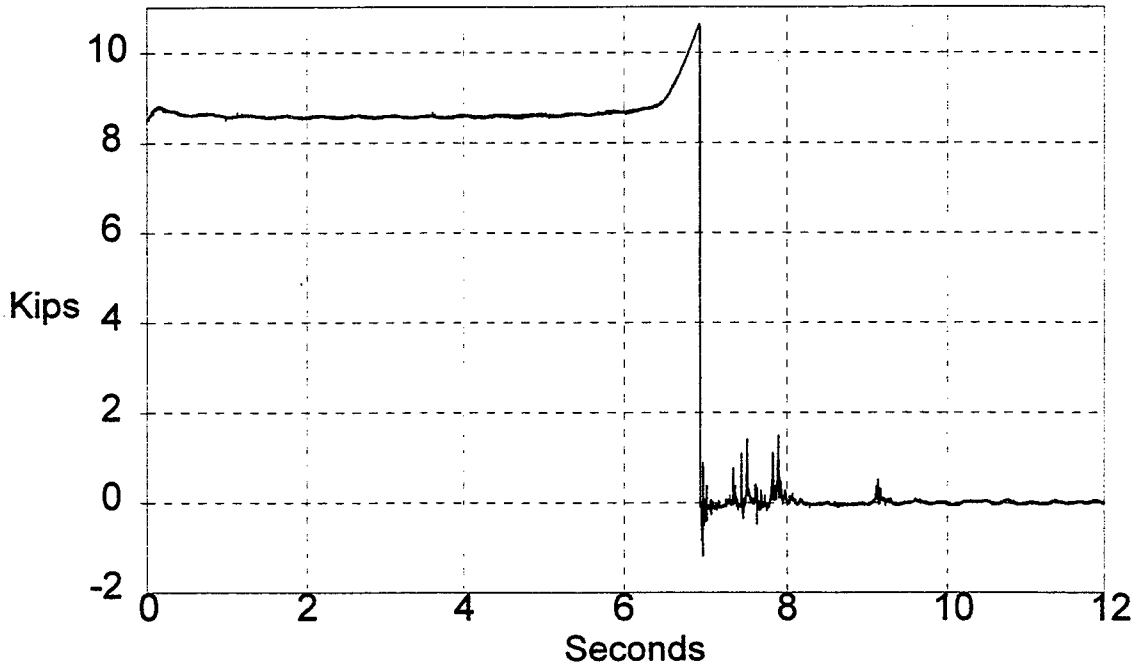

Figure 15: Load Cell History at Release

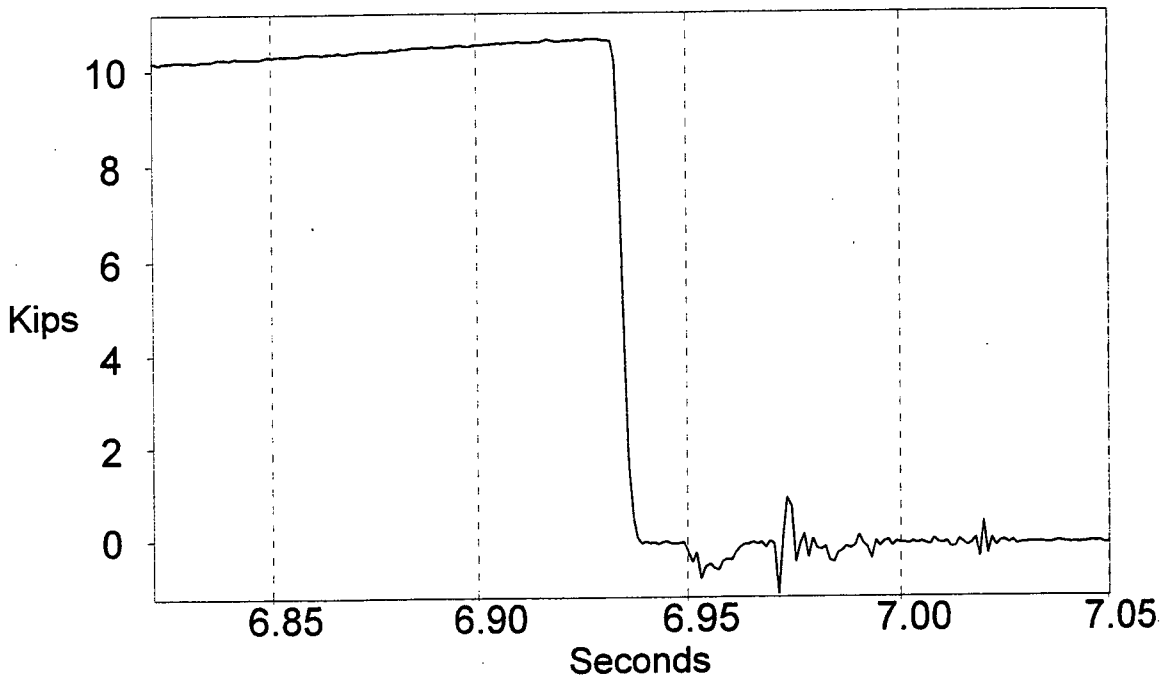

Figure 16: Quick-Release

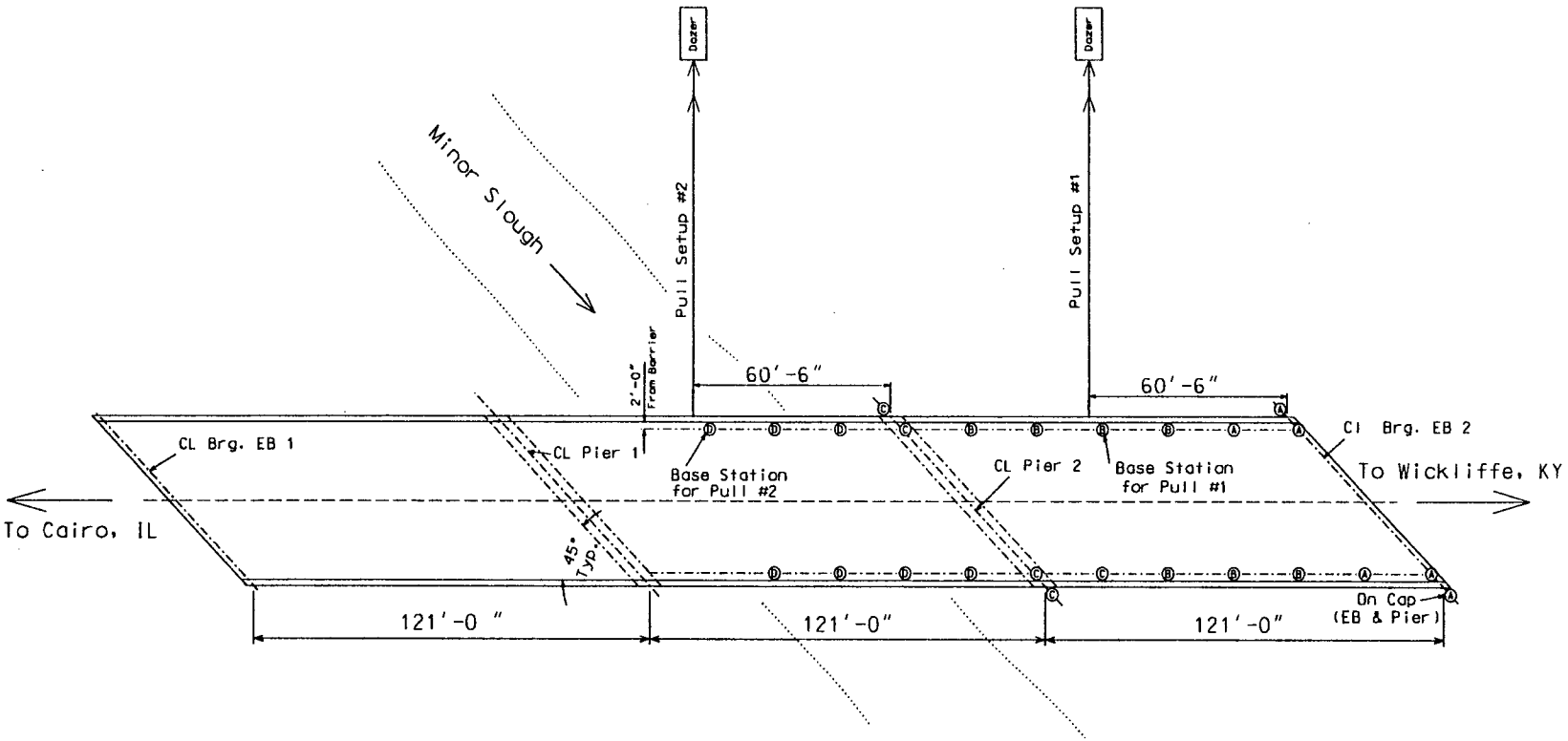

Figure 17: Plan Showing Accelerometer (¤) Locations (Pulls A-D)

Figure 18: Technician Positioning Accelerometer Block

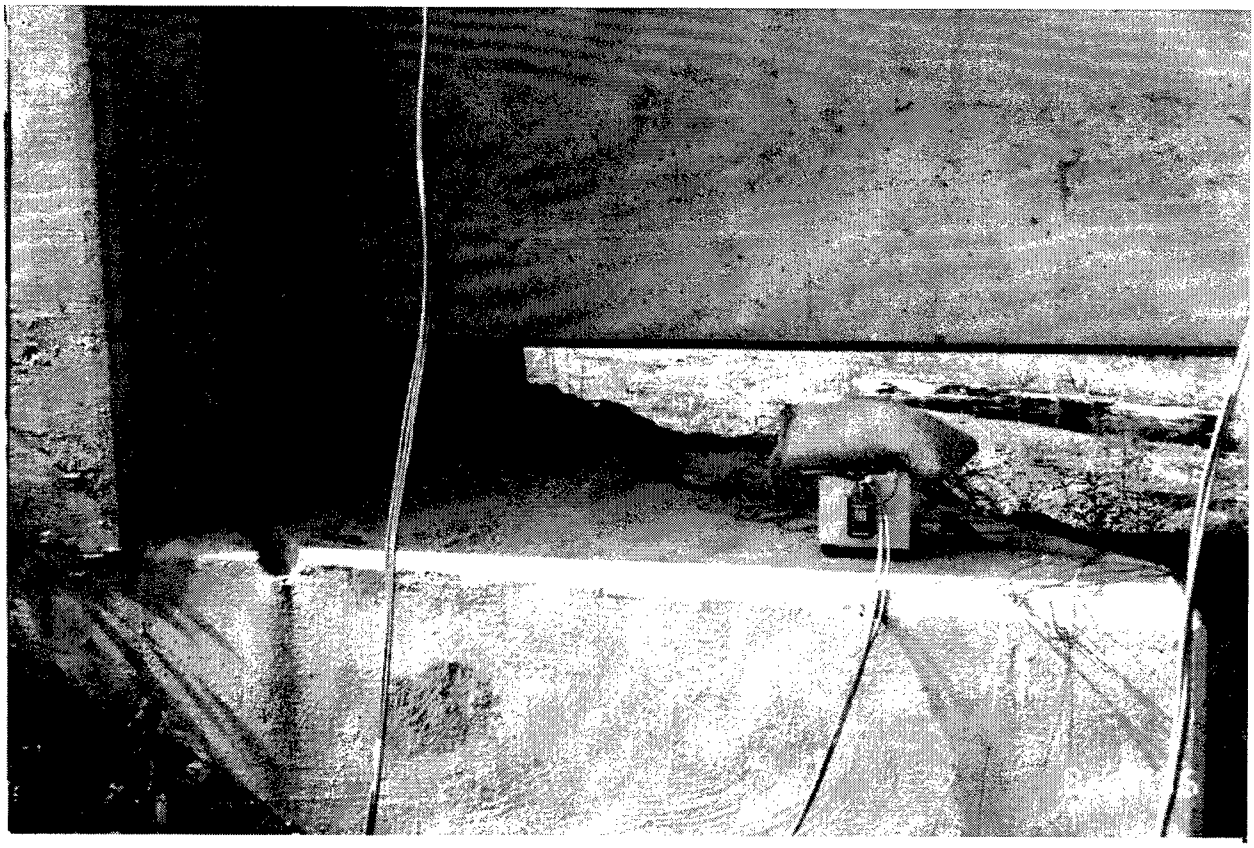

Figure 19: Accelerometer Block on End Bent Cap

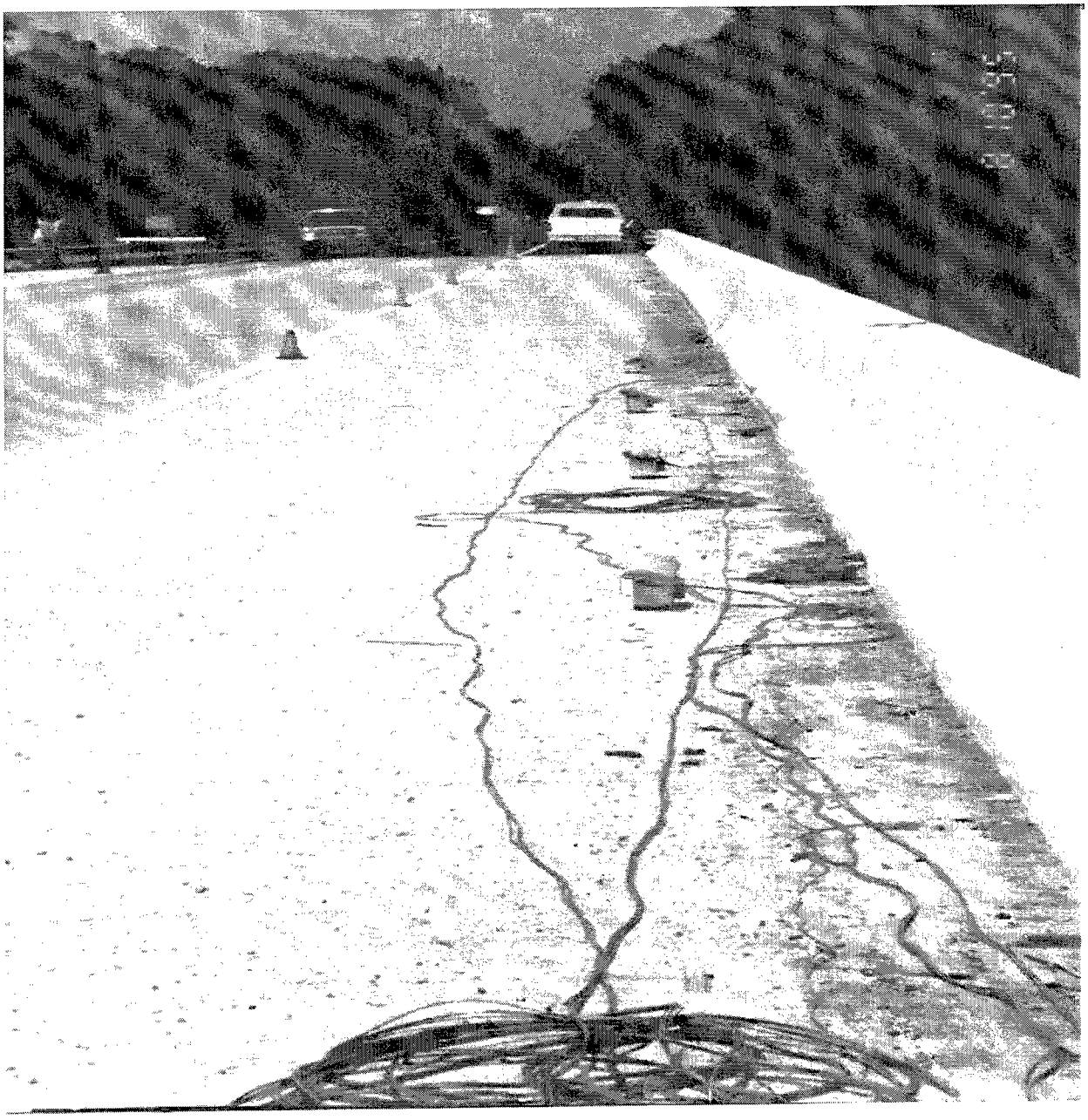

Figure 20: Four Accelerometer Blocks on Bridge Deck

Figure 21: Bulldozer During Pullback Testing

Figure 22: Bulldozer Tensioning Pullback Cable

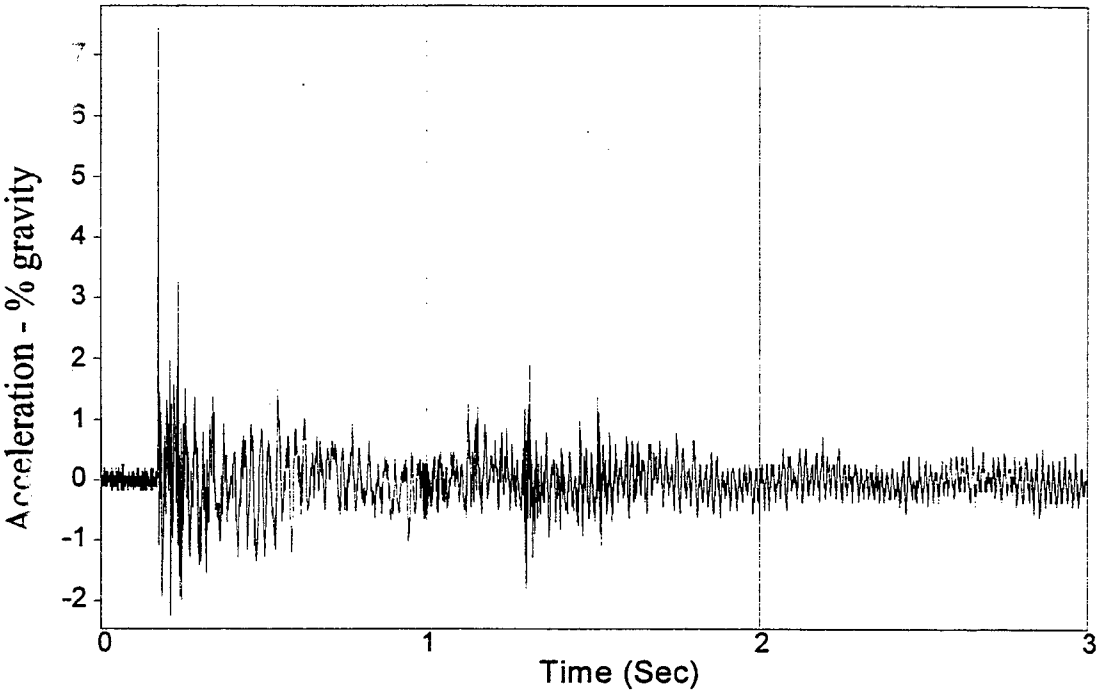

Figure 23: Typical Transverse Acceleration History

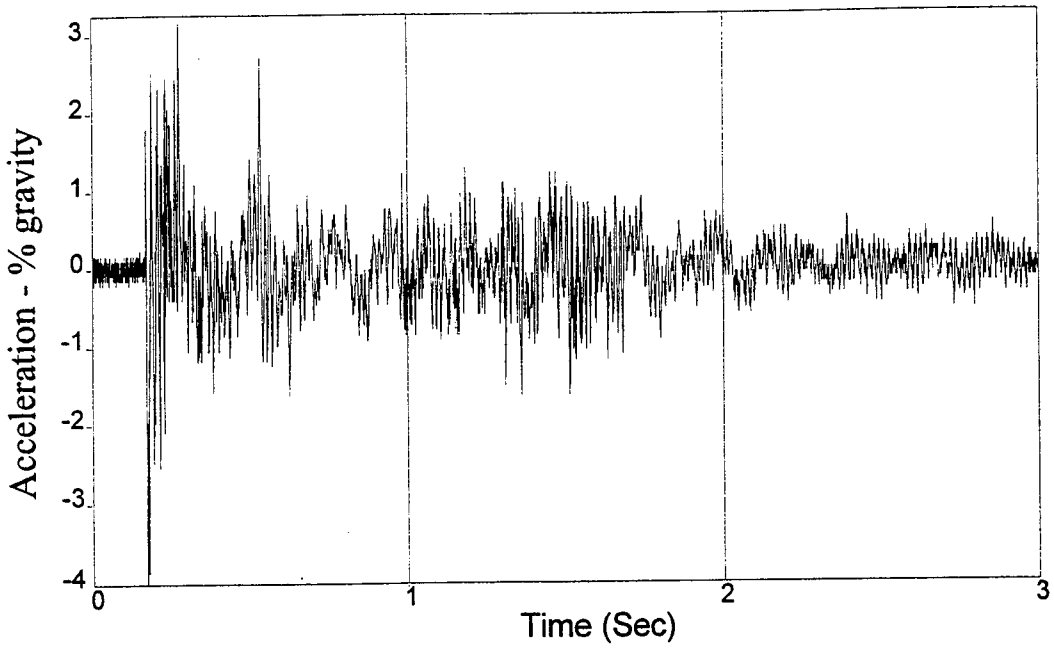

Figure 24: Typical Vertical Acceleration History

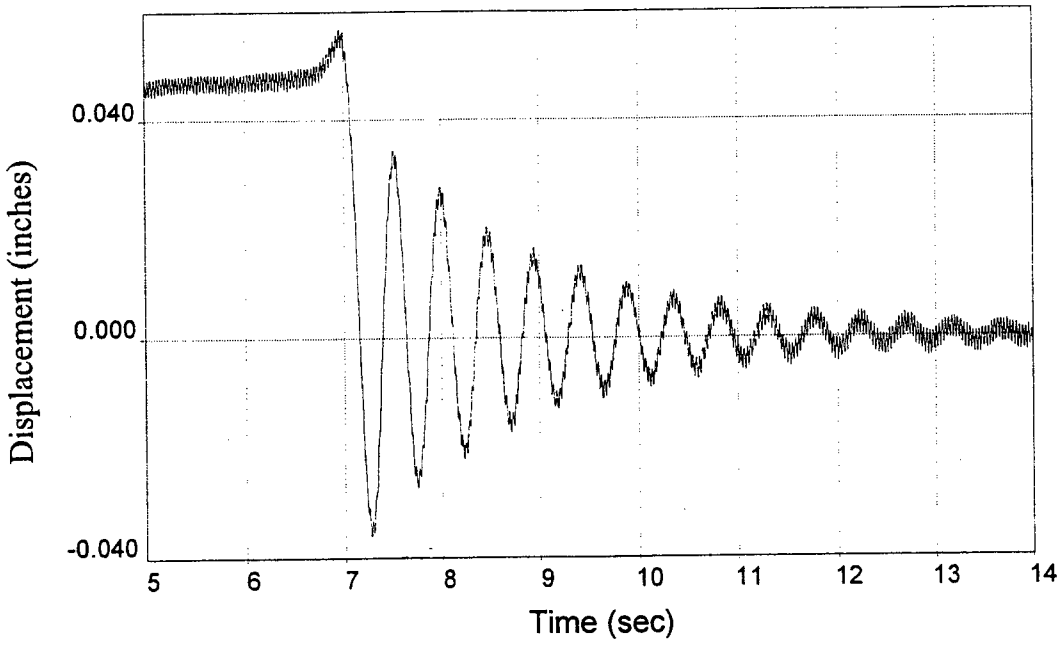

Figure 25: Relative Displacement Across Bearing

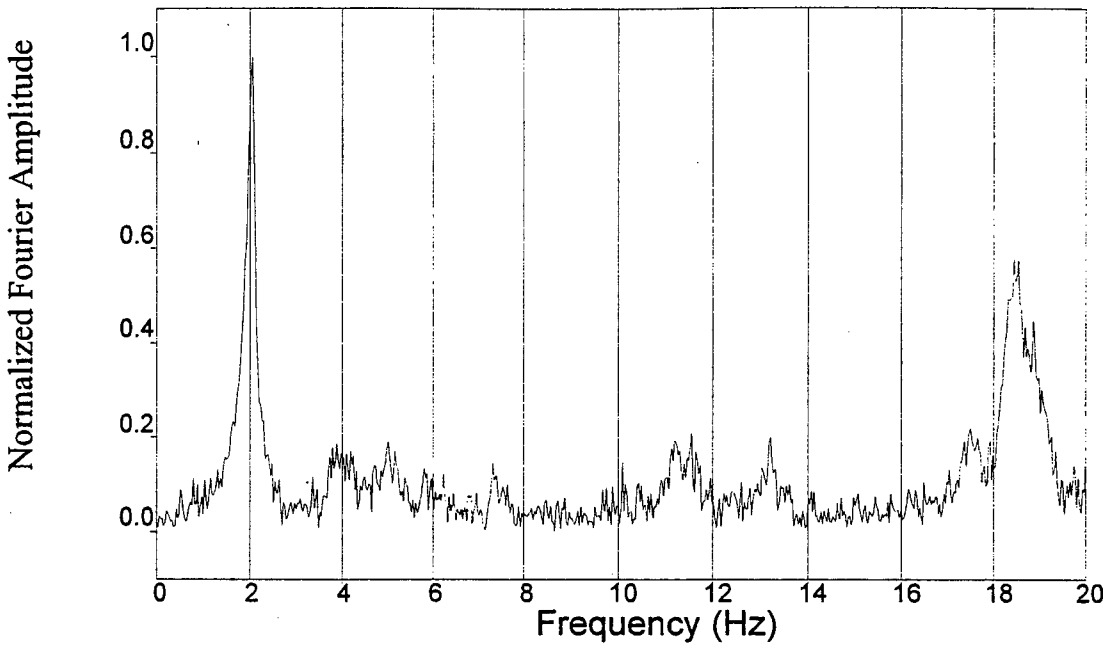

Figure 26: FFT of Transverse Acceleration

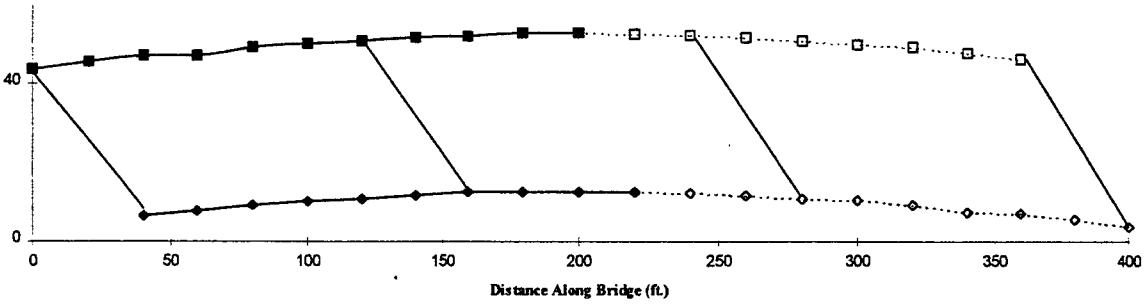

Figure 27: First Transverse Mode @ 2.08 Hz

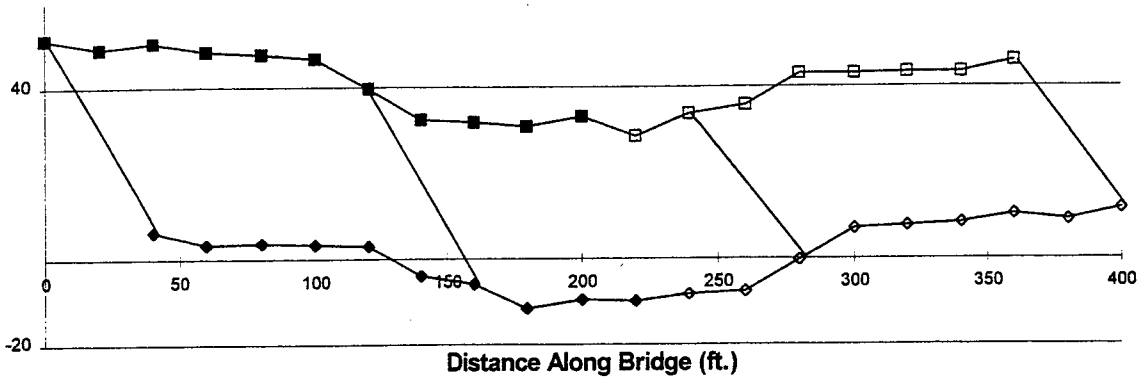

Figure 28: Second Transverse Mode @ 8.20 Hz

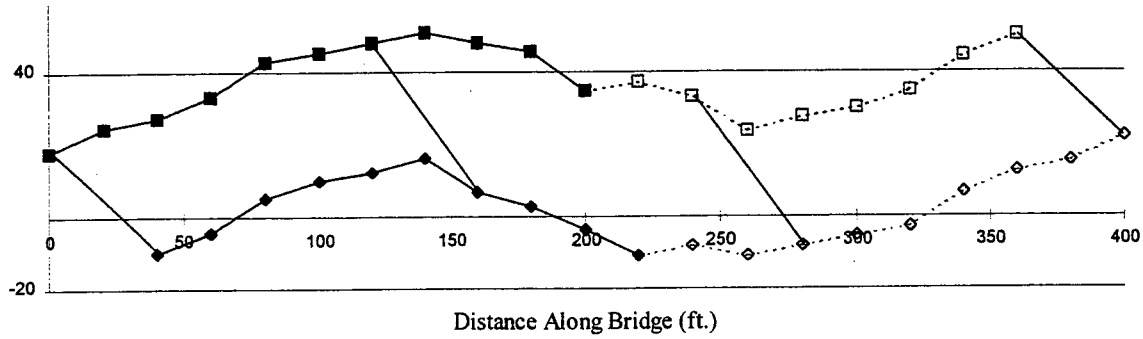

Figure 29: Third Transverse Mode @ 11.2 Hz

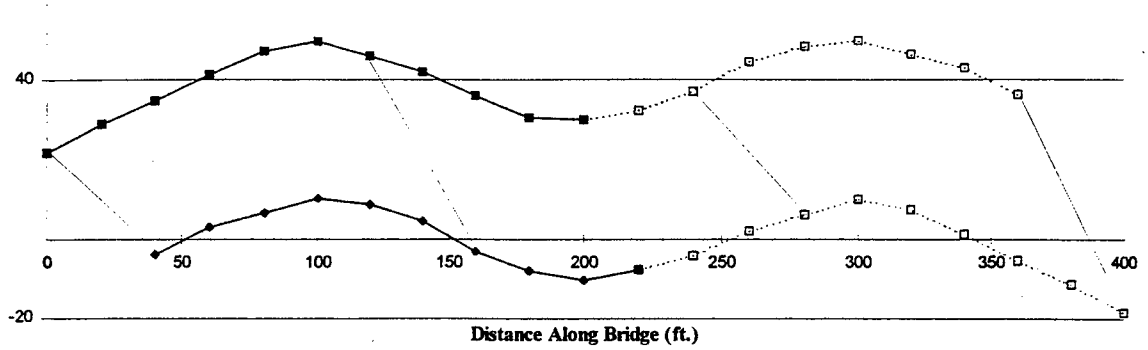

Figure 30: Fourth Transverse Mode @ 18.7 Hz

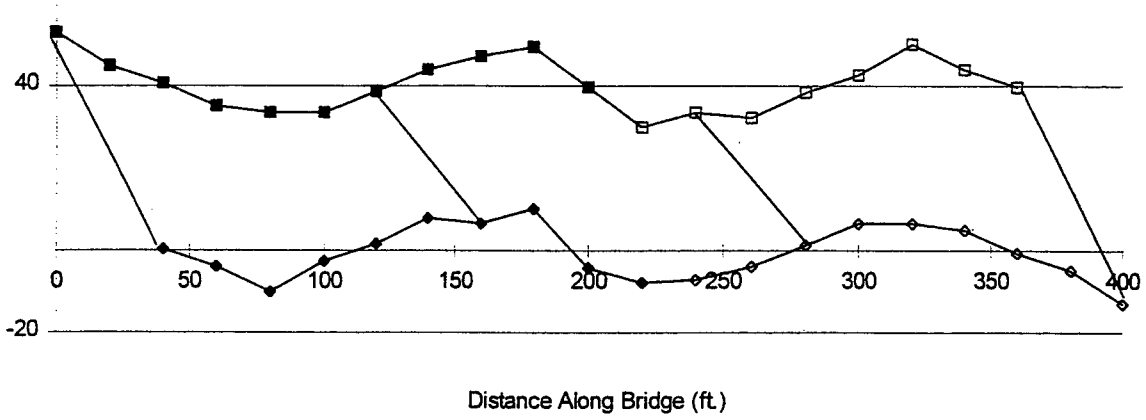

Figure 31: Fifth Transverse Mode @ 24.7 Hz

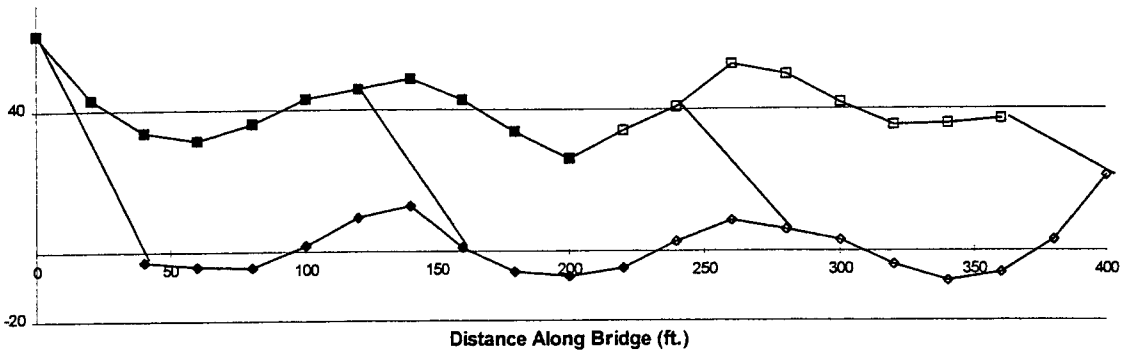

Figure 32: Sixth Transverse Mode @ 30.2 Hz

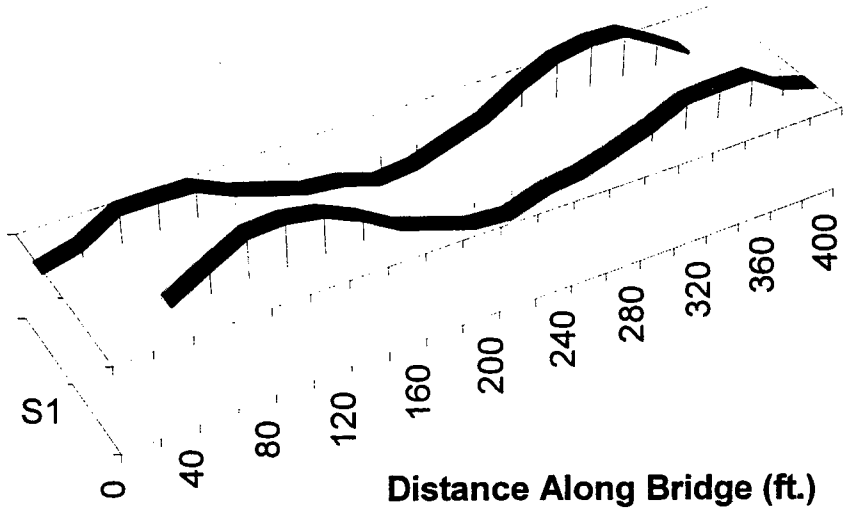

Figure 33: 1st Vertical Bending Mode @ 3.42 Hz

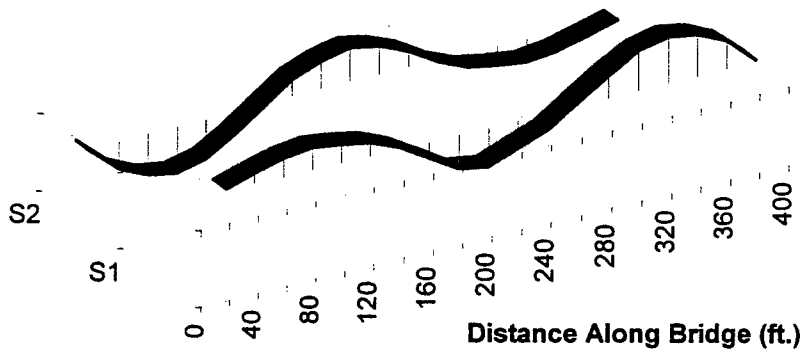

Figure 34: 1st Torsional Mode @ 4.21 Hz

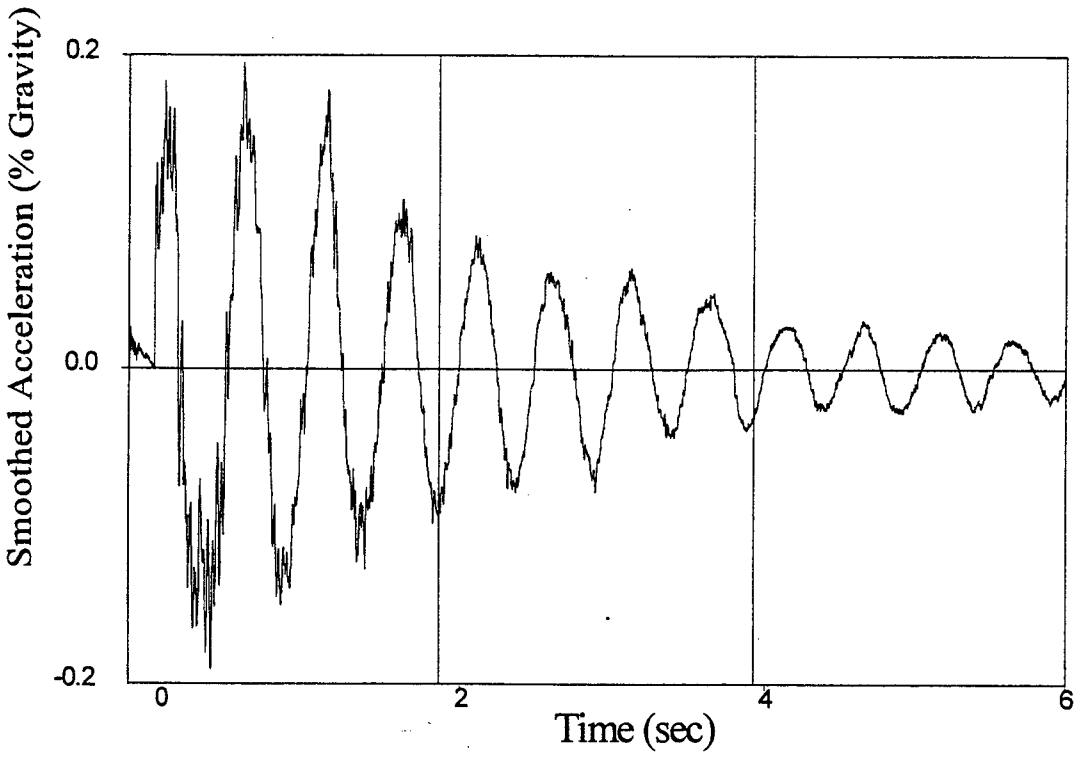

Figure 35: Moving Average on Figure 4.1

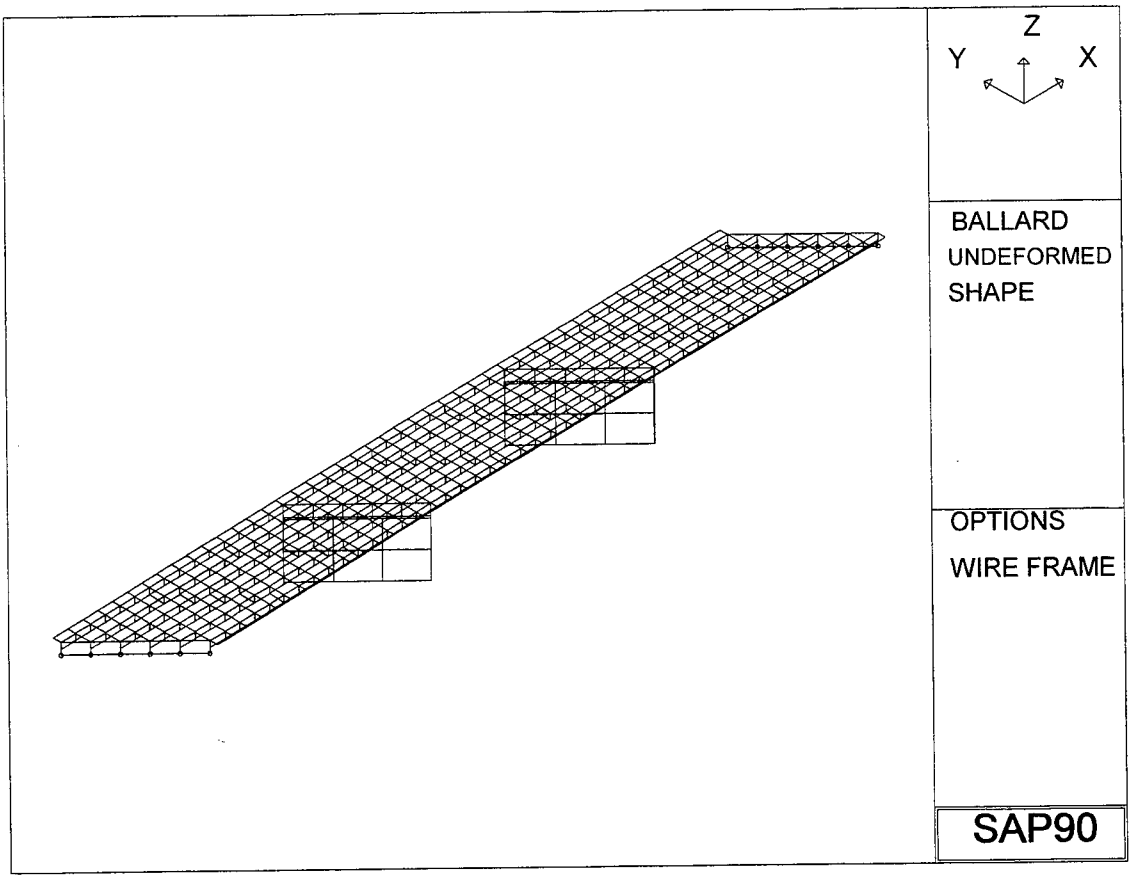

Figure 36: SAP 90 Model of Bridge

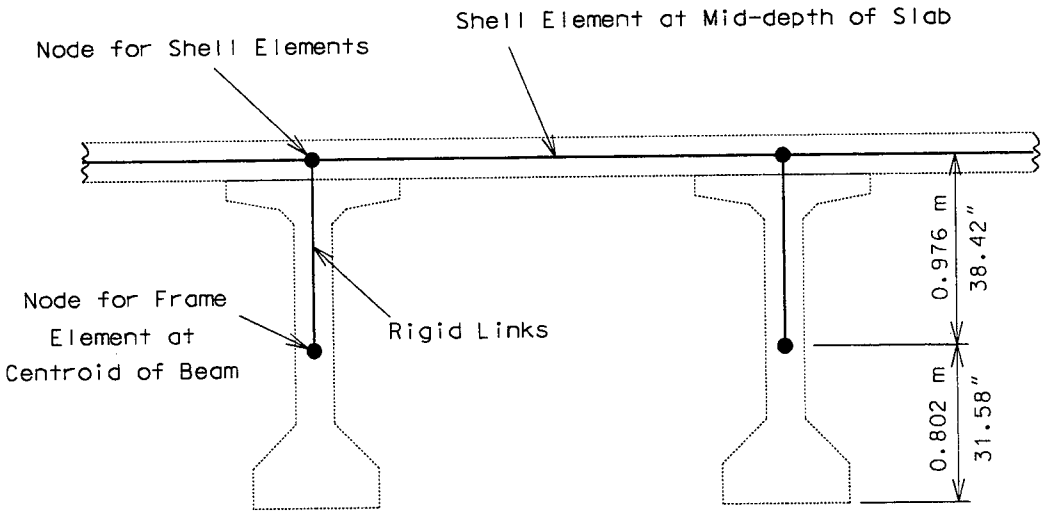

Figure 37: Typical Cross Section Model of Bridge

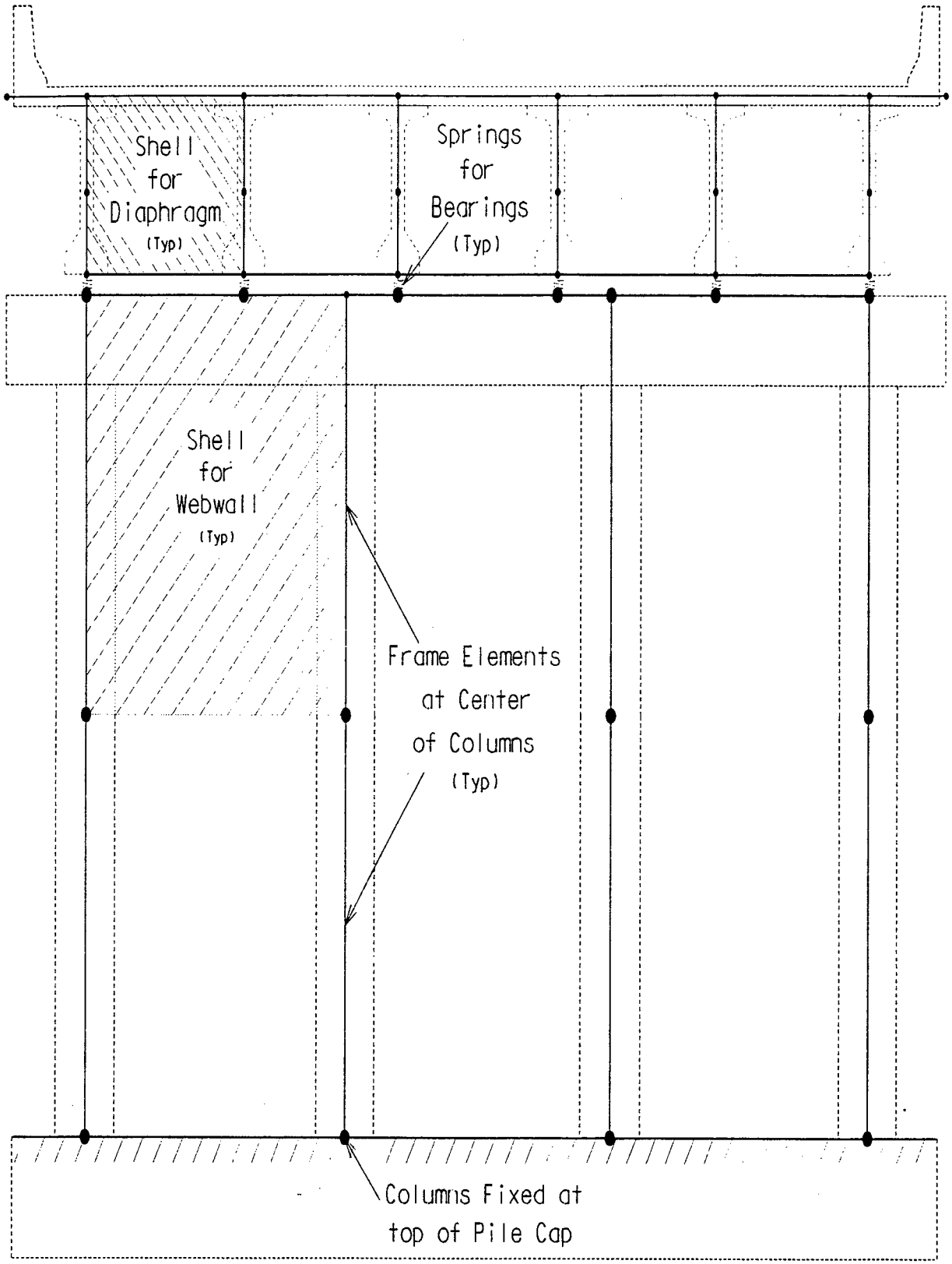

Figure 38. Model Of Pier

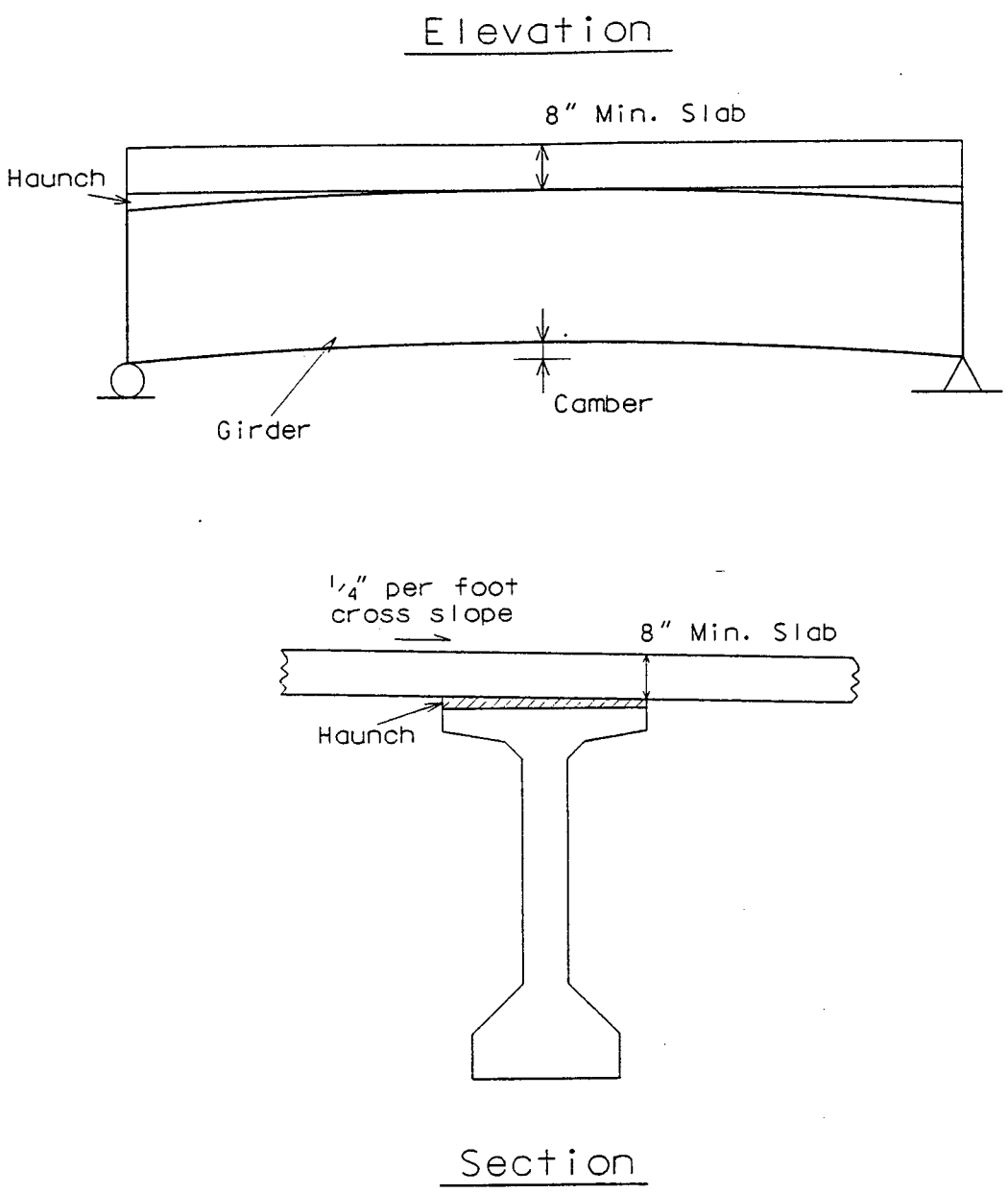

Figure 39. Camber And Haunch Of Girders

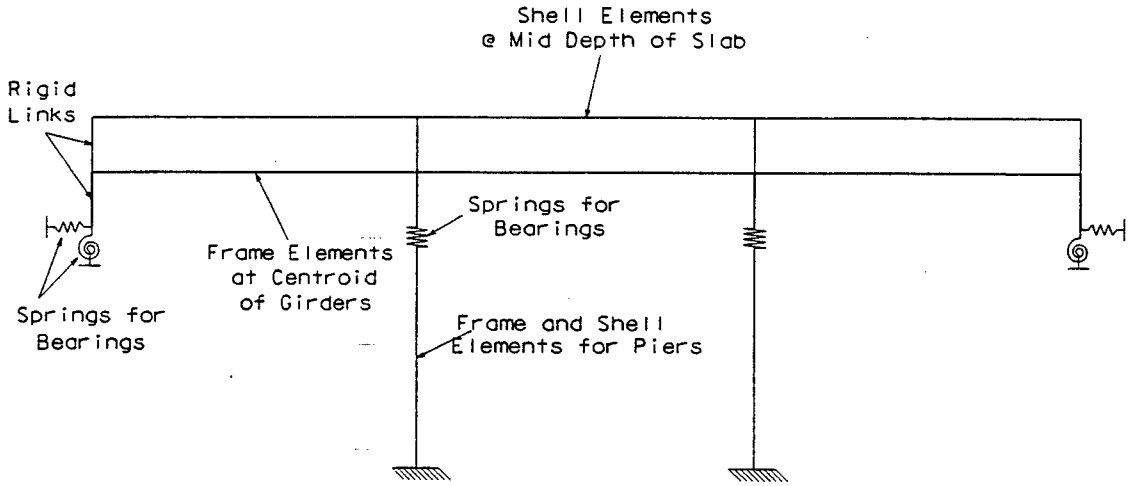

Figure 40. Model of Bridge Supports

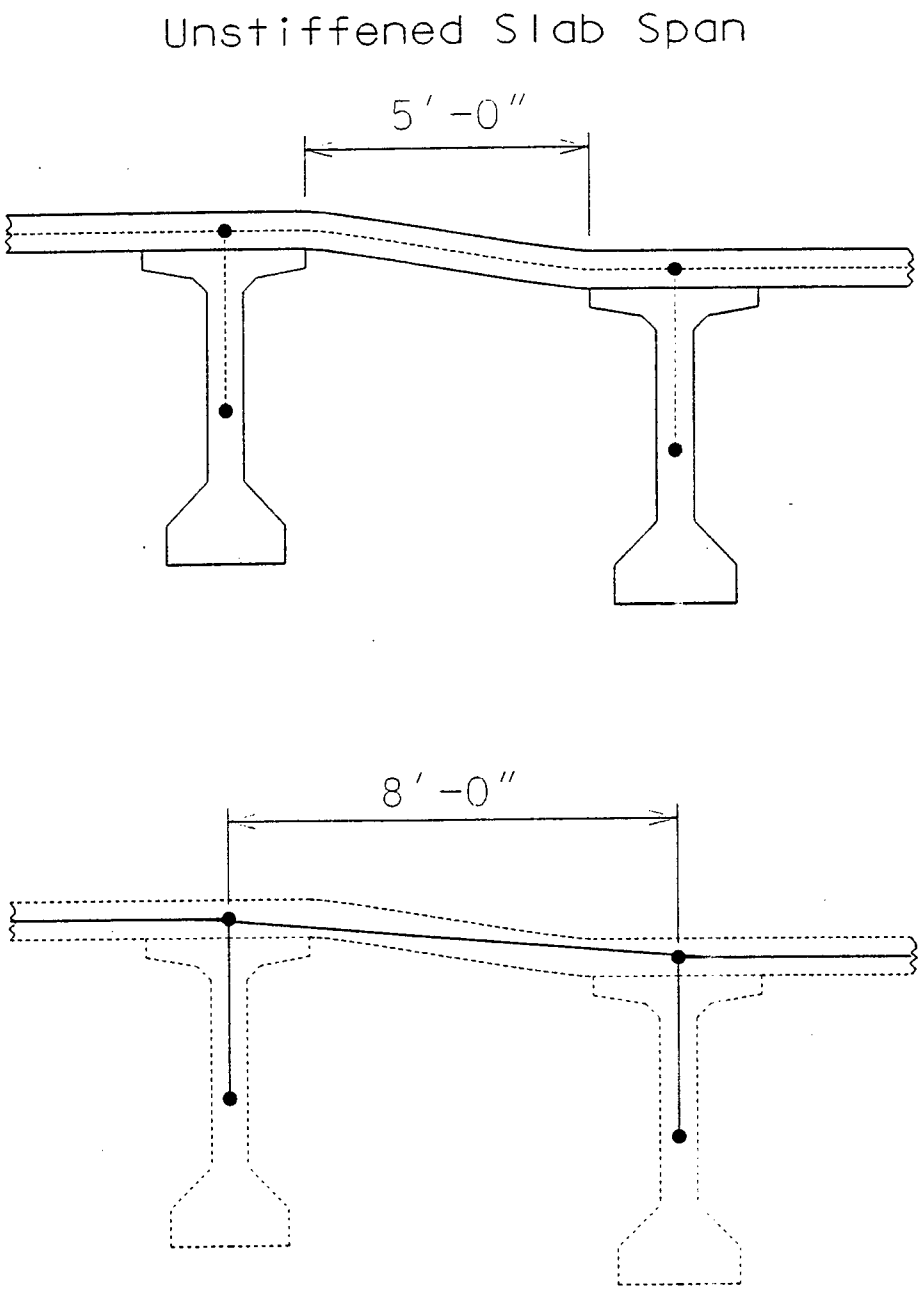

Figure 41. Slab Modeling Considerations

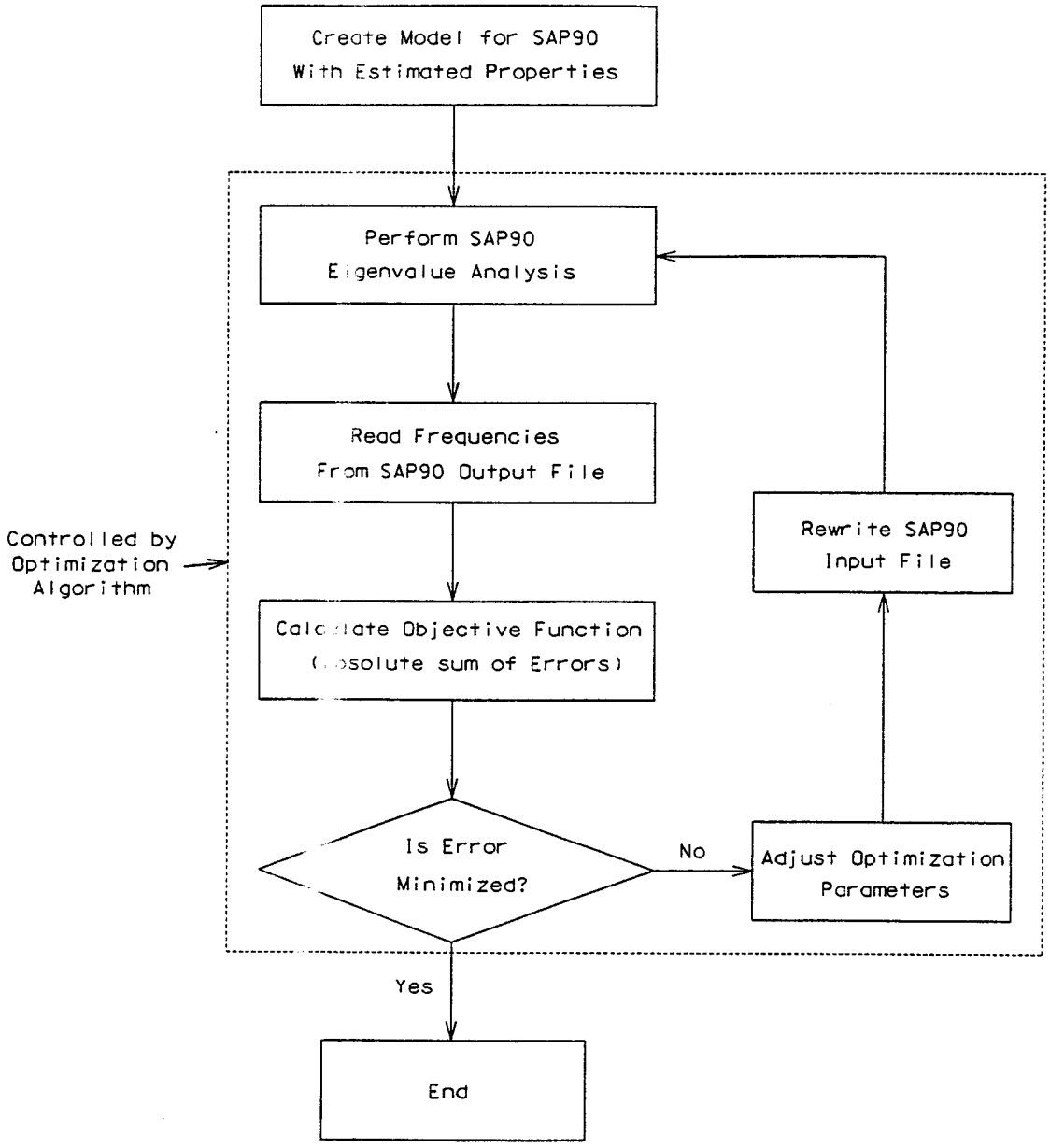

Figure 42. Flow Chart Of Optimization Process

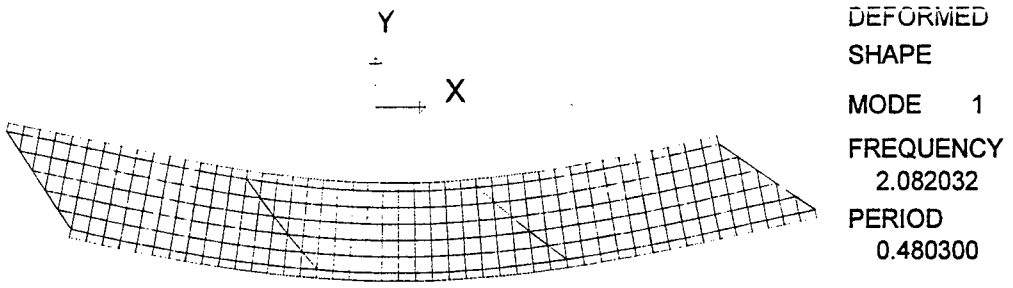

Figure 43: Plan of 1st Transverse Mode @ 2.08 Hz.

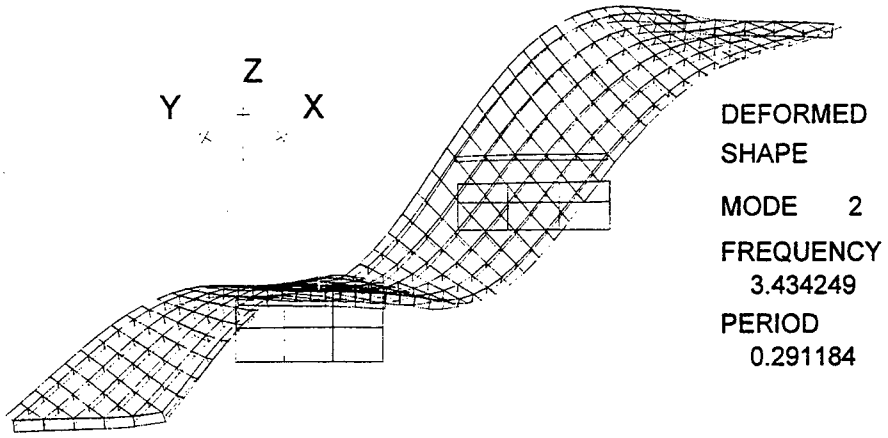

Figure 44: 1st Vertical Bending Mode @ 3.43 Hz.

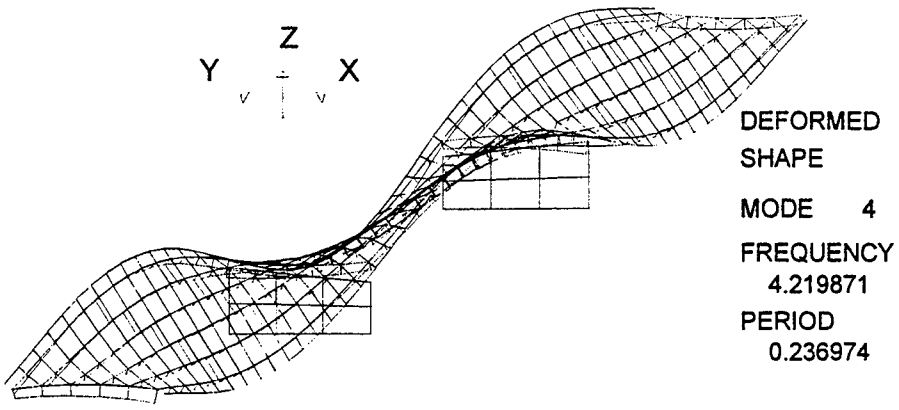

Figure 45 1st Vertical Torsional Mode @ 4.22 Hz.

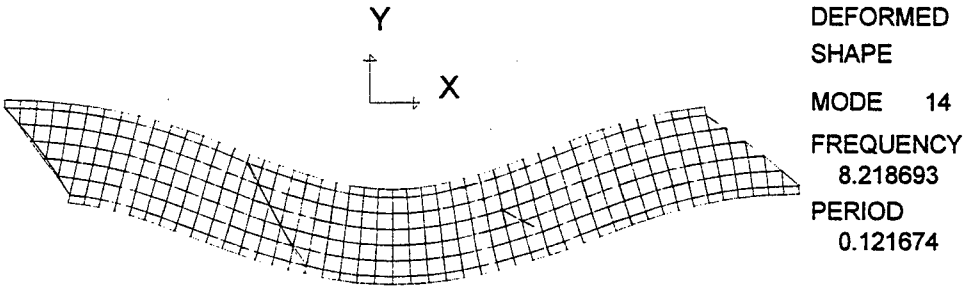

Figure 46: Transverse Mode @ 8.22 Hz.

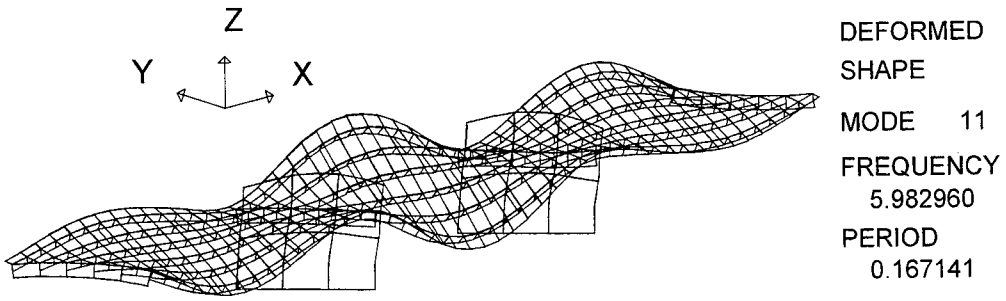

Figure 47: Vertical Torsional Mode @ 5.98 Hz.

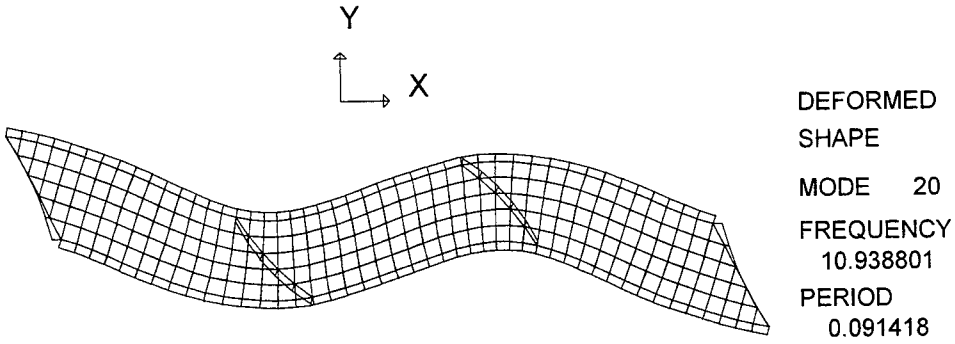

Figure 48: Plan of Transverse Mode @ 10.9 Hz.

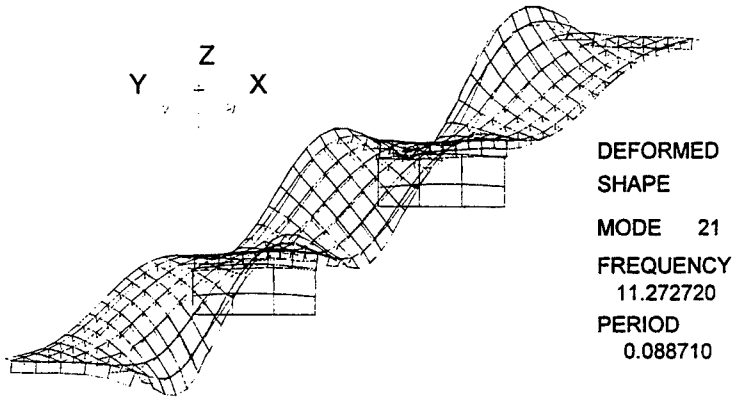

Figure 49: Vertical Bending Mode @ 11.3 Hz.

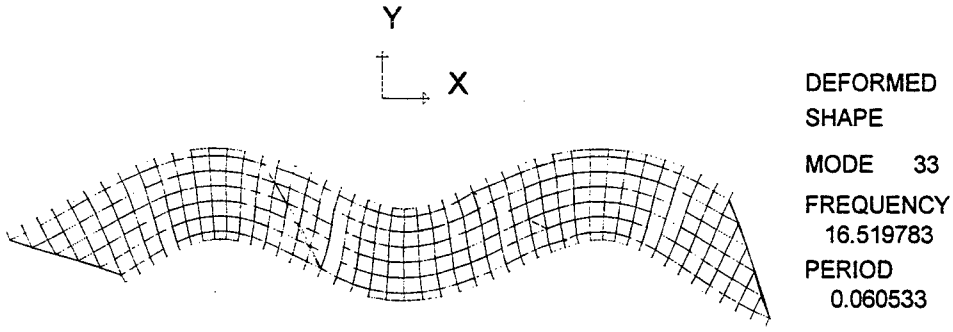

Figure 50: Transverse Mode @ 16.5 Hz.

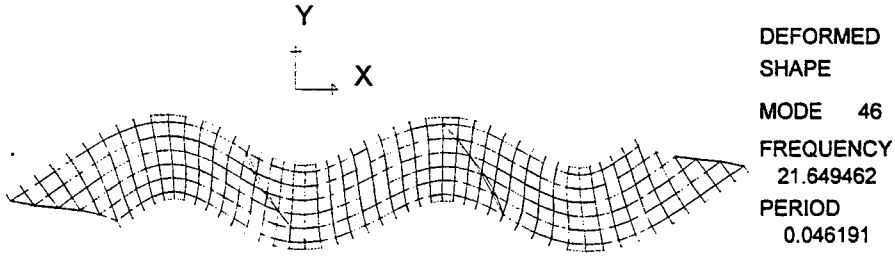

Figure 51: Transverse Mode @ 21.6 Hz.

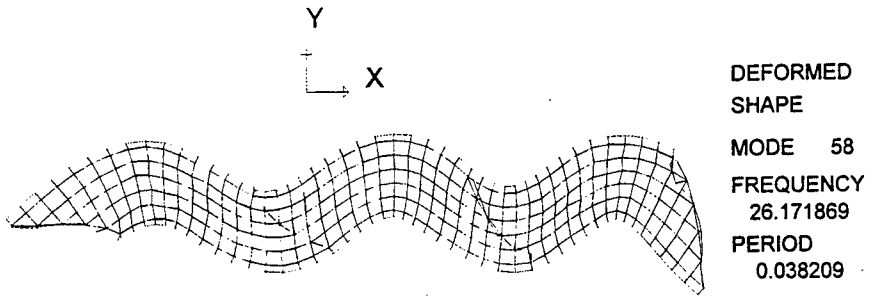

Figure 52: Transverse Mode @ 26.2 Hz.

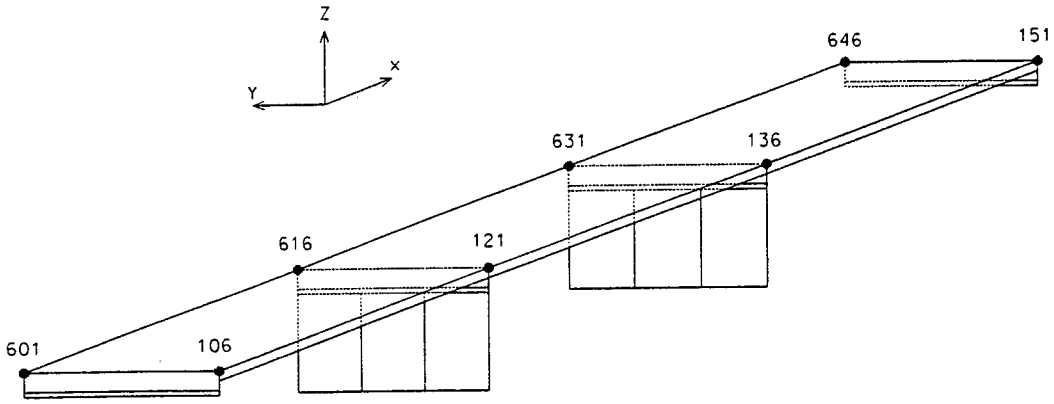

Figure 53: Nodes for Deck-Level Response

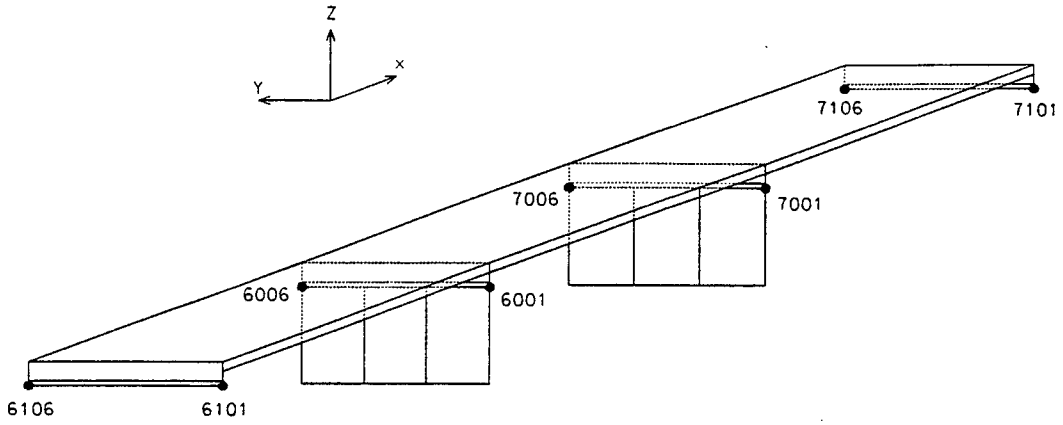

Figure 54: Elements for Bearing-Level Response

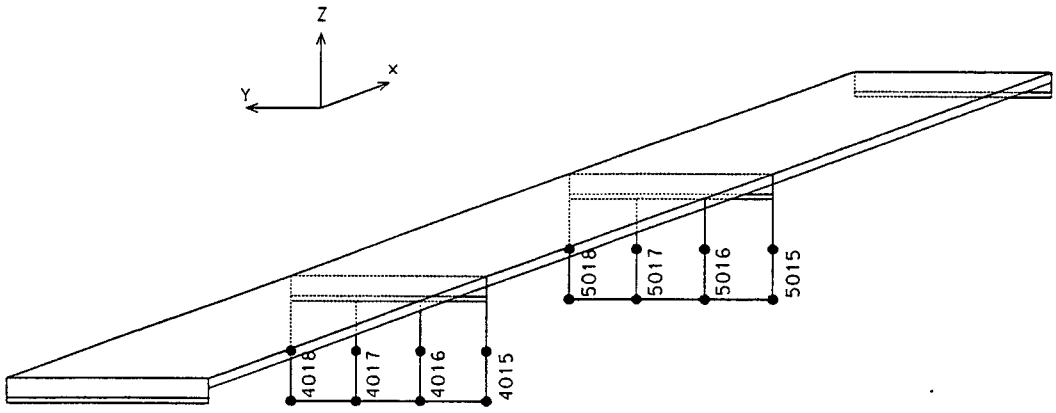

Figure 55: Elements for Pier Response

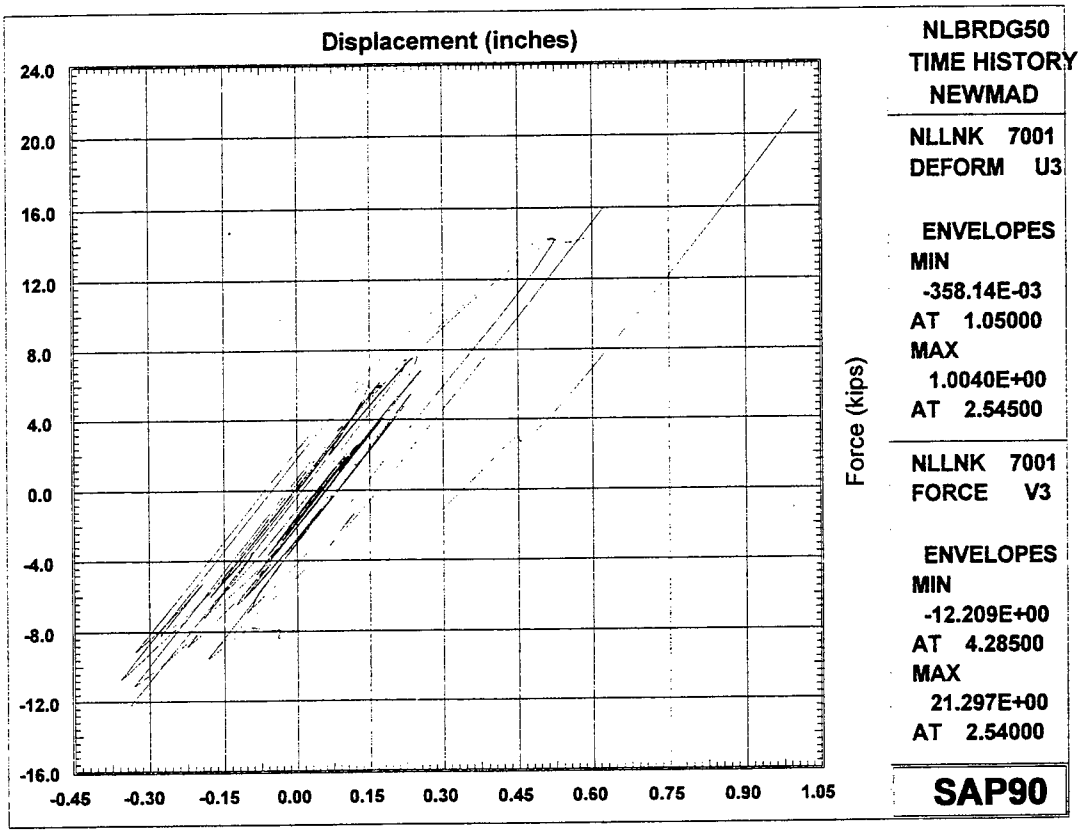

Figure 56: Typical Pier Bearing Response (Transverse Response - Design Earthquake)

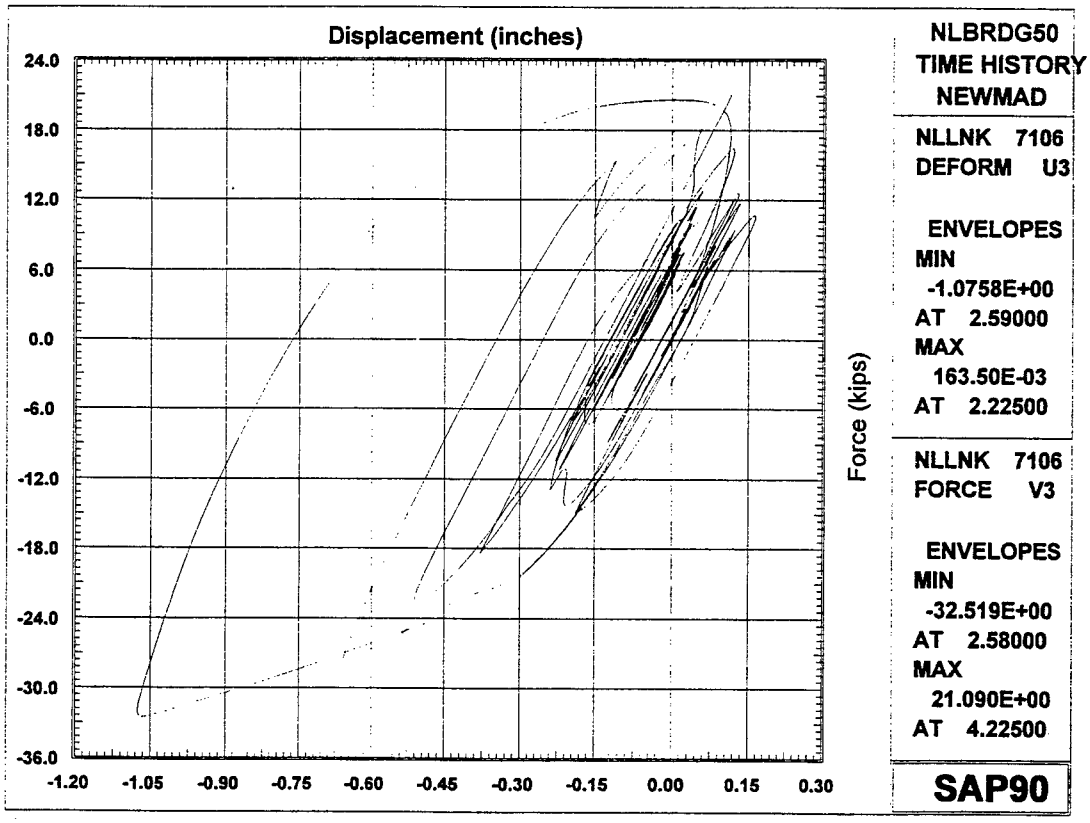

Figure 57: Typical End Bent Bearing Response (Transverse Response - Design Earthquake)

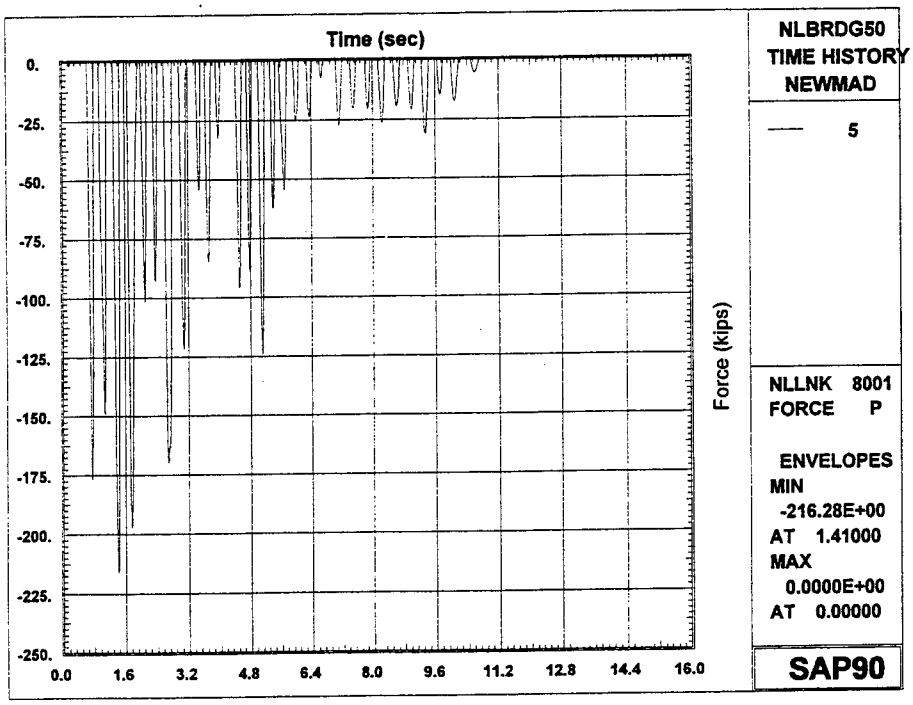

Figure 58: Typical Displacement History of Expansion Dam (Longitudinal Response - Design Earthquake)

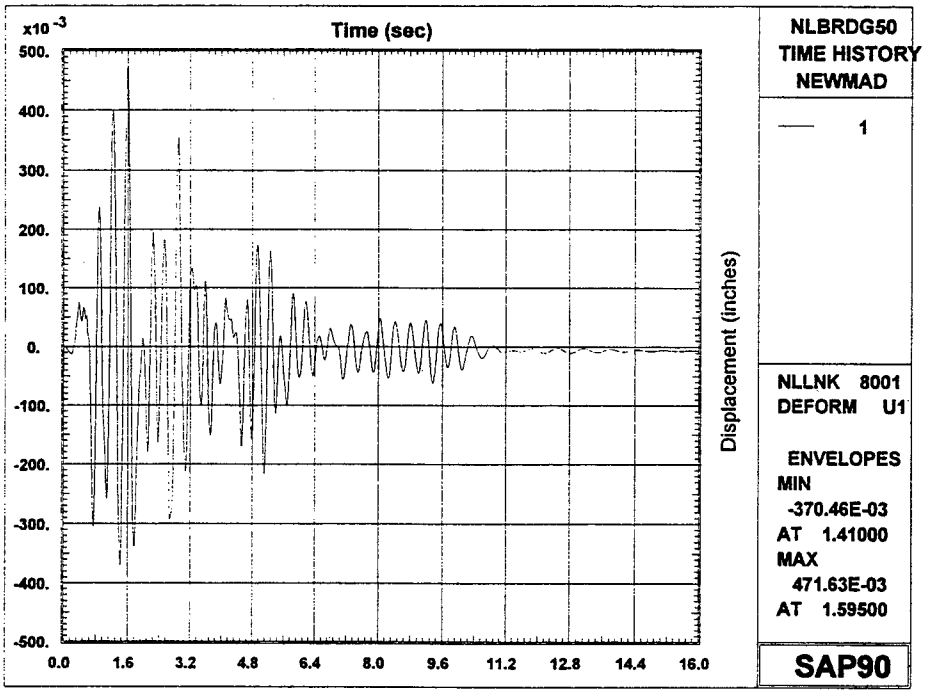

Figure 59: Force History of Expansion Dam Element (Longitudinal Response - Design Earthquake)

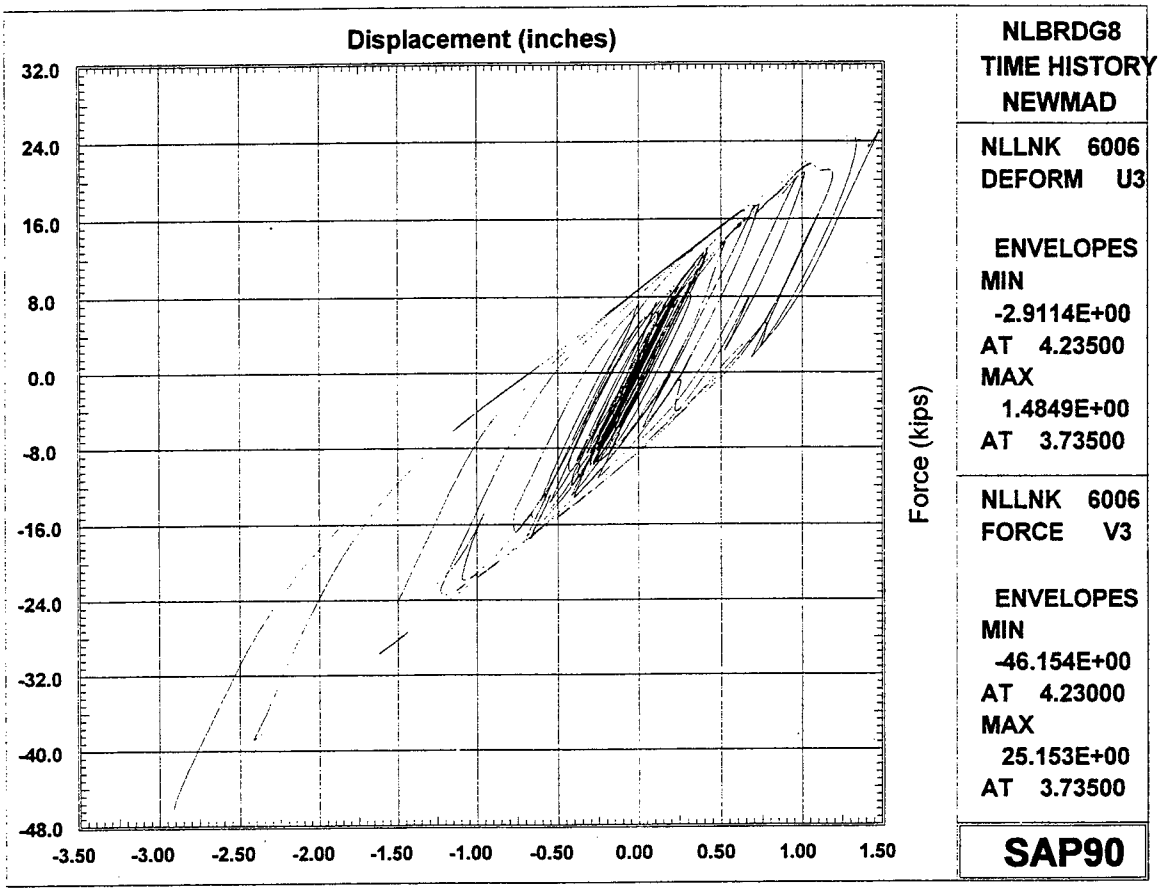

Figure 60: Typical Pier Bearing Response (Transverse Response - Maximum Earthquake)

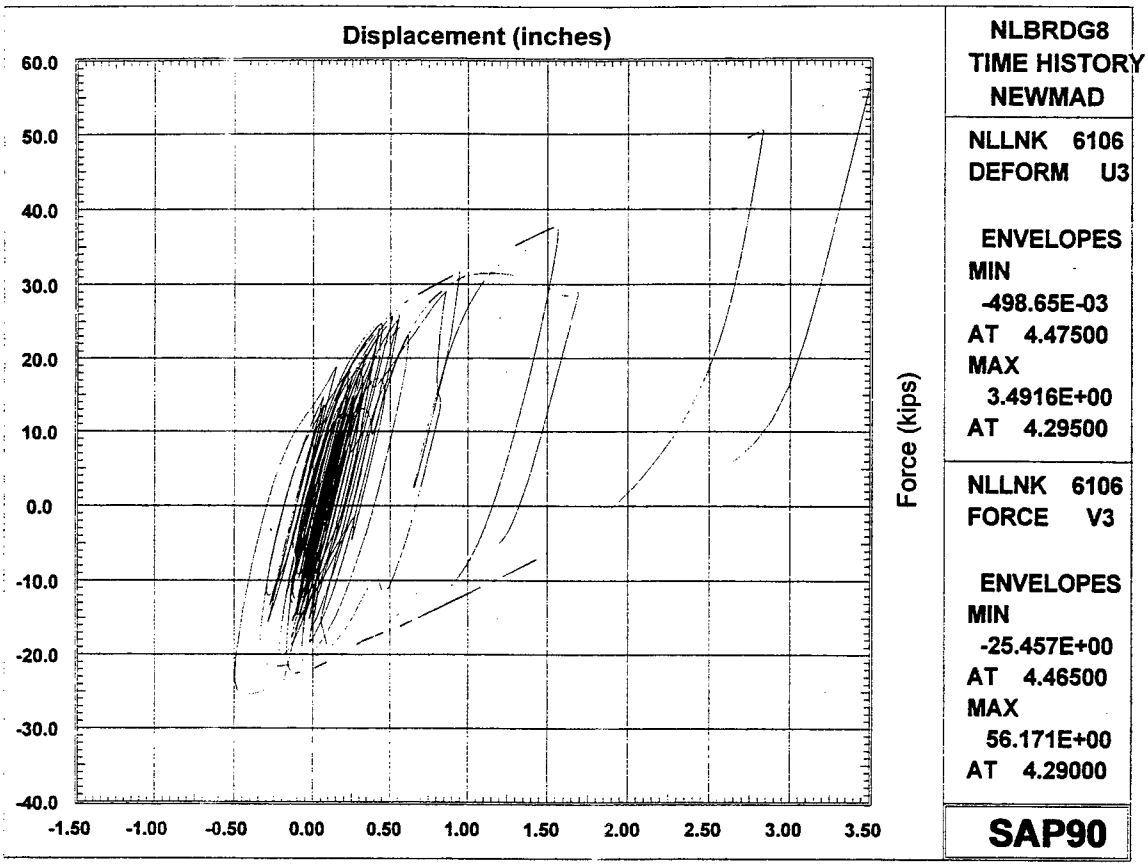

Figure 61: Typical End Bent Bearing Response (Transverse Response - Maximum Earthquake)

APPENDIX A

EXPERIMENTAL DATA

A.1 MEASURED DATA

A load cell, accelerometers, and an LVDT measured pullback force, deck accelerations, and bearing displacement histories, respectively. Representative examples of these records measured during pull 1A follow. The first acceleration set is from a midspan location (Black), the second set is from above the end bent bearing location (white).

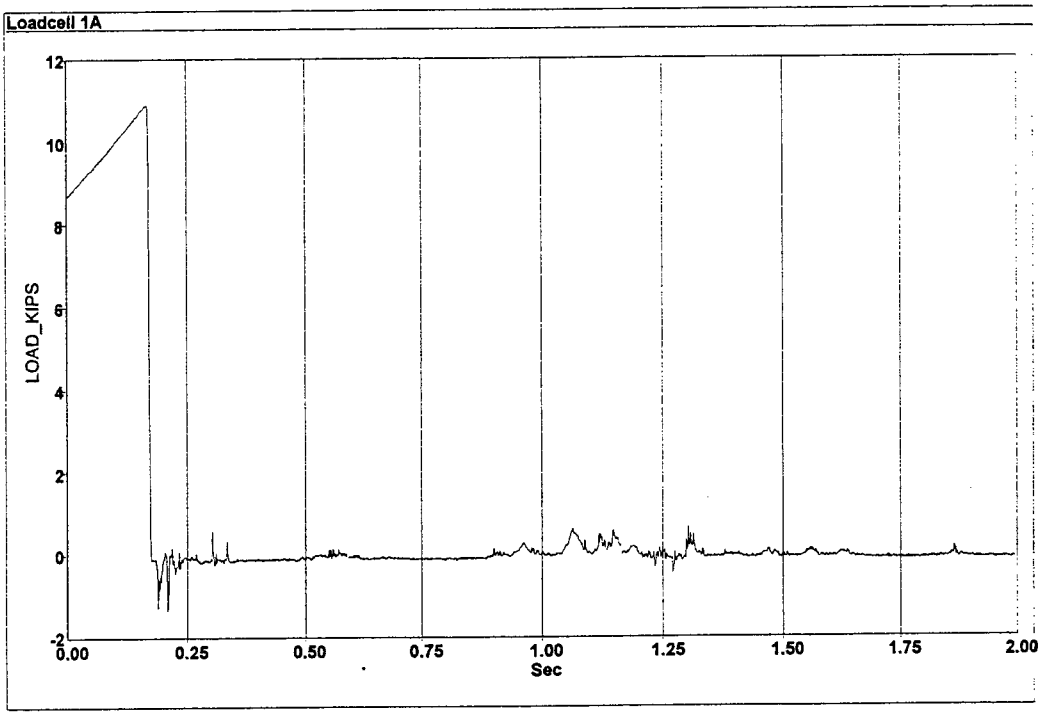

Figure A1: Load Cell History for Pull 1A

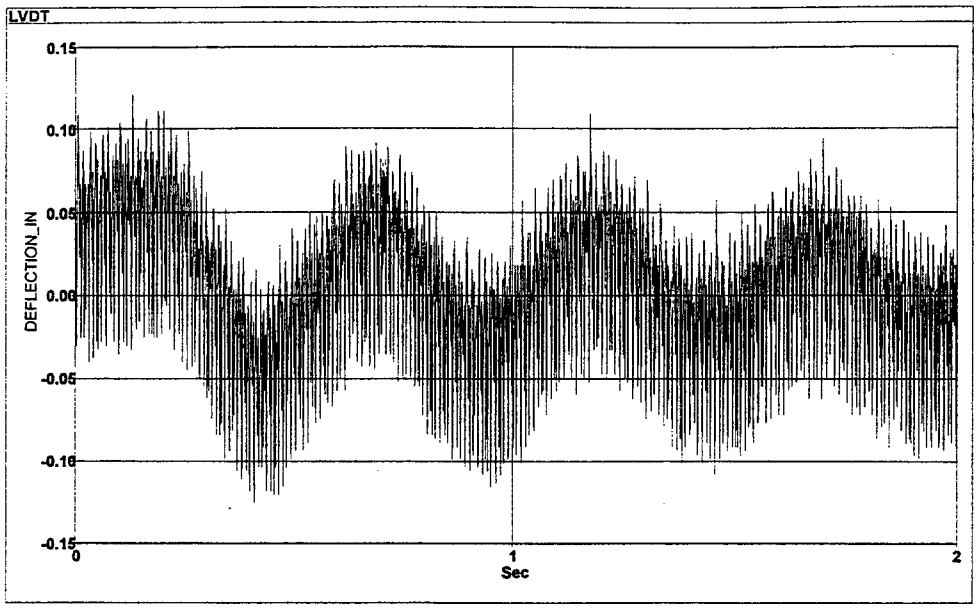

Figure A2: LVDT Measured Bearing Displacement - Pull 1A

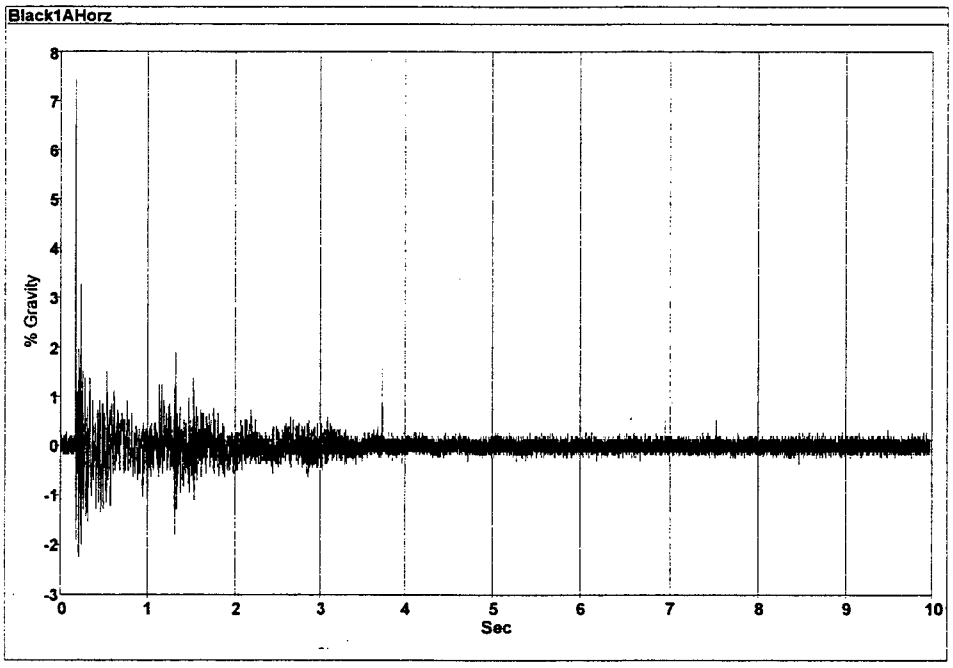

Figure A3: Transverse Acceleration - Black

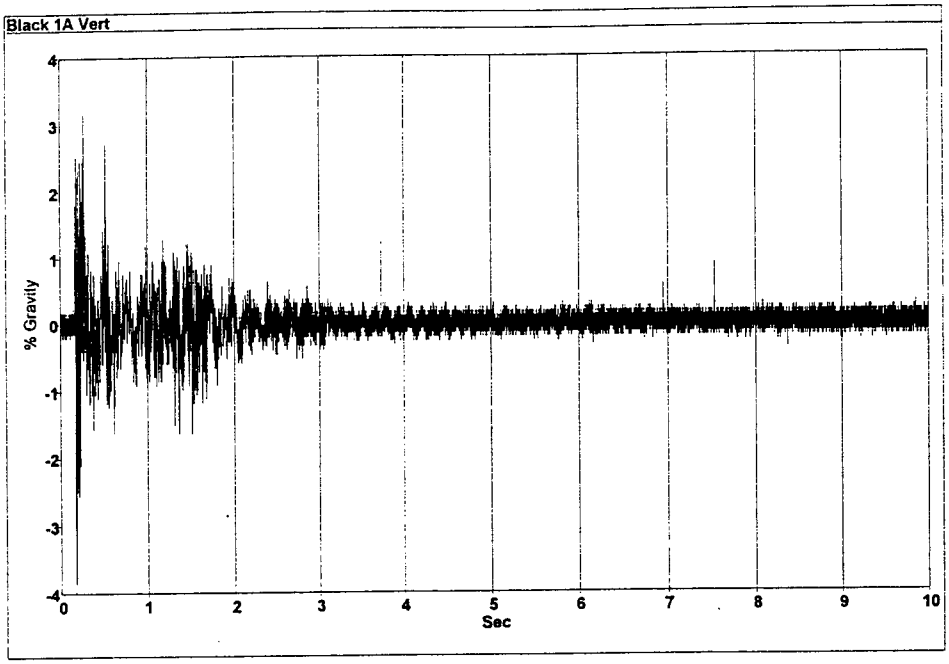

Figure A4: Vertical Acceleration - Black

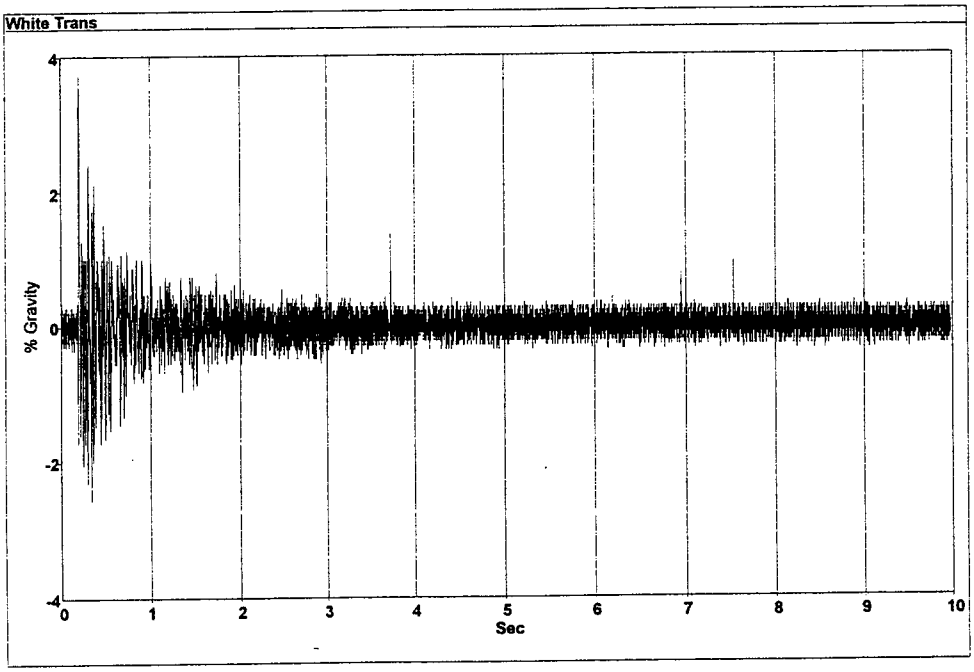

Figure A5: Transverse Acceleration - White

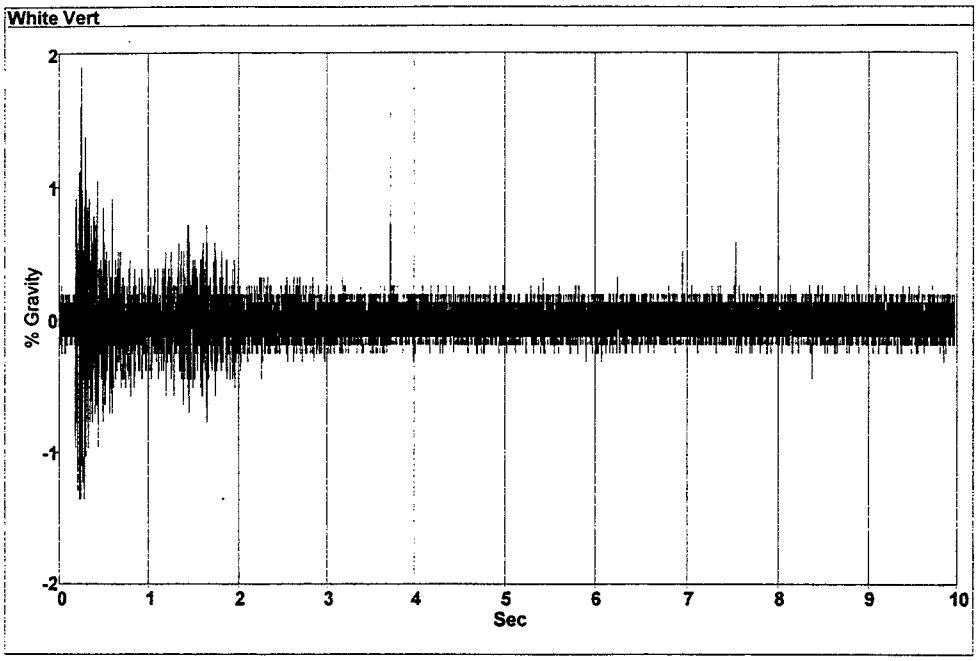

Figure A6: Vertical Acceleration - White

APPENDIX B

ANALYSIS OF EXPERIMENTAL DATA

B.1 ANALYSIS OF DATA

Representative examples of the load cell, accelerometer, and LVDT bearing displacement histories measured during pullback, quick-release testing were shown in Appendix A. Following, are plots of the FFT's of those records along with the smoothed records from which the log-decrement damping ratio was calculated.

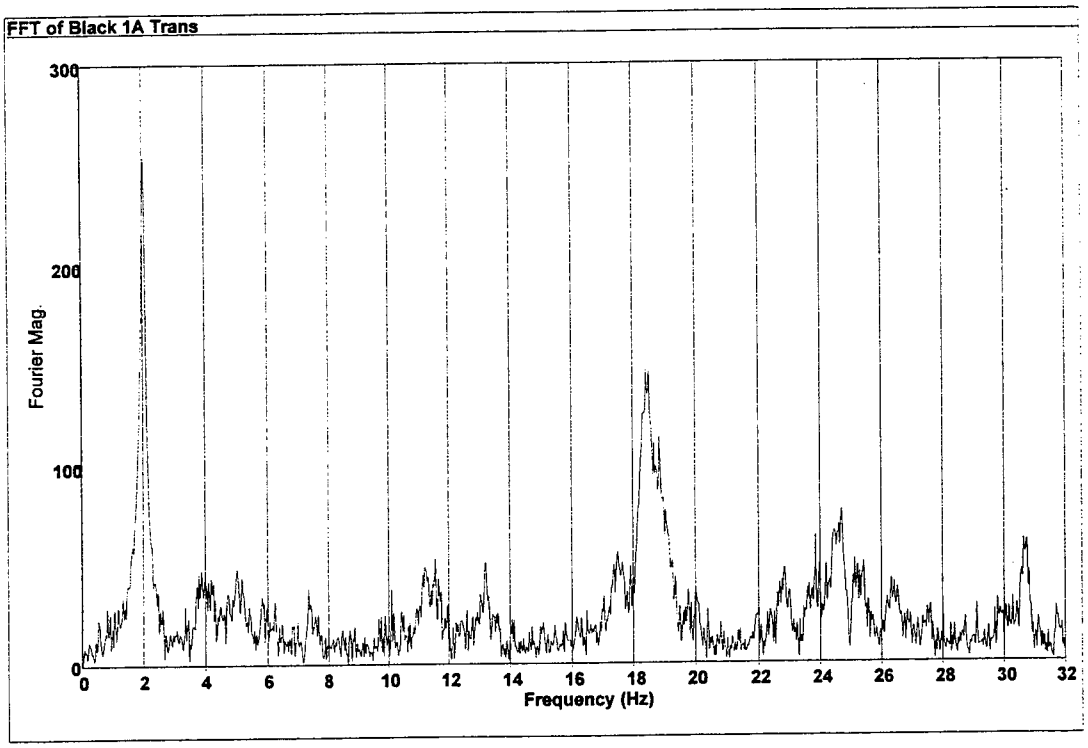

Figure B1: FFT of Figure A.3 (Transverse Acceleration - Black)

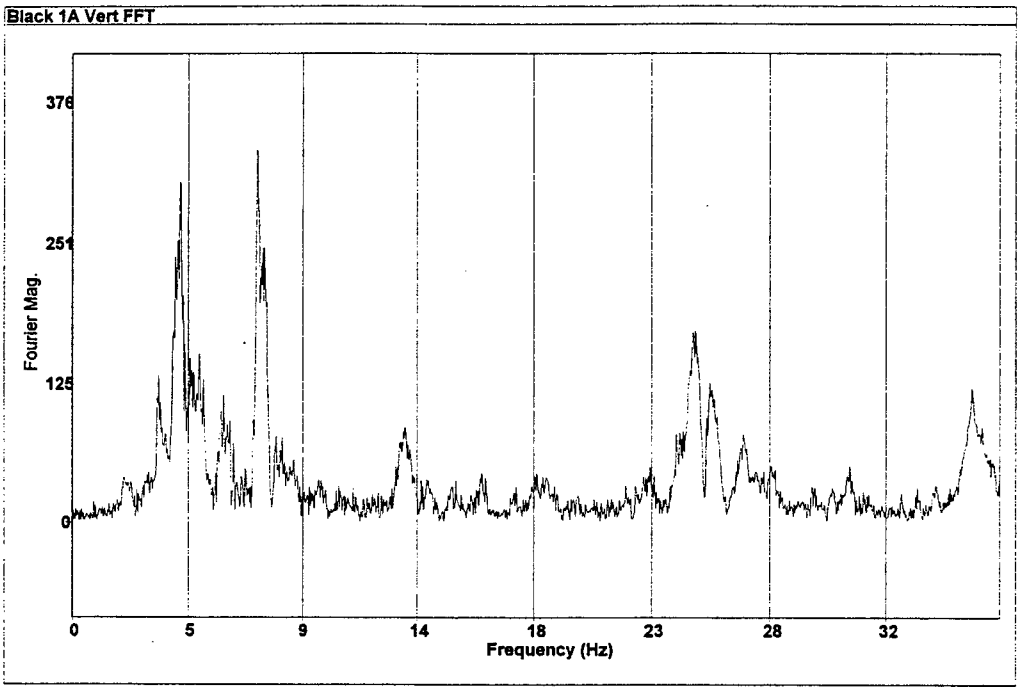

Figure B2: FFT of Figure A.4 (Vertical Acceleration - Black)

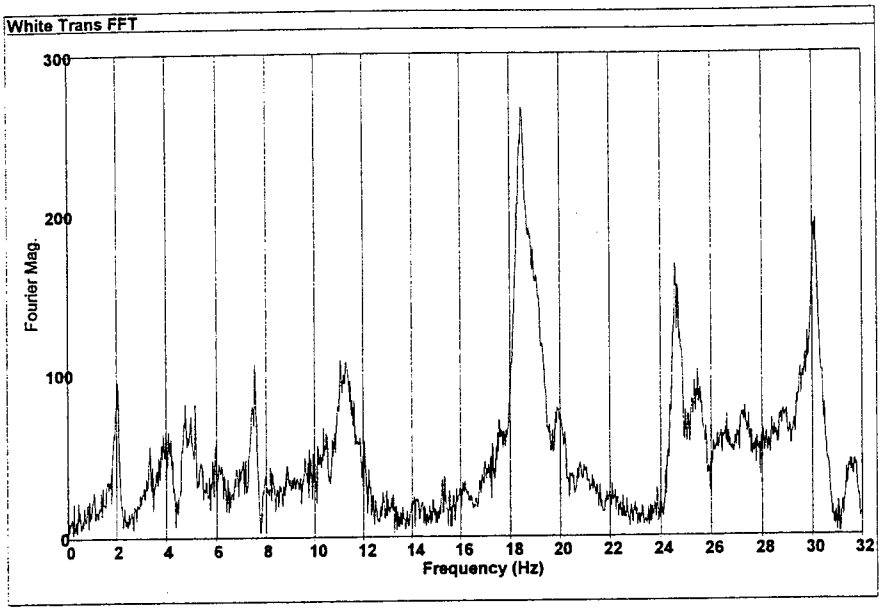

Figure B3: FFT of Figure A.5 (Transverse Acceleration - White)

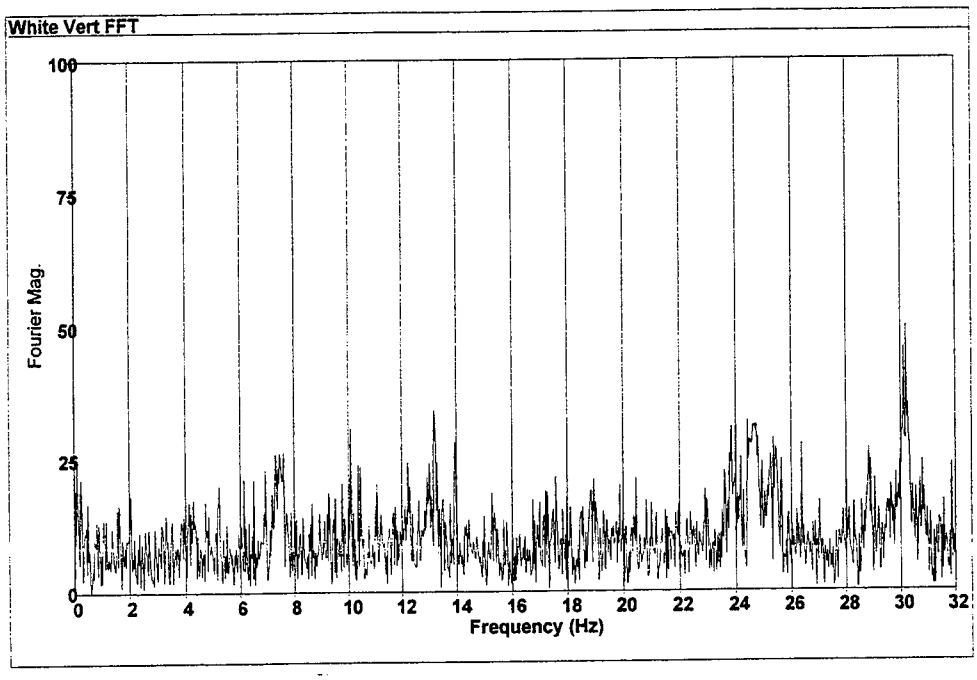

Figure B4: FFT of Figure A.6 (Vertical Acceleration - White)

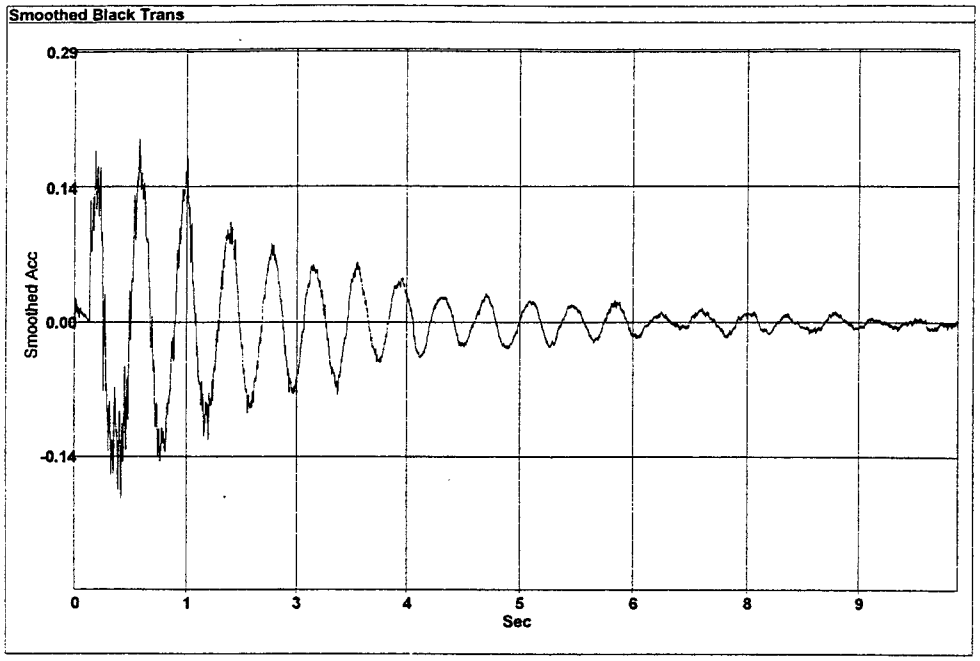

Figure B5: Smoothed Acceleration Record - Transverse Black

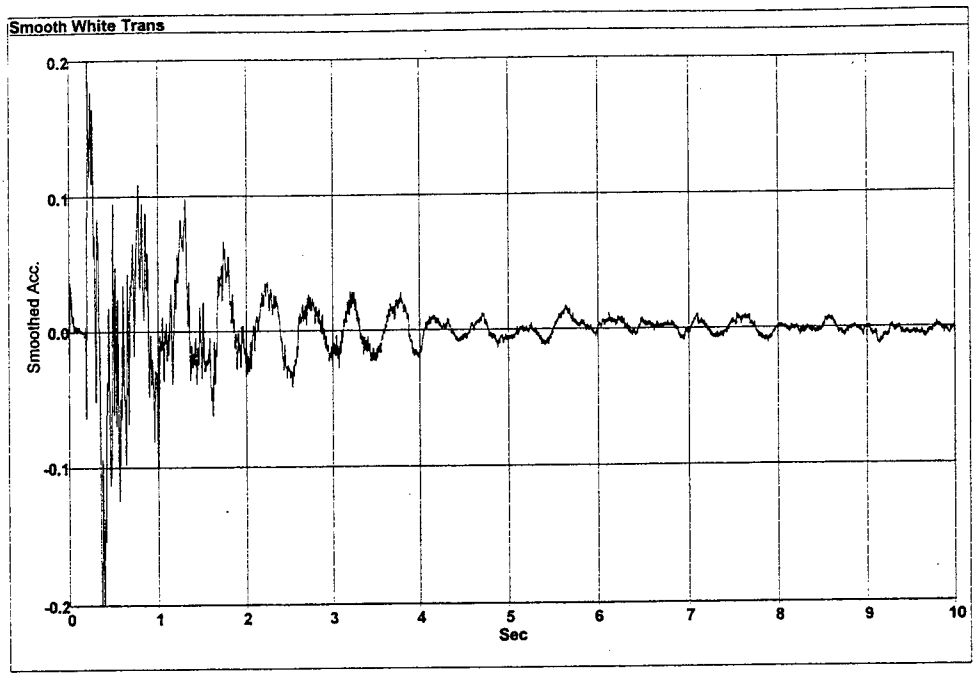

Figure B6: Smoothed Acceleration Record - Transverse White

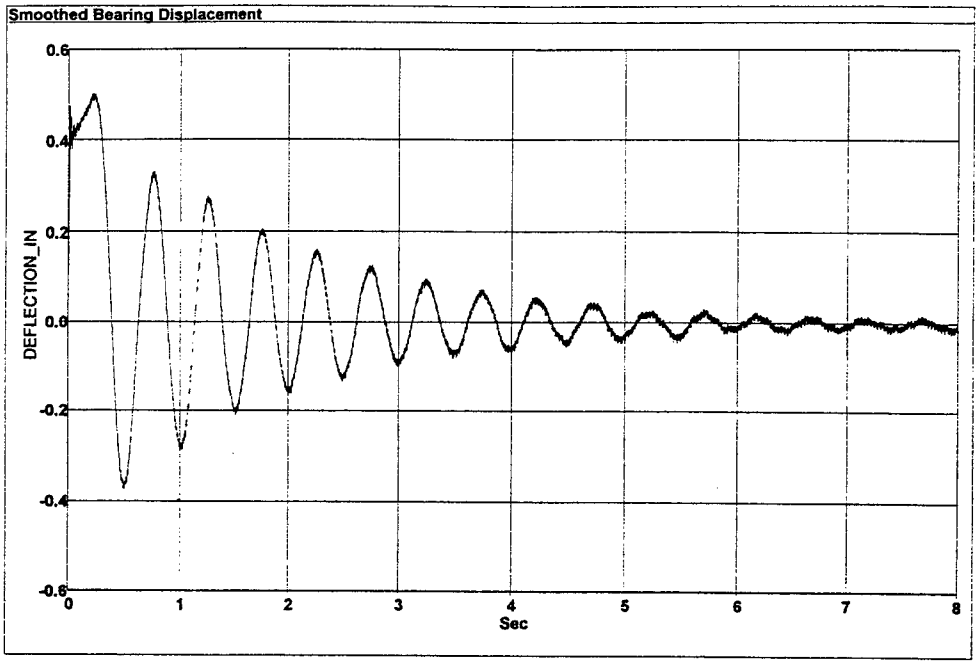

Figure B7: Smoothed Bearing Displacement Record

APPENDIX C

THEORY OF OPTIMIZATION PROGRAM

C.1 OPTIMIZATION PROGRAM

This section is an excerpt from Frangopol and Klisinski (1989) and is provided as a convenience for those who wish further explanation of the theory behind the optimization algorithm. A bold letter indicates a matrix while normal typeface indicates a scalar.

In the optimization program a vector base is defined in the n-dimensional space. The dimension of this space is determined by the number of optimization variables. The vector base constitutes the matrix

$$\mathbf{B} = [\mathbf{b}_1, \mathbf{b}_2, ..., \mathbf{b}_n]$$

This matrix has orthonormal properties, in which case any two of its columns (base vectors) satisfy the following requirement

$$\mathbf{b}_i \bullet \mathbf{b}_j = 0 \quad \text{if } i \neq j$$
$$\mathbf{b}_i \bullet \mathbf{b}_j = 1 \quad \text{if } i = j$$

where $\bullet$ denotes inner product.

The initial matrix is usually devised in terms of the unit matrix but it can change later on. Search directions are obtained when the base matrix is multiplied by the adequate step vectors

$$\mathbf{s}_i = s_i \mathbf{e}_i$$

where s_i denotes the step size and $\mathbf{e}_i$ is the unit vector

$$\mathbf{e}_i = [0_1, 0_2, ..., 0, 1_i, 0, ..., 0_n]$$

This vector has a unit component only at position i. Therefore:

$$\mathbf{B}s_i = s_i\mathbf{b}_i$$

Starting from the initial base point with an initial step value, the search proceeds according to the following scheme:

1. Compute the objective function F at the initial point and $F_{min} := F$, where := means substitute the left side with the right side;

2. For each i from 1 to n repeat the next two steps (i.e., 3 and 4).

3. Compute $F(\mathbf{x} + \mathbf{B}s_i)$.

4. If $F(\mathbf{x} + \mathbf{B}s_i) < F_{min}$ then
   $\mathbf{x} := \mathbf{x} + \mathbf{B}s_i$
   $F_{min} := F$
   $s_i = \alpha s_i$ where: $\alpha > 1$
   else
   $s_i := \beta s_i$ where: $-1 < \beta < 0$

5. If for all i the search was unsuccessful (i.e., F_{min} was not improved), then:
   (a) Perform the base change;
   (b) continue from point 1 in the preceding scheme; or
   else (a) continue from point 2.

The base change operation substitutes the actual base **B** by another orthonormal base, which takes into account the previous results, especially the direction of maximum improvement. In the preceding scheme, the loop 2-4 for each base vector is treated as one optimization step. The program searches for any improvement of the objective function in all base directions and when the search is successful, an increase in the step size in the particular direction is produced. If the search is unsuccessful, the program will search in the opposite direction using a smaller step size during the next loop. This procedure is repeated until there is no improvement. In such a case the base matrix is changed and the search begins from point 1 using a new initial starting point $\dot{\mathbf{x}}$ and a new base.

The only remaining problem is that the optimization program has not been specifically designed for structural optimization, but rather as a general purpose program, and may not be the most efficient. It can be, however, easily changed and other algorithms may be used. The optimization program uses two control parameters: accuracy and initial step size. The accuracy parameter controls a termination condition. When, after a few optimization steps, the improvement of the

objective function is smaller than the value of this parameter, the program stops. If the new value of the objective function is denoted by F_n and the previous value by F_{n-1}, the termination condition can be expressed as follows

$$\frac{2(F_{n-1} - F_n)}{F_{n-1} + F_n} < accuracy$$

Within the program, all variables are normalized so they vary from 0 to 1. The initial step size is applied to these normalized variables and defines the distance between the initial point and the point at which the new value of the objective function is computed. The input to this program requires also: number of optimization parameters; lower bound of all optimization parameters; upper bound of all optimization parameters; initial values of optimization parameters.

APPENDIX D

OPTIMIZATION PROGRAM

D.1 OPTIMIZATION PROGRAM

This section is a listing of the source code for the basic optimization program used in this research. The program is written in FORTRAN 77 compatible language with some FORTRAN 90 extensions (Microsoft FORTRAN PowerStation, 1993).

```
**********************************************************************
*******
*
      *
*                                   NLOPTVIB
      *
```

```
*
      *
*                  Nonlinear Optimization of Vibrations
      *
*
      *
*     Constrained Minimization Program for Optimizing a
Structural     *
*  Bridge Model Based on Experimentally Measured Natural
Frequencies.  *
*                       Runs SAP90 as a subprogram
      *
*
      *
*      Written By:
      *
*                      BRADLEY N. ROBSON, P.E.
      *
*                      DEPARTMENT OF CIVIL ENGINEERING
      *
*                      UNIVERSITY OF KENTUCKY
      *
*                      LEXINGTON, KENTUCKY  40506-0281
      *
*
      *
*                                  1997
      *
*
      *
*                     As part of Doctoral Research on:
      *
*                     Seismic Isolation of Prestressed
      *
*                        Concrete I-Girder Bridges
      *
*
      *
*****************************************************************
*******
*   MAIN PROGRAM VARIABLES:
      *
*
      *
*      N      - NUMBER OF PARAMETERS TO BE OPTIMIZED
      *
*      X( )   - INITIAL VALUES OF OPTIMIZATION PARAMETERS
      *
```

```
*       XL( ) - LOWER BOUNDS OF X
*
*       XU( ) - UPPER BOUNDS OF X
*
*       NSAMP - # OF EXPERIMENTAL FREQUENCIES TO USE IN OBJECTIVE
*
*               FUNCTION EVALUATION; READ FROM FILE NLUS51
*
*       NSPRG - # LINEAR SPRING SETS IN SAP90 FILE
*
*       NNLP  - # NONLINEAR PROPERTY SETS
*
*       EXPFREQ( ) - EXPERIMENTALLY DETERMINED FREQUENCIES
*
*       SAPFREQ( ) - ANALYTICAL FREQUENCIES FROM SAP90
*
*       SPRGK( )   - LINEAR SPRING STIFFNESSES
*
*       SPRGNL( )  - SPRING STIFFNESSES OF NONLINEAR SPRINGS
*
*       YMOD( )    - YOUNG'S MODULUS FOR SLAB & BEAMS
*
*
*
**********************************************************************
*******
      INCLUDE 'flib.fi'
      INCLUDE 'flib.fd'

      COMMON/STIFF/EXPFREQ(10),SAPFREQ(25),SPRGK(6),SPRGNL(6)
      COMMON/VLIMITS/X(50),XL(50),XU(50)
      CHARACTER*20 ADD(4)
      CHARACTER*6  COM
      CHARACTER*3  DOF(6)
      CHARACTER*2  ENAME
      CHARACTER*10 NLDOF(6)
      CHARACTER*20 PROG
      CHARACTER*90 INPUT(500),BEAMCONC,SLABCONC,NLSPRING
      LOGICAL*4 SUCCESS
      DIMENSION XN(50),R(50),YMOD(5)
      DIMENSION D(50,50),T(50),TP(50),S(50),W(50,50),V(50)


      OPEN(UNIT=10,FILE='NLBRDG8',STATUS='UNKNOWN')
      OPEN(UNIT=11,FILE='NLUS51',STATUS='UNKNOWN')

      OPEN(UNIT=20,FILE='OPTIMIZE.OUT',STATUS='UNKNOWN')

1000  FORMAT(A4,3F10.2,6(A3,F10.2))
```

```
1100   FORMAT(A20,A3,F6.0)
1150   FORMAT(A20,A3,F6.0,2X,'UY=',F6.0)
1200   FORMAT(A10,F10.0)
1300   FORMAT(A2,F8.0)
2000   FORMAT(A90:)
2050   FORMAT(A10,F10.0,2X,'KE=',F10.0)
2100   FORMAT(A2,F8.0,3X,'U=0.167')

       READ(11,*) NSAMP
       READ(11,*)(EXPFREQ(I),I=1,NSAMP)
       NSPRG = 2
*****************************************************************
*******
*         FIND LINE NUMBERS OF 'SPRING', 'MATERIALS', 'NLPROP',
*               & End of File IN SAP INPUT FILE
*****************************************************************
*******
       PRINT*, 'BEGINNING SEARCH THROUGH FILE NLBRDG8'
       REWIND(10)

       DO 10 I=1,500
          READ(10,2000,END=20) INPUT(I)
          LINEND = I
10     CONTINUE

20     PRINT*, 'STORED SAP INPUT FILE'
       NNLP = 0
       REWIND(10)

       DO 40 K=1,500
          READ(10,'(A6)',END=50) COM
          IF(COM.EQ.'SPRING') THEN
             LINESPRG = K
             DO 30 I=1,NSPRG
                READ(10,1100)ADD(I),DOF(1),SPRGK(I)
30           CONTINUE
             X(1) = SPRGK(1)
          ELSE IF(COM.EQ.'NLPROP') THEN
             NNLP = NNLP + 1
             IF (NNLP.LT.2) THEN
                LINEPROP = K + NSPRG
                READ(10,'(A90)')NLSPRING
                DO 35 I=1,6
                   READ(10,1200)NLDOF(I),SPRGNL(I)
35              CONTINUE
                X(2) = SPRGNL(2)
                X(3) = SPRGNL(5)
                X(4) = SPRGNL(6)
             ENDIF
```

```
         ELSE IF(COM.EQ.'MATERI') THEN

            LINECONC = K + NSPRG + 7
            READ(10,'(A90)')BEAMCONC
            READ(10,1300)ENAME,YMOD(1)
            X(5) = YMOD(1)
            READ(10,'(A90)')SLABCONC
            READ(10,1300)ENAME,YMOD(2)
            X(6) = YMOD(2)
            GOTO 60
         ENDIF
40     CONTINUE

50     PRINT*,'################ END OF INPUT FILE
###################'

**** READ UPPER AND LOWER LIMITS OF VARIABLES TO OPTIMIZE FROM
FILE ****

60     N = 6

       DO 70 I=1,N
          READ(11,*)XL(I),XU(I)
70     CONTINUE
**********************************************************************
*******
*       OPTIMIZATION PORTION OF PROGRAM
**********************************************************************
*******
*
* PROGRAM VARIABLES:
*        XN( )   = POSITION OF VARIABLE X( ) IN ITS RANGE; 0< XN()
<1
*        ALPHA   = INCREASE IN STEP SIZE IN SAME DIRECTION
*        BETA    = INCREASE IN STEP SIZE IN OPPOSITE DIRECTION
*        NF      = MAXIMUM # OF OBJECTIVE FUNCTION EVALUATIONS
*        NB      = # LOOPS TO BASE CHANGE ON
*        ST      = INITIAL STEP SIZE (PORTION OF VARIABLE RANGE)
*        ACC     = ACCURACY FOR TERMINATION
*        R( )    = RANGE OF VARIABLES TO BE OPTIMIZED
*        LF      = COUNTER OF OBJECTIVE FUNCTION EVALUATIONS
*        T( ),TP( )= VECTORS OF STEP SIZES
*        D( , )  = DIRECTION MATRIX
*        S( )    = SUM OF ALL SUCCESSFUL STEPS IN DIRECTION
*        V( )    = VECTOR USED IN ORTHOGONALIZATION & NORMALIZATION
*        W( , )  = MATRIX USED IN BASE MATRIX CHANGE

*        IR      = LOGICAL =0 -> OK;   =1 -> ADJUST XN( )
*        IBC     = COUNTER OF # OF BASE MATRIX CHANGES
```

```
*       IS      = # OF T( )'s LESS THAN ACCURACY; QUIT WHEN ALL
N<ACC
*       IK      = COUNTER OF # OF S( )'s < EPSILON
*
*****************************************************************
*******
      EPSI = 1E-7

C  SET Maximum Number of Function Calculations (NF)
      NF = 30

C  SET Number of Loops to Base Change (NB)
C  NB Must be Less Than of Equal to (NF/N)
      NB = 2

C  SET CONTROL PARAMETERS: Accuracy and Initial Step Size
C  SET Initial Step Size (0 TO 1)
      ST = 0.25

C  SET Accuracy (ACC > 0)
C  Controls Termination Condition
      ACC = 0.01

C  SET ALPHA (>1) & BETA (-1< BETA <0)
      ALPHA =  1.618
      BETA  = -0.3819

C  INITIALIZE DIRECTION MATRIX D(I,J)
      DO 90 I=1,N
         DO 80 J=1,N
            D(I,J) = 0.0
80       CONTINUE
         D(I,I) = 1.0
90    CONTINUE

C  CALC VARIABLE RANGES
      DO 100 I=1,N
         R(I) = XU(I) - XL(I)
         IF(R(I).LT.EPSI) THEN
            R(I) = EPSI
         ENDIF
         XN(I) = (X(I) - XL(I)) / R(I)
         TP(I) = ST
100   CONTINUE
***************************** 1ST SAP RUN
*******************************
      PROG = 'SAP NLBRDG8'
      SUCCESS = SYSTEMQQ(PROG)
```

```
**************** 1ST OBJECTIVE FUNCTION EVALUATION
*******************
      CALL OBJECT(FMIN,N,NSAMP)

*!!!!!!!!!!!!!!!!!!!!!!!!!!!!!!!!!!!
*      BASE MATRIX CHANGE LOOP      !
*!!!!!!!!!!!!!!!!!!!!!!!!!!!!!!!!!!!
      LF=0

200   DO 220 I=1,N
         T(I) = 0.0
         DO 210 J=1,N
            T(I) = T(I) + D(J,I)*TP(J)
210      CONTINUE
         S(I) = 0.0
220   CONTINUE

      IBC = 0
230   IBC = IBC + 1
      IS = 0
*!!!!!!!!!!!!!!!!!!!!!!!!!!!!!!!!!!!
*      ENTER MAIN LOOP --> TO 500   !
*!!!!!!!!!!!!!!!!!!!!!!!!!!!!!!!!!!!
      DO 500 K=1,N
         IR=0
         IF(ABS(T(K)).LT.ACC)THEN
            IS = IS + 1
            GOTO 500
         ENDIF


         DO 300 I=1,N
            XN(I) = XN(I) + D(I,K)*T(K)
            IF(XN(I).LT.0.) THEN
               IR=1
            ENDIF
            IF(XN(I).GT.1.) THEN
               IR=1
            ENDIF
            X(I) = XL(I) + XN(I)*R(I)
300      CONTINUE


         IF(IR.EQ.1)THEN
            DO 310 I=1,N
               XN(I) = XN(I) - D(I,K)*T(K)
310         CONTINUE
            T(K) = BETA * T(K)
            GOTO 500
```

```
      END IF
*%%%%%%%%%%%%%%%%%%%%%%%%%%%%%%%%%%%%%%%%%%%%%%%%%%%%%%%%%%%%%%%%%%%%%
%%%%%%%
*      REWRITE SAP INPUT FILE WITH NEW ADJUSTED PROPERTIES
*     STORE NEW SPRING STIFFNESSES & MODULI OF ELASTICITY TO
ARRAYS
*%%%%%%%%%%%%%%%%%%%%%%%%%%%%%%%%%%%%%%%%%%%%%%%%%%%%%%%%%%%%%%%%%%%%%
%%%%%%%
      SPRGK(1) = X(1)
      SPRGK(2) = SPRGK(1)
      SPRGNL(2)  = X(2)
      SPRGNL(3)  = SPRGNL(2)
      SPRGNL(5)  = X(3)
      SPRGNL(6)  = X(4)
      YMOD(1)    = X(5)
      YMOD(2)    = X(6)
************ FIND SPRING IN INPUT FILE AND WRITE NEW STIFFNESSES


      REWIND(10)
      DO 370 KK=1,500
         READ(10,'(A6)') COM
         IF(COM.EQ.'SPRING') THEN
            DO 330 I=1,NSPRG
              WRITE(10,1150)ADD(I),DOF(1),SPRGK(I),SPRGK(I)
330         CONTINUE
            DO 340 I = (LINESPRG + NSPRG + 1), (LINEPROP + 1)
               WRITE(10,'(A90)') INPUT(I)
340         CONTINUE
            DO 343 I = 1,6
               WRITE(10,2050) NLDOF(I),SPRGNL(I),SPRGNL(I)
343         CONTINUE
            DO 345 I = (LINEPROP + 8), (LINECONC + 1)
               WRITE(10,'(A90)') INPUT(I)
345         CONTINUE
            WRITE(10,2100)ENAME,YMOD(1)
            WRITE(10,'(A90)') INPUT(LINECONC + 3)
            WRITE(10,2100)ENAME,YMOD(2)
            DO 350 I = LINECONC + 5, LINEND
               WRITE(10,'(A90)') INPUT(I)
350         CONTINUE
            GOTO  380
         ENDIF
370   CONTINUE
*%%%%%%%%%%%%%%%%%%%%%%%%%%%%%%%%%%%%%%%%%%%%%%%%%%%%%%%%%%%%%%%%%%%%%
%%%%%%%
*      FINISHED REWRITING SAP INPUT FILE WITH NEW ADJUSTED
PROPERTIES
```

```
*%%%%%%%%%%%%%%%%%%%%%%%%%%%%%%%%%%%%%%%%%%%%%%%%%%%%%%%%%%%%%%%%%%%%%%%
%%%%%%

****************************** RUN SAP
*********************************
380       SUCCESS = SYSTEMQQ(PROG)
          PRINT*,'SAP RUN COMPLETE'

****************** OBJECTIVE FUNCTION EVALUATION
**********************
          CALL OBJECT(ERROR,N,NSAMP)

          LF = LF + 1
*** IF IMPROVEMENT, TAKE STEP IN SAME DIRECTION; ELSE, STEP
BACKWARD
          IF(ERROR.LT.FMIN) THEN
             FMIN = ERROR
             S(K) = S(K) + T(K)
             T(K) = ALPHA * T(K)
          ELSE
             DO 390 I=1,N
                XN(I) = XN(I) - T(K)*D(I,K)
390          CONTINUE
             T(K) = BETA * T(K)
          ENDIF

500    CONTINUE
*!!!!!!!!!!!!!!!!!!!!!!!!!!!!!!!!!!!!!!!!!!!!!!!!!!!!!!!!!!!!!!!!!!!!!!!
!!!!!!!
*       CHECK FOR CONVERGENCE ==> FINISHED IF
*!!!!!!!!!!!!!!!!!!!!!!!!!!!!!!!!!!!!!!!!!!!!!!!!!!!!!!!!!!!!!!!!!!!!!!!
!!!!!!!
       IF(LF.GE.NF.OR.IS.EQ.N) THEN
          GOTO 640
       ENDIF

       IF(IBC.LT.NB) THEN
          GOTO 230
       ENDIF
       IK=0

       DO 510 I=1,N
          IF(ABS(S(I)).GT.EPSI) THEN
             IK=IK+1
          ENDIF
510    CONTINUE

       IF(IK.EQ.0) THEN
          GOTO 230
```

```
      ------
************************* BASE MATRIX CHANGE
***************************
      DO 520 I=1,N
         TP(I)=0.
         DO 520 J=1,N
            TP(I) = TP(I) + D(I,J)*T(J)
520   CONTINUE


      DO 530 J=1,N
         DO 530 I=1,N
            NJ= N + 1 - J
            W(I,NJ) = D(I,NJ)*S(NJ)
            IF(J.EQ.1)  THEN
               GOTO 530
            ENDIF
            W(I,NJ) = W(I,NJ+1) + W(I,NJ)
530   CONTINUE


      DO 540 I=1;N-1
         DO 540 J=I+1,N
            W(I,J)=0.0
540   CONTINUE
************************** ORTHOGONALIZATION
***************************
      DO 630 K=1,N
         DO 550 I=1,N
            V(I) = W(I,K)
550      CONTINUE


         IF(ABS(V(K)).LT.EPSI) THEN
            V(K) = EPSI
         ENDIF

         IF(K.EQ.1) THEN
            GOTO 580
         ENDIF


         DO 570 J=1,K-1
            YY=.0
            DO 560 I=1,N
               YY = YY + W(I,K)*D(I,J)
560         CONTINUE
            DO 570 I=1,N
               V(I) = V(I) - YY*D(I,J)
```

```
570       CONTINUE
************************** NORMALIZATION
*****************************
580       YY = 0.0

          DO 590 I=1,N
             YY = YY + V(I)*V(I)
590       CONTINUE

          YY=SQRT(YY)
          IF(ABS(YY).LT.EPSI)THEN
             DO 610 I=1,N
                DO 600 J=1,N
                   D(I,J) = 0.0
600             CONTINUE
                D(I,I) = 1.0
610          CONTINUE
             GOTO 200
          END IF


          DO 620 I=1,N
             D(I,K) = V(I)/YY
620       CONTINUE
630    CONTINUE
************************ End of Orthogonalization
************************
*       LOOP BACK TO 200 UNTIL OBJECTIVE FUNCTION IS MINIMIZED
       *
**********************************************************************
*******

       GOTO 200
****************** FINAL RESULTS  **************
640    DO 650 I=1,N
          X(I) = XL(I) + XN(I)*R(I)
650    CONTINUE


       STOP
       END

**********************************************************************
*******
       SUBROUTINE OBJECT(ERROR,N,NSAMP)
**********************************************************************
*******
*                      OBJECTIVE FUNCTION TO MINIMIZE
*
```

```
*           MODERR( )   = ABSOLUTE ERROR IN THE FREQUENCY OF
*                         THE 4 OPTIMIZED MODES
*           ERROR       = SUM OF ABSOLUTE ERRORS IN 4 OPTIMIZED
MODES
*
**********************************************************************
*******
      COMMON/STIFF/EXPFREQ(10),SAPFREQ(25),SPRGK(6),SPRGNL(6)
      COMMON/VLIMITS/X(50),XL(50),XU(50)
      REAL*4 MODERR(32)
      CHARACTER*8 ISMODE
      CHARACTER*20 BEGIN

      OPEN(UNIT=20,FILE='OPTIMIZE.OUT',STATUS='UNKNOWN')
      OPEN(UNIT=12,FILE='NLBRDG8.OUT',STATUS='UNKNOWN')

      OPEN(UNIT=21,FILE='ROSEFUNC',STATUS='UNKNOWN')

1000  FORMAT(A20,F12.4)
2000  FORMAT(7X,40H     LOWER           TRIAL           UPPER/
     C7X,40H      LIMIT           VALUE           LIMIT/)
2100  FORMAT(3H  X,I2,2H =,F10.1,5X,F11.1,3X,F12.1)
2200  FORMAT(12X,43H  SAP-90        EXPERIMENTAL          MODAL  /
     C12X,41H FREQUENCY       FREQUENCY            ERROR/)
2300  FORMAT(6H  MODE,I3,2H =,F8.2,9X,F8.2,8X,F8.2)


      REWIND(12)

      DO 140 I=1,9999
         READ(12,'(A8)',END=150) ISMODE
         IF(ISMODE.EQ.'    MODE') THEN
            GOTO 160
         ENDIF
140   CONTINUE

150   PRINT*,'ERROR READING FREQUENCIES FROM OUTPUT FILE'

160   READ(12,'(A8)')ISMODE
      READ(12,'(A8)')ISMODE

      DO 200 I=1,14
         READ(12,1000)BEGIN,SAPFREQ(I)
200   CONTINUE

      ERROR = 0.0
      MODERR(1) = ABS(SAPFREQ(1) - EXPFREQ(1))
      MODERR(2) = ABS(SAPFREQ(2) - EXPFREQ(2))
      MODERR(3) = ABS(SAPFREQ(4) - EXPFREQ(3))
```

```
      MODERR(4) = ABS(SAPFREQ(14) - EXPFREQ(4))

      DO 300 I=1,NSAMP
         ERROR = ERROR + MODERR(I)
300   CONTINUE

      WRITE(20,*)'        '
      WRITE(20,*)'-------------------------------'
      WRITE(20,*)'|     MODEL PROPERTIES        |'
      WRITE(20,*)'-------------------------------'
      WRITE(20,*)'        '
      WRITE(20,2000)

      DO 400 I=1,N
         WRITE(20,2100)I,XL(I),X(I),XU(I)
400   CONTINUE

      WRITE(20,*)'        '
      WRITE(20,*)'>>>>>>>>>>>>>>>>>>>>>>>>>>>>>>>'
      WRITE(20,*)'      RESULTS AND ERRORS      >'
      WRITE(20,*)'>>>>>>>>>>>>>>>>>>>>>>>>>>>>>>>'
      WRITE(20,*)'        '
      WRITE(20,2200)
*%%%%%%%%%%%%%%%%%%%%%%%%%%%%%%%%%%%%%%%%%%%%%%%%%%%%%%%%%%%%%%%%%%%%%%%
%%%%%%%
*       WRITE CALCULATED SAP FREQUENCIES TO OPTIMIZE.OUT
*%%%%%%%%%%%%%%%%%%%%%%%%%%%%%%%%%%%%%%%%%%%%%%%%%%%%%%%%%%%%%%%%%%%%%%%
%%%%%%%
      I1=1
      I2=2
      I5=4
      I10=14

C      DO 500 I=1,NSAMP
      WRITE(20,2300)I1,SAPFREQ(1),EXPFREQ(1),MODERR(1)
      WRITE(20,2300)I2,SAPFREQ(2),EXPFREQ(2),MODERR(2)
      WRITE(20,2300)I5,SAPFREQ(4),EXPFREQ(3),MODERR(3)
      WRITE(20,2300)I10,SAPFREQ(14),EXPFREQ(4),MODERR(4)
C500   CONTINUE

      WRITE(20,*)'        '
      WRITE(20,*)'!!!!!!!!!!!!!!!!!!!!!!'
      WRITE(20,*)'!!!!  TOTAL ERROR  ====> ',ERROR
      WRITE(20,*)'!!!!!!!!!!!!!!!!!!!!!!'
      WRITE(21,*) ERROR
      CLOSE(12)
      RETURN
      END
```

APPENDIX E

BASE ACCELERATION TIME-HISTORIES

E.1 DESIGN EARTHQUAKE

This section shows graphs of the vertical and two orthogonal, horizontal bedrock-level acceleration histories developed in the study by Street et al. (1996) for the 50-year event (i.e. 90% probability of not being exceeded in a 50 year period).

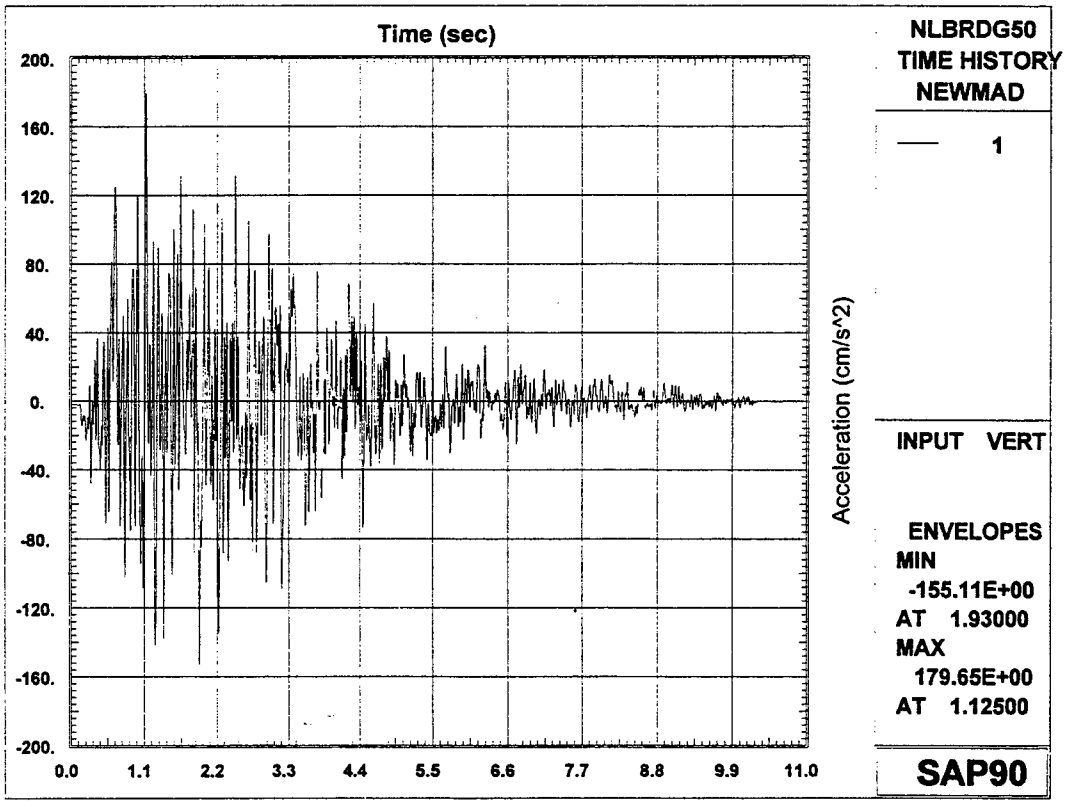

Figure E.1: Vertical Base Acceleration for 50-year Event

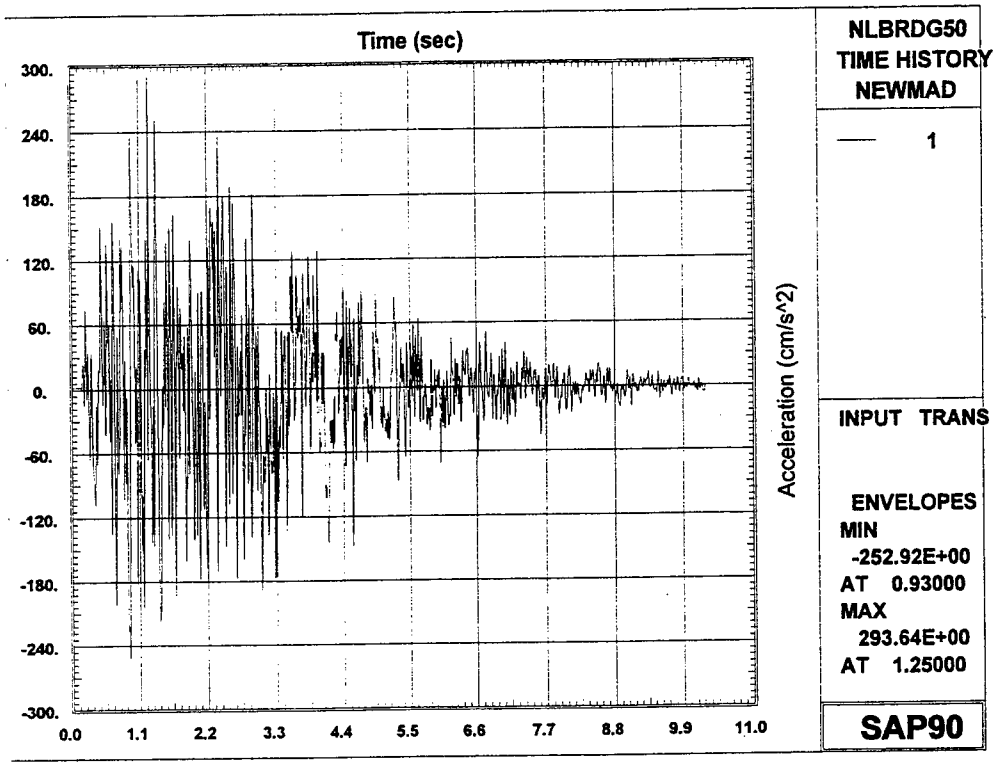

Figure E.2: Transverse Base Acceleration for 50-year Event

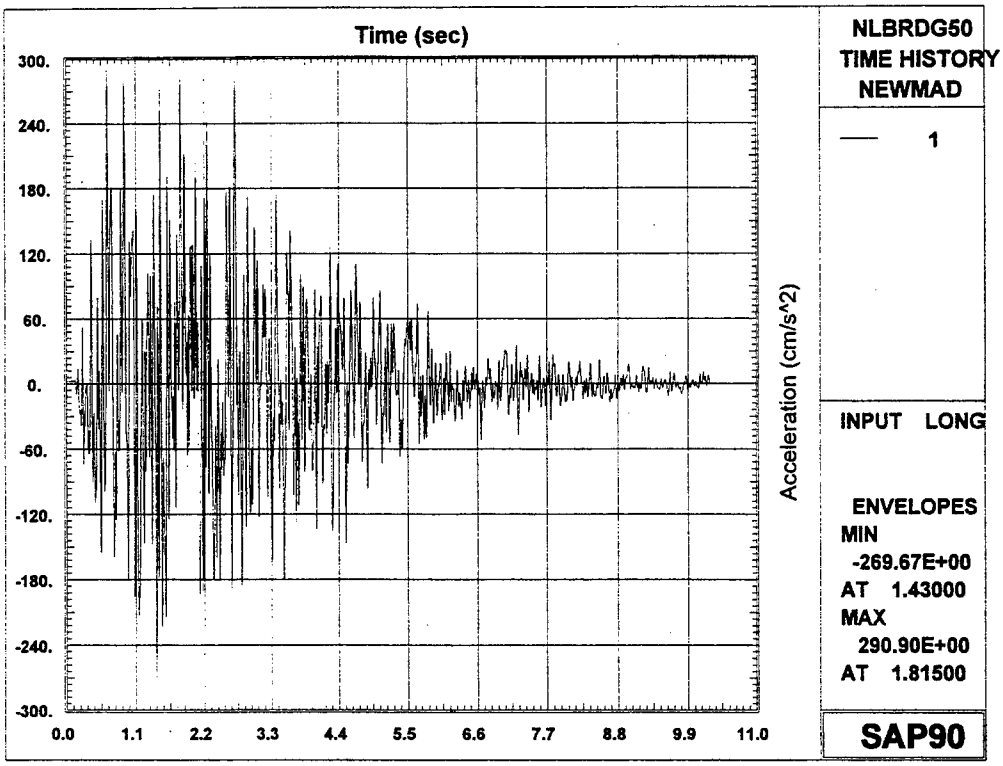

Figure E.3: Longitudinal Base Acceleration for 50-year Event

E.2 MAXIMUM EARTHQUAKE

This section shows graphs of the vertical and two orthogonal, horizontal bedrock-level acceleration histories developed in the study by Street et al. (1996) for the 500-year event (i.e. 90% probability of not being exceeded in a 500 year period).

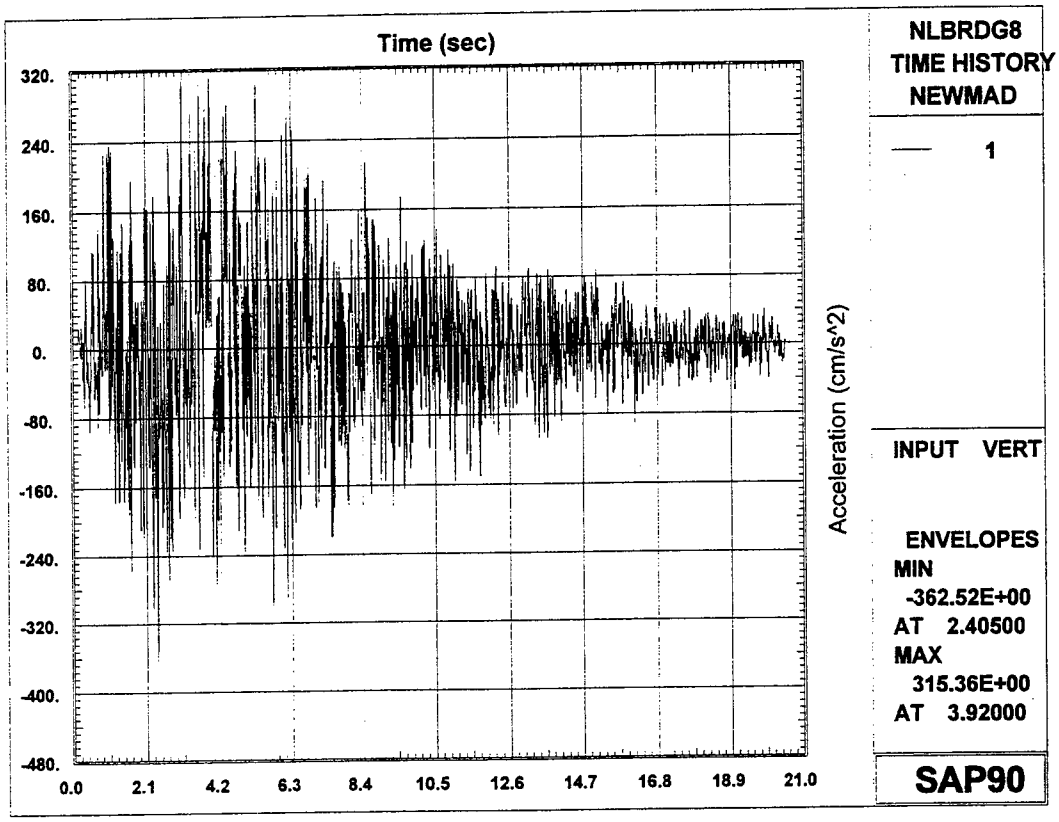

Figure E.4: Vertical Base Acceleration for 500-year Event

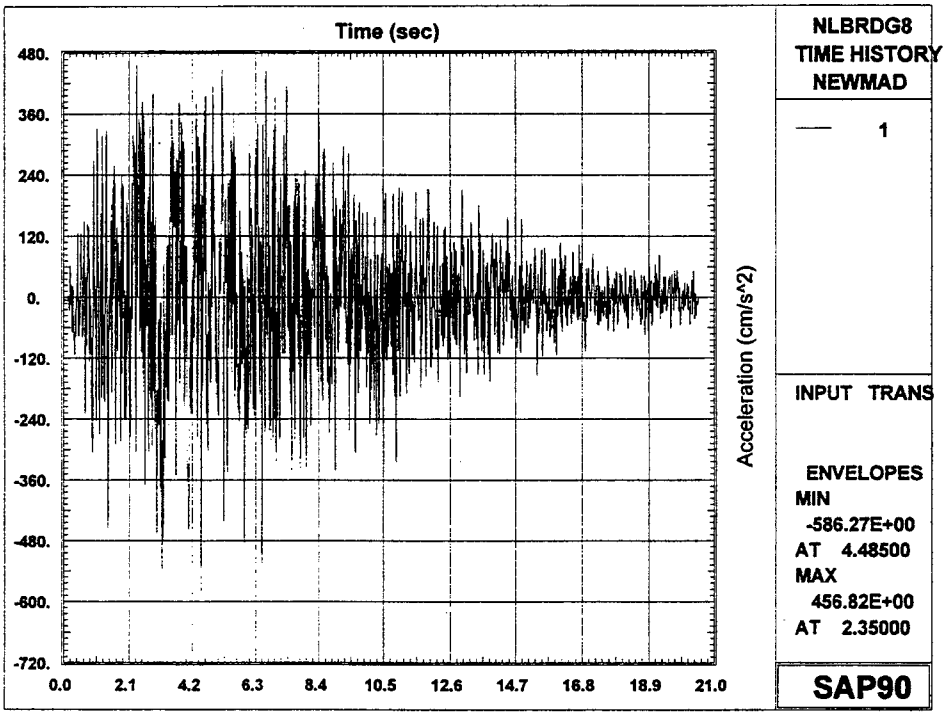

Figure E.5: Transverse Base Acceleration for 500-year Event

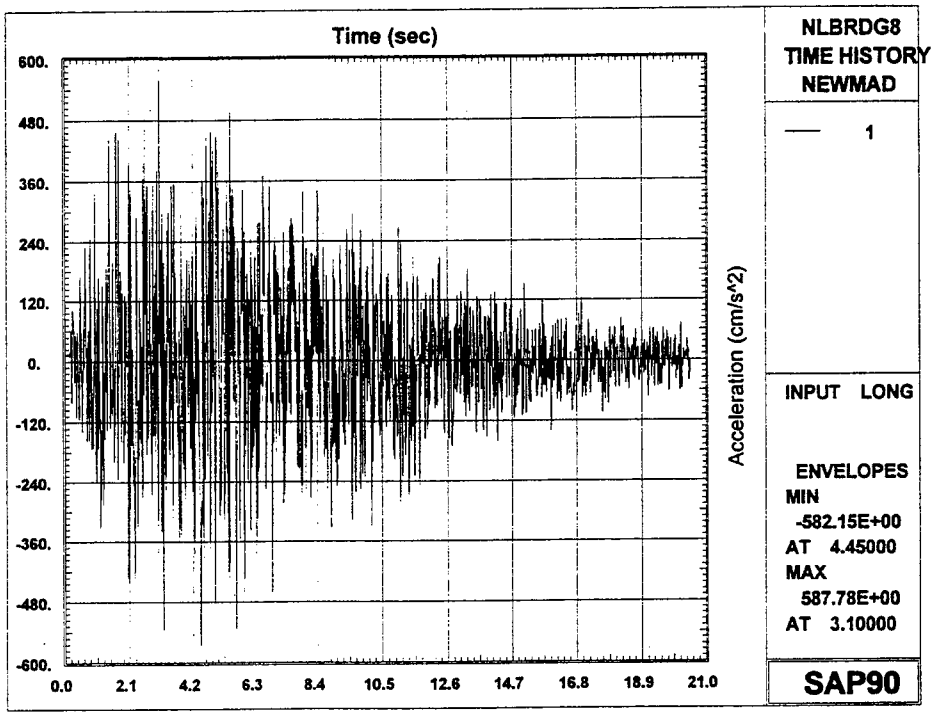

Figure E.6: Longitudinal Base Acceleration for 500-year Event

APPENDIX F

ANALYSIS METHODS

F.1 RITZ VECTOR ANALYSIS

Inherent in using the exact eigenvectors in a mode-superposition analysis are the following problems: (1) solving the exact eigenvalue problem is computationally "expensive" for large systems, (2) it is not known how many eigenvectors are required to obtain an accurate dynamic solution until after the eigenvalue problem is solved, and (3) it has not been proven that using the exact eigenvectors in a mode superposition analysis is better than the use of any other set of orthogonal vectors (Wilson, Yuan, and Dickens 1982). The purpose of time-history analysis is to calculate the theoretical response of a structure to a time-varying load. Many types of loading can be accurately solved only by time-history analysis. One of its most important uses for structural engineers is in earthquake analysis. The dynamic equilibrium equations in nodal coordinates are:

$$\mathbf{M}\,\ddot{\mathbf{u}}(t) + \mathbf{C}\,\dot{\mathbf{u}}(t) + \mathbf{K}\,\mathbf{u}(t) = \mathbf{f}(t) \qquad \text{(F.1)}$$

where:

M, C, K = mass, damping, and stiffness matrices

$\ddot{\mathbf{u}}(t)$, $\dot{\mathbf{u}}(t)$, $\mathbf{u}(t)$=joint accelerations, velocities, and displacements, respectively, relative to the ground, in physical coordinates, as a function of time

f (t) = applied nodal load vector as a function of time

The mode superposition method is a way of parsing the displacement function **u(t)** into two functions: one function of time only, and one function of space only. For linear systems, the method can transform the set of N (number of degrees of freedom) coupled equations, in nodal coordinates, into a set of N uncoupled equations in modal coordinates. The transformation is:

$$\mathbf{u}(s,t) = \Phi(s)\,\mathbf{a}(t) \quad \text{or} \quad \mathbf{u} = \Phi\,\mathbf{a} \qquad \text{(F.2)}$$

where $\mathbf{a}$ is an array of L unknown functions of time and Φ is an N x L matrix of shape functions describing the spatial distribution of loading and is not a function of time. The corresponding velocities and accelerations are

$$\dot{\mathbf{u}} = \Phi \dot{\mathbf{a}} \qquad \text{(F.3)}$$

$$\ddot{\mathbf{u}} = \Phi \ddot{\mathbf{a}} \qquad \text{(F.4)}$$

Substituting equations F.2, F.3, and F.4 into equation F.1 and premultiplying by Φ^T yields

$$\mathbf{M}^* \ddot{\mathbf{a}} + \mathbf{C}^* \dot{\mathbf{a}} + \mathbf{K}^* \mathbf{a} = \mathbf{f}^* \qquad \text{(F.5)}$$

in which

$$\mathbf{M}^* = \Phi^T \mathbf{M} \Phi \qquad \text{(F.6)}$$

$$\mathbf{C}^* = \Phi^T \mathbf{C} \Phi \qquad \text{(F.7)}$$

$$\mathbf{K}^* = \Phi^T \mathbf{K} \Phi \qquad \text{(F.8)}$$

$$\mathbf{f}^* = \Phi^T \mathbf{f} \qquad \text{(F.9)}$$

In traditional mode superposition analysis of linear structures, Φ is a matrix of the lowest eigenvectors of the structure and $\mathbf{M}^*$ and $\mathbf{K}^*$ are diagonal. If modal damping is assumed, the matrix $\mathbf{C}^*$ is also diagonal. Therefore, equation F.5 is reduced to a set of uncoupled, linear, second-order, ordinary differential equations.

On the other hand, if Φ is a matrix of Ritz vectors, the L x L matrices $\mathbf{C}^*$ and $\mathbf{K}^*$ are not diagonal. However, the solution of this set of coupled equations can be obtained with a minimum of numerical effort since L is always small compared to the size of the complete system N. This method is especially efficient for earthquake analysis where a small number of modes contribute most to the response (Wilson, Yuan, and Dickens 1982). The reduced equation set (F.5) can be solved by using a step-by-step, direct integration method.

Selection of appropriate Ritz vectors is essential to achieve superior numerical performance over the use of the system's eigenvectors in a mode superposition analysis. A judicious process of selecting Ritz vectors will successfully approximate the actual modes of vibration due to the applied loading. Ritz vectors used in a SAP2000 time-history analysis are generated from the recurrence relationship:

$$\mathbf{K}\, \varphi_i^* = \mathbf{M}\, \varphi_{i-1}, \qquad i = 2,\ldots, \text{Number of Ritz vectors sought} \qquad \text{(F.10)}$$

where: φ^*_i is the Ritz vector before orthogonalization and normalization

φ_i is the final Ritz vector

The first vector is obtained from the solution of

$$\mathbf{K}\varphi_1^* = \mathbf{f} \qquad \text{(F.11)}$$

At each step, the Ritz vectors are orthogonalized and normalized by standard eigensolution techniques (SAP2000 1996).

The first Ritz vector can be physically interpreted as the static displacement due to the applied load vector **f**. The dynamic forces which were neglected in computing the first vector are of the form $\omega^2 \mathbf{M}\varphi_1$, where ω is a typical frequency component of the loading. The second Ritz vector is determined from the static displacements due to the inertial force distribution associated with the first Ritz vector. (Chopra 1995, Wilson, Yuan, and Dickens 1982)

The process continues until a pre-defined number of Ritz vectors are found. Each Ritz-vector mode consists of a mode shape and frequency. These vectors may be good approximations to the exact mode shapes and frequencies of the structure but are distinctly different. However, because Ritz modes are orthogonal with respect to the mass and stiffness matrices, they can be used just like the exact modes in classical modal analysis.

It should be noted that by using this method to generate load-dependent Ritz vectors, all vectors will participate in the response to the basic loading. When using exact eigenvectors in a mode superposition analysis, there is no assurance that any one eigenvector will participate in the structural response.

F.2 NONLINEAR TIME-HISTORY ANALYSIS

When structures contain members that exhibit nonlinear material or geometric behavior, the governing differential equations become more complex. In general, the left-hand side and right-hand side of the equilibrium equations become coupled because forces are displacement dependent. For a mostly linear structure, with predefined nonlinear elements, subjected to arbitrary loading, the dynamic equilibrium equations can be written as (SAP2000 1996):

$$\mathbf{M}\,\ddot{\mathbf{u}}(t) + \mathbf{C}\,\dot{\mathbf{u}}(t) + \mathbf{K}_L\,\mathbf{u}(t) + \mathbf{f}_N(t) = \mathbf{f}(t) \qquad \text{(F.12)}$$

where:

M = diagonal lumped mass matrix

C = proportional damping matrix

$\mathbf{K}_L$ = stiffness matrix of linear elastic elements

$\ddot{\mathbf{u}}(t)$, $\dot{\mathbf{u}}(t)$, $\mathbf{u}(t)$ = joint accelerations, velocities, and displacements, respectively, relative to the ground, in physical coordinates, as a function of time

$\mathbf{f}(t)$ = applied nodal load vector

$\mathbf{f}_N(t)$ = vector of forces from the nonlinear elements

Direct integration of the coupled equations of motion can be used to solve for the dynamic response of the system. However, the direct integration approach is numerically efficient only for short-duration loads in which a large number of high frequencies are excited (Ibrahimbegovic and Wilson 1988).

Classical modal analysis is precluded from being used since the equations cannot be decoupled into independent modal equations. Despite this apparent obstacle, the mode superposition method can still be used efficiently for some systems. Systems which can be accurately modeled for dynamic response by a structure composed of linear subsystems connected through nonlinear elements are ideal for a modified version of the mode superposition method (Chopra 1995, Ibrahimbegovic and Wilson 1988). The number of significant modes (J) is much smaller than the total degrees of freedom (N) of the system. That much smaller set of coupled equations can be solved in modal coordinates instead of the much larger set of N coupled equations in nodal coordinates.

Direct integration of the equations of motion is equivalent to including all N modes in a mode superposition analysis, even though only the first J modes may be sufficient to represent the dynamic response of the structure. Accuracy of the time integration method is required only for J modes, but stability must be ensured for all N modes (Chopra 1995). Requiring stability for all modes is a severe restriction on time step length for conditionally stable algorithms and causes excessive computational expense. It is, therefore, prudent to use unconditionally stable numerical procedures for the direct integration of the equations of motion. SAP2000 uses closed-form, unconditionally stable integration of the modal equations assuming a linear variation of the loading excitation between input time steps.

The nonlinear time-history analysis method used in SAP2000 is an extension of the method developed by Wilson (Ibrahimbegovic and Wilson 1989, SAP2000 1996). For the purpose of analysis, a linear effective stiffness is defined for each nonlinear element. The equilibrium equation can then be rewritten as:

$$\mathbf{M}\,\ddot{\mathbf{u}}(t) + \mathbf{C}\,\dot{\mathbf{u}}(t) + \mathbf{K}\,\mathbf{u}(t) = \mathbf{f}(t) - [\mathbf{f}_N(t) - \mathbf{K}_N\,\mathbf{u}(t)] \qquad \text{(F.13)}$$

where $\mathbf{K} = \mathbf{K}_L + \mathbf{K}_N$, and $\mathbf{K}_N$ is the linear effective-stiffness matrix for all the nonlinear elements. Modal analysis is performed using the full stiffness matrix, **K**, and the mass matrix, **M**. Coordinate transformation is performed in the same manner as described in section F.1:

$$\mathbf{u}(t) = \Phi\,\mathbf{a}(t) \qquad \text{(F.14)}$$

where Φ is the matrix of mode shapes and $\mathbf{a}(t)$ is the vector of modal displacement amplitudes which varies with time. Equilibrium equations can now be written as:

$$\mathbf{M}^* \ddot{\mathbf{a}}(t) + \mathbf{C}^* \dot{\mathbf{a}}(t) + \mathbf{K}^* \mathbf{a}(t) = \mathbf{f}^*(t) - \mathbf{f}_N(t) \qquad \text{(F.15)}$$

using transformations similar to those of equations F.6 to F.9:

$\mathbf{M}^* = \Phi^T \mathbf{M} \Phi = \mathbf{I}$, where $\mathbf{I}$ is the identity matrix

$\mathbf{C}^* = \Phi^T \mathbf{C} \Phi$ = modal damping matrix which is assumed to be diagonal

$\mathbf{K}^* = \Phi^T \mathbf{K} \Phi$ = diagonal matrix of squared structural frequencies

$\mathbf{f}^*(t) = \Phi^T \mathbf{f}(t)$ = vector of modal applied loads

$\mathbf{f}^*_N(t) = \Phi^T [\mathbf{f}_N(t) - \mathbf{K}_N \mathbf{u}(t)]$ = vector of modal forces from the nonlinear elements

In the above equations, the nonlinear forces, $\mathbf{f}^*_N(t)$, will couple the modes since they are functions of the modal displacements, $\mathbf{a}(t)$. At each time step, they are solved iteratively until convergence is achieved. SAP2000 assumes a piecewise linear variation of the right-hand side of the equilibrium equations and uses exact, closed-form integration to solve the equations in each iteration. A more complete description of the algorithm can be found in Ibrahimbegovic and Wilson (1989) and Wilson (1993).